ROLE OF THE ANTERIOR INSULAR CORTEX IN SALIENCE DETECTION AND BEHAVIORAL FLEXIBILITY

Dissertation an der Fakultät für Biologie
der Ludwig-Maximilians-Universität München
zur Erlangung des akademischen Grades
eines Doktor der Naturwissenschaften (Dr. rer. nat.)

Alja Podgornik

München, 7. November 2022

All work described in this dissertation was conducted

under the supervision of Dr. Nadine Gogolla and Prof. Dr. Rüdiger Klein,

in the department Molecules-Signaling-Development,

in the research group Circuits for Emotion,

at Max Planck Institute for Biological Intelligence (previously Neurobiology)

in Martinsried, Germany.

Supervisor:	Dr. Nadine Gogolla
First examiner:	Prof. Dr. Rüdiger Klein
Second examiner:	Prof. Dr. Laura Busse
Submission date:	7. November 2022
Date of oral examination:	22. February 2023

Eidesstattliche Erklärung

Ich versichere hiermit an Eides statt, dass die vorgelegte Dissertation von mir selbständig und ohne unerlaubte Hilfe angefertigt ist.

München, den 2. 3. 2023 ALJA PODGORNIK
(Unterschrift)

Erklärung

Hiermit erkläre ich,

☐ dass die Dissertation nicht ganz oder in wesentlichen Teilen einer anderen Prüfungskommission vorgelegt worden ist.

☐ dass ich mich anderweitig einer Doktorprüfung ohne Erfolg **nicht** unterzogen habe.

München, den 2. 3. 2023 ALJA PODGORNIK
(Unterschrift)

ABSTRACT

The main role of the nervous system is to detect, interpret and respond to changes in an organism's internal and external environment. The ability to swiftly and appropriately switch behaviors in response to change is termed behavioral flexibility. Human imaging studies have identified three large-scale brain networks involved in behavioral flexibility, and identified anterior insular cortex (AIC) as the core region regulating switching between the networks through detection of salient stimuli. However, until recently, no rodent study has investigated the role of anterior insular cortex in salience detection, and only this year have two studies attempted to characterize its causal involvement in network switching. As such, we lack understanding of whether and how rodent AIC participates in salience detection and regulates flexible behavior.

In this study, I demonstrate that rodent AIC acts as a salience detector and regulates behavioral switching during flexible behavior. Using a novel behavioral paradigm that allows freely moving mice to flexibly transition between three different behaviors in combination with optogenetic perturbation, I show that AIC stimulation increases behavioral switching and shifts behavioral preference towards externally-focused behaviors. Using fiber photometry recordings of excitatory neuronal activity, I next show that mouse AIC responds to salient stimuli independent of their valence. In addition, I show that AIC activity increases during externally focused and decreases during internally focused behaviors. Finally, using viral tracings in Sim1-Cre, Rgs14-Cre ad GRP-Cre transgenic mouse lines, I examine structural connectivity of three neuronal subpopulations within the AIC, revealing distinct labelled cell localization, projection patterns and preferential connectivity to the major hubs of the rodent salience network. Lastly, I examine the functional properties of the GRP-Cre neuronal subpopulation with fiber photometry, revealing that its functions differ from that of bulk AIC excitatory neuron activity.

Overall, this study is the first to show that rodent AIC detects salient stimuli and regulates behavior switching during flexible behavior. Furthermore, the optogenetic and fiber photometry experiments indirectly suggest that, similar to humans, rodent AIC may regulate switching between large-scale brain networks.

ACKNOWLEDGMENTS

First, I want to thank Nadine for accepting me into her work group, and for all her support and scientific guidance over the past four years. I also want to thank my TAC members Rüdiger Klein, Laura Busse and Carsten Wotjak for all their feedback, as well as my graduate school IMPRS, for providing many great learning opportunities over these years.

The last four years would have been a lot more difficult without all the great people that I got to work with. A huge thanks to Onur, who worked with me on a technically really challenging part of the project, not only doing work that exceeded any expectations, but also remaining motivated and positive throughout. I also want to thank my fellow PhDs, Caro and Anna, for always being willing to listen and discuss not only scientific but also personal (and cat-related) matters. Thanks to Brad, for all the conversations, outdoor adventures and for keeping me alive during lead climbing. Big thanks to our postdocs Meryl, Jeong, Stoyo and Silvia, for your feedback, scientific insights and offering help whenever needed, as well as to our technicians Frederique, Andrea and, especially, Eunjae, who not only helped with surgeries and imaging for the tracing experiments, but whose efficiency and skill have made our lab work infinitely easier. I also want to thank the "original" lab crew: Alex, for teaching me the technical know-how, Daniel, for always inspiring me to own my truth regardless of whether people like it or not, Nejc, for being so full of life, and to all three of you for welcoming me into the lab with such warmth and kindness.

Finally, I want to deeply thank my family who has stood by my side all these years. It has been incredibly supportive to not only have parents who truly understand what it means to do a PhD, but who, despite their personal academic successes, understand and support your decision to choose your own, different path. From the bottom of my heart I also want to thank my partner Matt, who has been on this journey with me since day one. If I were to describe all the ways in which you supported me during these years, I would have to write another dissertation. I am unbelievably lucky to have a partner like you.

Last, but most certainly not least, I want to express my deepest gratitude to all our little furry mouse friends, who sacrificed more than anyone else for the work described in this dissertation. May your contribution to science never be forgotten or taken for granted.

TABLE OF CONTENTS

ABBREVIATIONS AND ACRONYMS

AAV	Adeno-associated virus
AcbC	Nucleus accumbens Core
ACC	Anterior cingulate cortex
ACh	Acetylcholine
ADD	Attention deficit hyperactivity disorder
AIC	Anterior insular cortex
AP	Antero-posterior
BAC	Bacterial artificial chromosome
BLA	Basolateral amygdala
CaMKII	Ca^{2+}/calmodulin-dependent protein kinase
CeA	Central amygdala
CEN	Central executive network
ChR2	Channelrhodopsin
CPu	Caudate Putamen
CTb	Cholera toxin subunit B
DA	Dopamine
DMN	Default mode network
DNA	Deoxyribonucleic acid
DREADD	Designer Receptors Exclusively Activated by Designer Drugs
DV	Dorso-ventral
eNpHR3.0	Enhanced *Natronomonas pharaonis* Halorhodopsin 3.0
ENT	Entorhinal cortex
EPM	Elevated plus maze
eYFP	Enhanced yellow fluorescent protein
fMRI	Functional magnetic resonance imaging
fUS	Functional ultrasound
FP	Fiber photometry
GRP	Green fluorescent protein
GECI	Genetically-encoded calcium indicators
HPC	Hippocampal formation

IC	Insular cortex
IPAC	Interstitial nucleus of the posterior limb of the anterior commissure
IPS	Inferior parietal sulcus
LC	Locus coeruleus
MeA	Medial amygdala
MIC	Medial insular cortex
ML	Medio-lateral
NTS	Nucleus of the solitary tract
OFC	Orbitofrontal cortex
OFT	Open field test
PBN	Parabrachial nucleus
PETH	Peri-event time histogram
PCC	Posterior cingulate cortex
PFC/PF	Prefrontal cortex
PIC	Posterior insular cortex
PPC	Posterior parietal cortex
RSP	Retrosplenial cortex
SN	Salience network
SNG	Substantia nigra
ZI	Zona Incerta

1. INTRODUCTION

1.1 Behavioral flexibility

An important role of one's nervous system is to detect, recognize and evaluate one's internal and external environment in order to dynamically adjust our behavior to the ever-changing world around us. Whether this is an internal sensation of hunger, the perception of a loud, potentially threatening sound, or a response to a large-scale catastrophe such as an earthquake or pandemic, an organism's survival and thrive depend on its ability to flexibly adapt to novel circumstances.

An appropriate and timely adaptation of one's behavior in response to change is termed "behavioral flexibility"[1]. Research done in developmental and lifespan fields has shown that greater behavioral flexibility correlates with both greater academic success[2] and smoother transitioning into adulthood, as well as increased chance of employment and better life outcomes[3]. Furthermore, maintaining greater behavioral flexibility later in life has been shown to correlate with decreased negative effects of ageing and cognitive decline[4].

When we talk about human behavioral flexibility, two components are generally considered - cognitive and behavioral. The cognitive component denotes an individual's ability to switch his or her thinking process between two different concepts depending on situational context[5]. The behavioral component addresses an organism's ability to adjust its behavior in response to a change in its environment[6]. The two components are highly intertwined: most laboratory tests used to asses an organism's flexibility require behavioral output, which is then used to draw conclusions about an individual's flexibility. Likewise, it is hard to conceptualize that flexible behavior could emerge without underlying cognitive flexibility[1]. Therefore, since this work has been conducted in animals where the cognitive components are difficult to isolate, I will not explicitly differentiate between the two, but will cumulatively refer to them as "behavioral flexibility".

1.1.1 Neural correlates of behavioral flexibility in humans

To date, a large number of studies have looked at behavioral flexibility, particularly in humans. There, the neural substrates for behavioral flexibility are assessed using task-switching or set-shifting paradigms while simultaneously measuring brain activity using functional magnetic resonance imaging (fMRI)[7]. To determine the extent to which individuals successfully shift their behavior, flexible problem-solving, tolerance of change, transition making, attention switching and change of focus are assessed[8]. Functional imaging studies using task-switching and set-shifting have illuminated the brain structures underlying flexible behavior switching. Three major brain networks involved in this process have been highlighted:

Central executive network

A central role in behavioral flexibility is governed by the central executive network (CEN). This network is comprised of the dorsolateral and ventrolateral prefrontal cortices (PFC), as well as the inferior parietal lobule, posterior inferior temporal lobes and portions of the midcingulate gyrus[1]. The CEN shows strong activation during cognitively demanding tasks[9], such as solving a complex mathematical problem. This network is especially important for actively manipulating information retrieved from working memory, as well as decision-making, discernment and judgement during goal-directed behavior[10–12]. Overall, the CEN is involved in externally-focused, goal-directed and cognitively demanding tasks.

Default mode network

As opposed to the CEN, the default mode network (DMN) is a set of structures that increase their activity during internally focused- and decrease their activity during cognitively demanding tasks. The DMN comprises the medial temporal lobes, the angular gyrus, as well as posterior cingulate cortex (PCC) and the ventro-medial PFC. The abovementioned structures are involved in a number of processes, including autobiographical memory and self-referential processes as well as social cognitive processes related to self and others[13–16]. Over the past decades, a number of brain imaging studies have converged to define the DMN as a key network involved in internal modes of cognition and self-referential functions, some of which

have been considered to be unique to humans: empathy, conceptual processing, recollection and imagination, and conscious awareness[17]. However, the uniqueness of the DMN to humans has been challenged, as analogous systems and behaviors have been found in other species, such as primates and even rodents[18–21]. While the precise functions of the DMN are still not fully understood, its overall functioning appears to be involved in internally focused and self-referential processes, rather than externally focused, cognitively demanding processes.

Salience network

It is important to note that CEN and DMN activation is largely opposing and mutually exclusive – as the activity in the CEN increases, the activity in the DMN decreases, and vice versa[22,23]. This begs the obvious question: what structure, or set of structures, mediates the transition from one network to the other? Human imaging studies have indeed identified a third large-scale brain network, responsible for switching between the CEN and DMN, allowing one to flexibly shift their focus between externally and internally oriented behaviors. This network is called the salience network (SN) (**Figure 1**). The SN is composed of two major cortical structures, the anterior insular cortex (AIC) and anterior cingulate cortex (ACC), as well as subcortical structures like the thalamus, nucleus accumbens and the amygdala[24]. It has been shown that the main role of the AIC within the SN is to identify salient stimuli that are homeostatically most relevant to the organism from a multitude of stimuli competing for an organism's attention at any given moment. Once the salient stimulus is correctly identified, the ACC is recruited to facilitate a sensory-motor transformation that guides appropriate motor output and externally detectable behavior change[25,26]. Indeed, multiple studies have now shown that the AIC plays a causal role in guiding the bi-directional switching between the DMN and the CEN[22,27]. Since the ability to smoothly transition between internally and externally focused behaviors depending on the change in the environment is crucial to correct behavioral adaptation, the AIC is hypothesized to play a major, and potentially causal role, in behavioral switching and flexibility[9].

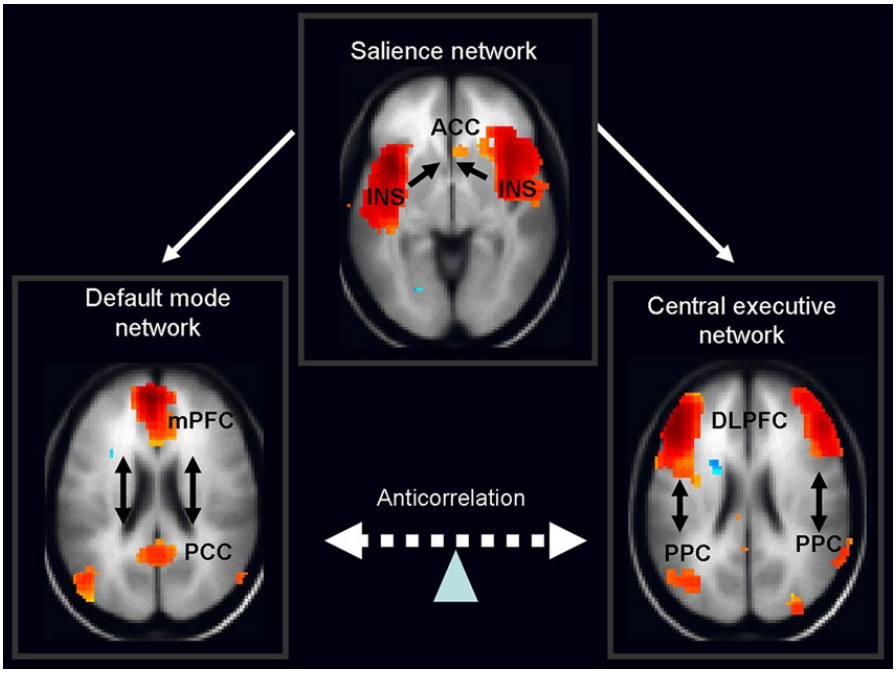

Figure 1. Salience network and AIC guide switching between large-scale brain networks. *The salience network and its primary nodes, anterior insula and anterior cingulate cortex, guide appropriate transitioning between networks responsible for internally-focused (DMN - left) and externally-focused (CEN - right) processes. The activity patterns of the two networks are largely anti-correlated and serve opposing behavioral functions. As such, they require a third network – the so-called salience network - to guide appropriate transitioning between them. Abbreviations: PCC: posterior cingulate cortex; mPFC: medial prefrontal cortex; INS: insular cortex; ACC: anterior cingulate cortex; DLPFC: dorsolateral prefrontal cortex; PPC: posterior parietal cortex. Adapted with permission from*[28].

1.1.2 Large scale brain networks in rodents

While human studies offer great insight into the broad functional organization of the human brain, their technical and ethical limitations prevent precise exploration of specific neuronal circuits and their interactions within the networks. As such, a number of studies have attempted to elucidate the existence of large-scale brain networks in rodents (**Figure 2**). Multiple studies have by now confirmed the existence of rodent DMN and have convincingly demonstrated that it is anchored in the retrosplenial cortex (RSP)[29,30], which is thought to be a rodent analogue of human PCC. Similar to humans, the rodent DMN includes the midline structures and in addition to the RSP encompasses the cingulate, orbitofrontal, and peri- and ventro-hippocampal areas[20]. Furthermore, these studies also revealed the existence of an opposing, anti-correlated network, encompassing primary motor and somatosensory areas, posterior part of the thalamus, lateral caudate putamen and substantia nigra[18]. This network, often referred to

as a “lateral cortical network”, represents a mouse analogue of the human CEN. In addition, seed-based correlation maps show that, similar to the AIC’s role within the human SN, rodent AIC exhibits strong functional connectivity with a distributed anteroposterior network, including the areas such as dorsal cingulate cortex and ventral striatum[19,21,31].These studies have convincingly demonstrated that rodent brains also contain a SN, with the AIC being one of its main hubs[29,30,32].

However, many of the aforementioned studies have also reported contradictory findings: one of the main disagreements is whether or not medial prefrontal nodes are included in the DMN, with some paradoxical findings simultaneously assigning certain nodes, such as RSP and medial prefrontal cortex, to both the SN and DMN[30,33]. It is also important to note that these functional studies, while highly valuable, are based on observing and quantifying temporal correlations between anatomically dispersed brain regions in anaesthetized animals. As such, studies probing the direct function of specific network structures are needed to confirm and describe the properties of rodent large-scale brain networks important for behavioral flexibility. At the time when this project began, no such studies were published. However, in the last two years, three studies tackling this issue were published - two, at the time of writing, still only as pre-prints[34,35]. A study conducted by Mandino et al. convincingly demonstrated homology of the three large-scale brain networks between humans, macaques and mice, and showed that evoked activity within certain rodent SN nodes preferentially elicits activity within other SN nodes, confirming strong intra-network functional connectivity. Fascinatingly, that study also showed that depression-induced changes within rodent large-scale networks are similar to those observed in human patients, further suggesting similarity in their functions[18]. In another study conducted by Menon et al., the authors combined optogenetic-fMRI technology with computational modeling of brain-circuit dynamics to demonstrate that feedforward optogenetic stimulation of the AIC dynamically suppresses specific subdivisions of the rat DMN[34]. Finally, the third study, employing concurrent neural recordings using fiber photometry with fMRI, revealed that the rat AIC is activated by salient deviant stimuli, and that the AIC causally suppresses the RSP, an important rodent DMN hub[35]. While the last two studies still await peer review, they are pioneering evidence that the rodent AIC may play a causal role in switching between large-scale brain networks.

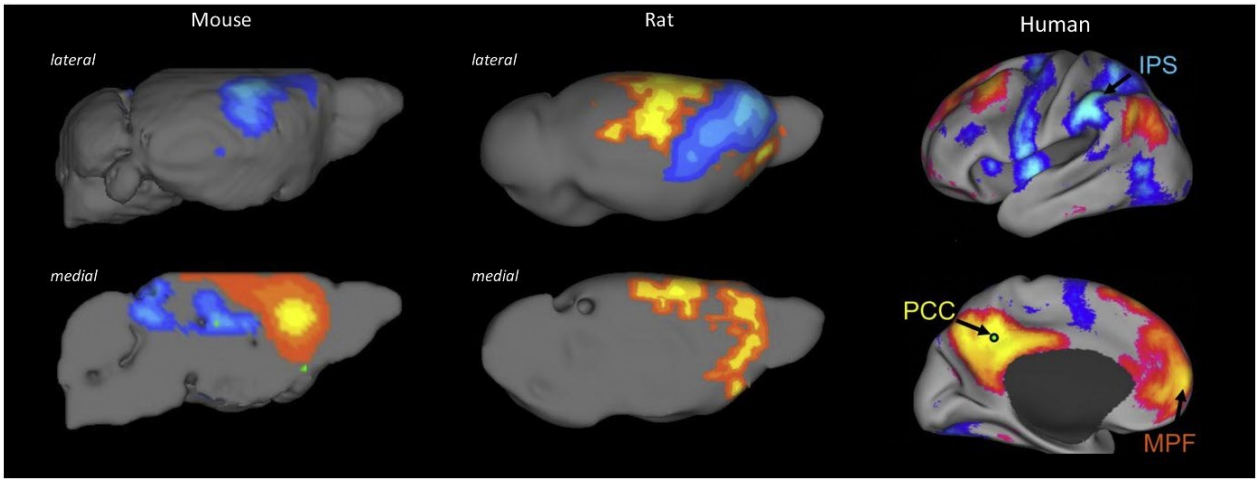

Figure 2. Comparison of large-scale brain networks between rodents and humans. *Medial and lateral views of the reconstructions of mouse (left), rat (center) and human (right) brain. The maps display clearly visible anticorrelations between midline DMN-like network and lateral cortical areas (analogue of the CEN). Such anticorrelations represent a fundamental topological feature of the human DMN. Abbreviations: MPF: medial prefrontal cortex; IPS: inferior parietal sulcus; PCC: posterior cingulate cortex) Red/yellow colors indicate positive correlations; blue colors indicate negative correlations. Adapted with permission from*[21].

While the above publications mark an important milestone in the study of rodent brain networks important in behavioral flexibility, we are still a long way from understanding how individual structures within these networks contribute to effective and appropriate behavioral switching. As such, **the main objective of my dissertation was to explore the role of rodent AIC in behavioral switching during flexible behavior.** To facilitate further understanding of this fascinating brain region, the following section will briefly review our current knowledge about the insular cortex. Furthermore, I will explore structural and functional evidence that the AIC indeed possesses the necessary attributes to serve as a hub guiding behavioral switching and flexibility not only in humans, but also mice, suggesting it may also there serve to detect salient events and guide switching between large-scale brain networks.

1.2 The Insular cortex

The insular cortex (IC), or simply “insula”, is a complex and heterogeneous region that has been associated with a number of functions, including, but not limited to, sensory, sensory-motor, cognitive, socio-emotional and interoceptive functions[36]. Furthermore, many human imaging studies have consistently identified the IC as an important hub whose functional connectivity is altered across a vast spectrum of neuropsychiatric disorders[37], ranging from

mood disorders such obsessive-compulsory disorder, anxiety and depression, to developmental, early-onset disorders, such as autism spectrum disorder and attention deficit hyperactivity disorder (ADHD)[1]. Interestingly, it has been shown that many of these disorders are characterized by a dysfunction in resting-state connectivity of large-scale brain networks[38–42]. In the following paragraphs I describe the current state of knowledge regarding functional and structural connectivity of the IC, with focus on the mouse, since this is the model organism used in this study. Furthermore, I will describe the functional role of the insula uncovered through both human and rodent studies, with emphasis on rodent research.

1.2.1 Structural organization of the insular cortex

In humans and other primates, the insular cortex is located in the Sylvian fissure, hidden under the junction of temporal, parietal and frontal lobes. In rodents, however, the IC is exposed on the lateral surface of the brain, positioned above the rhinal fissure[43] (**Figure 3**). In humans and rodents, the insular cortex tends to be subdivided based on its cytoarchitecture, function and structural connectivity[44].

In mouse and human alike, the IC is subdivided along the dorso-ventral axis into three subdivisions. Following the antero-posterior axis, these are the agranular, dysgranular and granular insula, their "granularity" being determined by the absence or presence of cortical layer IV, also called the granular layer[45,46]. The IC can thus be considered a six-layered cortex, however, along the postero-anterior axis layer IV is gradually lost, being fully absent in the anterior (agranular) insular cortex. The second way of subdividing the IC is based on its structural and functional connectivity, rather than its cytoarchitecture[47]. A rather arbitrary mode of division, the details of which are not agreed upon across various research labs, divides the IC into posterior (PIC) and anterior IC (AIC) (**Figure 3**). This mode of subdivision is very common in both rodent and human studies. It is worth noting that the entirety of the IC is heavily interconnected along the postero-anterior, as well the dorso-ventral axis[46,48,49].

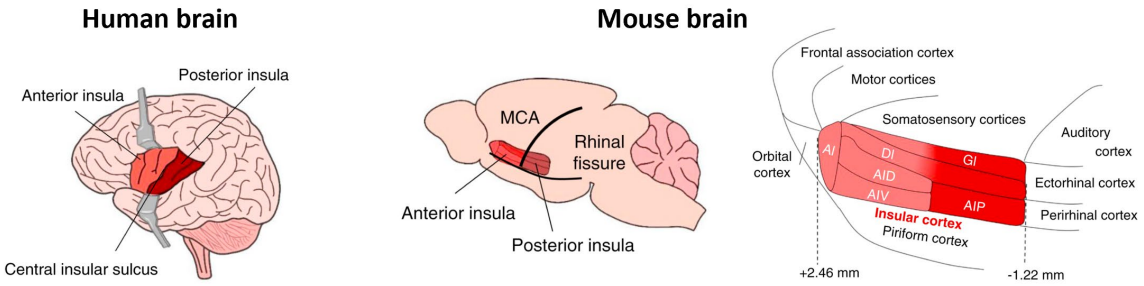

Figure 3. Location and subdivisions of mouse and human insular cortex. *In humans (left), the insular cortex (IC) is hidden under the junction of three cortical lobes and is normally divided along the antero-posterior axis into PIC and AIC. In mice (right), the IC is found on the lateral surface of the brain. Depending on the objective of a study, the IC may get divided along an antero-posterior axis into AIC and PIC, or according to its cyto-architecture into agranular, dysgranular and granular layers. Adapted with permission from*[50].

1.2.1.1 An overview of insular cortex connectivity

Like the majority of cortical regions, the IC displays highly diverse connectivity with a number of cortical and subcortical regions and displays strong internal connectivity. The IC receives extensive internal and external sensory inputs. As the primary gustatory cortex, it receives strong sensory input from the gustatory and olfactory senses as well as auditory, visual and somatosensory information via thalamic and cortical inputs[44,46,48,50,51]. Furthermore, the IC exhibits strong indirect connectivity with the internal organ systems, such as the stomach, gut, heart, lungs and bladder[52,53]. These interoceptive signals travel to the IC via vagal and glossopharyngeal afferents synapsing in the nucleus of the solitary tract (NTS)[54] and parabrachial nucleus (PBN), and from there travelling either directly or via the ventral posteromedial nucleus to the PIC[55–58]. In turn, the IC sends strong output connections to the autonomic centers of the brain, and the AIC in particular projects strongly to the NTS, which is known to be involved in gustatory, visceral, cardiac and respiratory functions[59]. The IC also exhibits connectivity with brainstem nuclei such as the PBN[58], and parts of the dorsal vagal complex involved in the regulation of gastric motility, as well lateral hypothalamus, which is important in cardiovascular regulation[56–58,60]. As such, the IC exhibits strong bidirectional connectivity with the brain and bodily systems regulating basic physiological functions.

In addition to strong connectivity with the sensory, autonomic and interoceptive hubs, the IC displays prominent connectivity with multiple structures of the “emotional” limbic system,

with noticeably strong bi-directional connectivity with the amygdaloid complex[49], as well as the nucleus accumbens, mediodorsal thalamus and the bed nucleus of the stria terminalis[44,49,61]. These regions have been implicated in representing information regarding both negative and positive stimulus valence, as well as motivation and addiction[62–65]. The IC also displays bidirectional connectivity to cortical regions involved in higher-order cognitive processes, such as the prefrontal, orbitofrontal and anterior cingulate cortices[44,45,47,66,67]. Intra-insular connectivity is thought to predominantly flow along the posterior-anterior axis in a feed-forward manner. This hypothesis is supported by the findings from a tracing study conducted in our lab, in which we showed that a larger number of intra-insular outputs are found in the AIC compared to the PIC[49].

Given the complex input-output connectivity pattern described above, the IC is oftentimes considered to be a "multisensory integration hub", integrating external sensory, interoceptive, cognitive, emotional and autonomic information into a coherent whole[36,50,68,69].

1.2.1.2 Rodent AIC connectivity with putative large-scale brain networks

Such complex and extensive whole-brain connectivity of the IC already suggests its possible involvement in coordination of large-scale networks. But what do we know about direct connectivity of rodent AIC with other putative core structures of the DMN, SN and CEN? One study, published soon after the start of this project, revealed the existence of direct projections between the AIC and ACC[70], a finding further confirmed by the data displayed in the Allen brain mouse connectome[71]. Furthermore, a tracing study from our lab revealed that the AIC also projects to the ventral striatum and the amygdala, two of the core subcortical SN regions[49]. Interestingly, no studies to date have found direct connectivity between the retrosplenial cortex (RSP), one of the main functional hubs within the DMN, and any part of the IC. AIC does, however, exhibit strong reciprocal connectivity with dorsal striatum, orbitofrontal cortex (OFC) and peri hippocampal regions[49], all of which are other important DMN nodes. As for the CEN, often referred to as the "lateral cortical network" in mice, the AIC has been shown to have strong connectivity with all major hubs. Specifically, AIC displays strong reciprocal connectivity with primary motor and somatosensory areas, as well as the ventral posterior part of the thalamus. In addition, the AIC sends strong output projections to the lateral striatum and

substantia nigra (SNG), both parts of the rodent CEN[18,49]. Taken together, these studies suggest that the in-so-far characterized AIC connectivity is in line with the input-output pattern one would expect from a region involved in regulating switching between large-scale networks in rodent brain.

1.2.2 Functional roles of the insular cortex

1.2.2.1 An overview of insular cortex function

Given the highly heterogeneous nature of IC connectivity, it is unsurprising that its functional roles are equally complex. A large body of literature, primarily done in humans, has shown the involvement of the IC, particularly the PIC, in a number of processes, including, but not limited to, nociception and pain[72,73], thermal sensation[74], chronic pain[75], itch[76] and sensual touch as well as muscular and visceral sensations[77,78]. Furthermore, particularly the AIC has been shown to be involved in representing subjective awareness of both positive and negative feelings such as anger, happiness, disgust and pain[79] as well as more complex processes such as judgment of trustworthiness[80]. Furthermore, the AIC has also been associated with higher-order functions such as bodily awareness and sense of agency[81,82], emotional awareness[83], time perception[84], attention[85,86], empathy[87] and has even been suggested to gate conscious access to incoming information[88]. It has been suggested that the PIC represents more "objective" sensory information, such as the absolute value of temperature or nociceptive signaling, whereas the AIC integrates this input with higher order processes to assign a "subjective" value to the incoming stimuli[74,79]. Interestingly, the AIC has repeatedly been shown to be affected in a number of neuropsychiatric conditions, including anxiety disorders, depression, addiction, obsessive-compulsory disorder, anorexia nervosa, schizophrenia and autism[89–95]. It is worth noting that many of these disorders are characterized by a marked reduction in behavioral flexibility; one of the hallmarks of addiction is an inability to give up a certain behavior despite its negative consequences, whereas restricted and repetitive behaviors are characteristic of ASD. Furthermore, patients suffering from a major depressive disorder exhibit decreased functional connectivity within the AIC and between the DMN and CEN, which may explain the patients' difficulty to disengage the processing of self-focused, negative thoughts[96].

As opposed to a vast pool or human literature, much less research has been conducted on the functional role of the rodent IC, especially the AIC. Yet, based on the studies done up until this point, we know the rodent IC to be involved in multisensory[68,69] and pain processing[97], valence and identity coding[98–100], learning and memory[101], social behavior[102], gustatory representation[98,100], conditioned taste aversion and malaise[103], as well as representation and modulation of aversive physio-emotional states such as hunger, thirst, fear and anxiety[47,104,105]. Furthermore, the IC has recently been shown to encode immune system information[106], motivational vigor[107] and even represent current and anticipated physiological states[108]. Similar to the human literature, these results suggest highly diverse and complex roles of the IC. It is important to note, however, that the majority of these studies have explored the role of more posterior, rather than anterior, regions of the IC. Since the anterior insular regions are anatomically far more expanded in humans than any other species[79], we do not yet know how its functional roles compare between humans and rodents.

1.2.2.2 Saliency detection, salience network and behavior switching

While the AIC has been implicated in a number of higher-order cognitive and emotional processes, another, much simpler set of paradigms, consistently shows its engagement. Across stimuli of various modalities, the AIC shows a strong response to deviant stimuli embedded in the stream of continuous stimuli[109–111]. Furthermore, it has been shown that once the familiar deviant stimuli are replaced with novel deviant stimuli, the latter elicit a greater response in the AIC, regardless of the stimulus modality[112,113]. Only a few months ago, this has, for the first time, been also shown in rodents[35]. These studies suggest that one of the roles of the AIC is to detect salient – novel, deviant or homeostatically relevant – stimuli across various modalities, which can then guide decision-making and behavioral adaptation[114].

Based on the above, a network model of the insula function, aiming to synthesize a large number of seemingly disparate functional roles of the AIC, has been proposed: the main role of the AIC is to detect salient stimuli, relevant to an organism in a given space and time. Once a stimulus is detected and marked as salient – and thus worthy of being engaged with - the AIC recruits other large-scale brain networks, predominantly the CEN, that gate access to attention and working memory. In this way, the AIC acts as a gatekeeper of executive control, gating the access to frontal and other brain regions that provide the neural substrate for executive

functions[114]. Once the information about the salient stimulus has been processed and integrated, it gets communicated to other regions, predominantly the ACC, which guide motor output, thus leading to outwardly detectable behavior change[9]. As such, the AIC is theorized to play a causal role in orchestrating the activity of large-scale brain networks and ultimately guiding correct behavioral response to increase the organism's chance for survival and thrive.

1.2.3.2 Attributes of rodent IC suggesting its involvement in behavioral flexibility

While the above model has been widely considered in the human insula research field, there has, so far, been little to no research evaluating the role of rodent AIC in either salience detection or behavioral flexibility. As such, it is important to consider if, based on the in-so-far obtained information about the structural and functional properties of the rodent IC, it is reasonable to assume that the AIC would serve a similar function in rodents as it does in humans. Below, I want to briefly discuss why I believe that rodent AIC possesses the necessary attributes to play a role in salience detection and behavioral flexibility.

First, I want us to first briefly consider components necessary for salience detection. It is important to keep in mind that in ethologically relevant situations, saliency detection is a far more complex process than just detecting deviant stimuli. An organism's ability to evaluate a stimulus as salient depends not only on the properties of the stimulus itself, but also on the current condition of the organism. For example, while a piece of bread may be highly salient to a hungry person, this same stimulus would be perceived as irrelevant to a sated person. Likewise, even to a hungry individual, this same stimulus would not be deemed as equally salient if they were being attacked by a lion. As such, successful salience detection requires integration and evaluation of external sensory information about the stimulus and the environment, with the internal experience of the subject, as well as higher cognitive processes needed to fine-tune and correctly regulate behavior.

Given the above, the region that would serve to correctly detect salient stimuli and guide flexible behavior would need to integrate and evaluate sensory, emotional, interoceptive and higher cognitive information. As mentioned in the previous sections, it has been shown that the rodent IC possesses structural connectivity with the regions encoding such information, as well as with putative core regions of the relevant large-scale brain networks. Furthermore, the rodent

IC has been shown to integrate external sensory information with interoceptive, cognitive and emotional components of a stimulus. In addition, studies have also shown that different parts of the rodent IC are important in positive and negative valence processing, as well as assigning value and identity to a given stimulus. The integration of all these components thus equips the rodent IC with a unique ability to construct a unified representation of an organism's current state at any given moment, and its connection to the motor hubs suggests it could indirectly guide behavioral output. Overall, these attributes give reasonable ground to pursue the exploration of the role of rodent IC in salience detection and behavioral flexibility.

In the final section of this chapter, and before I introduce the experimental protocol and results obtained in this study, I want to briefly discuss the experimental approaches that were used in my work.

1.3 Experimental approaches used in this study

1.3.1 Behavioral experiments in mice

Over the past decades, the field of neuroscience has become increasingly interested in identifying neural correlates that govern behavior. To achieve this, human studies generally use activity readouts, such as fMRI, combined with specific behavioral tasks to ascertain brain regions and networks involved in those tasks. While this approach gives us valuable information about relevant brains structures, and allows us to look at the large-scale brain networks, it nevertheless has a number of limitations. First of all, it measures indirect neural activity through changes in blood flow, serving only as a proxy of increased neural activity rather than its direct measurement. Second of all, its limited spatio-temporal resolution prevents the identification of precise neuronal activity in smaller regions, let alone looking at specific neuronal subpopulations[115]. Finally, such approaches are purely correlational, as proof of causal involvement generally requires the use of tools that allow direct neural manipulation.

To circumvent this, behavioral neuroscience has turned towards model organisms. Specifically, mice have turned out to be an extraordinarily useful model due to several reasons. Firstly, the exhibit a number of behaviors that are relevant to human research both in health and disease[116].

Secondly, many transgenic mouse lines are now available, allowing us to investigate how specific neuronal subpopulations contribute to behavior. Finally, over the past twenty years, a multitude of tools have been developed that allow precise spatio-temporal neuronal manipulation as well as the specific measurement of neuronal activity[117,118]. This has given researchers in the behavioral neuroscience field a unique opportunity – to manipulate and measure brain activity in awake, freely moving animals, with unprecedented precision.

Over decades, many behavioral assays were developed to study the involvement of the rodent brain during simple behaviors, such as locomotion and sensory processing, to more complex behaviors assessing cognitive and learning abilities, as well as emotion processing, fear and anxiety[116,119]. While commonly used tests such as the open field test, Morris water maze, elevated plus maze and fear conditioning have led to a number of insights, these paradigms have one large limitation: in an attempt to control the experimental conditions as precisely as possible, animals are normally placed in a highly constrained environment where they are either forced to perform a specific behavior, or given a very limited choice of actions. This makes for a very reductionist task, and can only give us a limited understanding of the brain's true capacity for information processing and regulation[120,121]. Recently, there has been a movement towards the use of ethologically more relevant behaviors[122], as well as the introduction of more complex behavioral setups that investigate higher dimensional and more loosely confined sets of behaviors[123].

Providing a complex and dynamic environment is especially important when we become interested in the question of neural circuits underlying flexible behavior switching in rodents. Compared to human studies, mice cannot be instructed to behave in a specific manner, making the construction of a relevant task even more difficult. As such, the vast majority of studies that aim to study behavior switching in rodents use reductionistic tasks, greatly limiting animal behavior, such as reversal learning, inhibitory learning, and set-shifting[124–127], or even choose to employ head-fixed tasks[128]. To date, however, no study investigating behavior switching in mice, has used a task that would allow freely moving animals to switch between different behaviors at their own volition. As I believe that an understanding of a complex brain regions such as the IC calls for more complex assessments, we designed a novel behavioral paradigm in which a mouse is allowed to freely switch between three different, ethologically relevant behaviors, namely eating, nesting and social interaction. As such, the novel paradigm

Multimaze, which is described in more detail in the methods and results sections, has allowed me to asses behavioral switching during flexible behavior in freely moving animals.

1.3.2 Transgenic Cre-recombinase mouse models

Since this work took advantage of transgenic Cre mice models to study specific neuronal subpopulations within the AIC, I here want to briefly discuss their generation and use. Transgenic Cre mice are genetically engineered mice in which a bacterial artificial chromosome (BAC) engineering system is used to introduce a Cre recombinase enzyme, which allows for site-specific DNA recombination upstream of the ATG start codon of a desired gene[129,130]. In this way, only neurons that express this specific gene will also express Cre recombinase. In such mice, the Cre-expressing neurons can be transfected with Cre-dependent viruses that can encode genes for proteins such as optogenetic channels or genetically encoded calcium indicators (both described in the following sections), allowing us to measure and perturb the activity of specific, genetically determined neuronal subpopulations. Today, transgenic Cre-mice are widely used to study neuronal sub-circuits in behaving mice.

1.3.3 Optogenetics

One of the largest breakthroughs in the field of neuroscience over the past decade has been the development of optogenetics. As the name suggests, optogenetics is a technique that combines optical and genetic tools to modulate neural activity in desired neuronal populations in both *in vitro* preparations, such as cell cultures, an *in vivo* animal models, like insects, rodents and primates[131]. The main benefit of this technique is the precise spatio-temporal regulation of neural activity[132,133]. Optogenetic tools use light-sensitive microbial opsins to regulate the flow of positively and negatively charged ions across a cell membrane, thus increasing or decreasing its membrane potential (**Figure 4**). The opsins used are transmembrane ion channels or pumps that respond to illumination by light of specific wavelength, leading to activation or inactivation of targeted cells with millisecond precision. Following the discovery of the "original", biologically present opsins, a number of different opsins with different kinetics, ionic selectivities and light sensitivities have been engineered[134–136]. To this date, the use of

optogenetics has been imperative in the study of brain circuits underlying various behaviors, and has tremendously increased our understanding of various brain circuits[131,132,136].

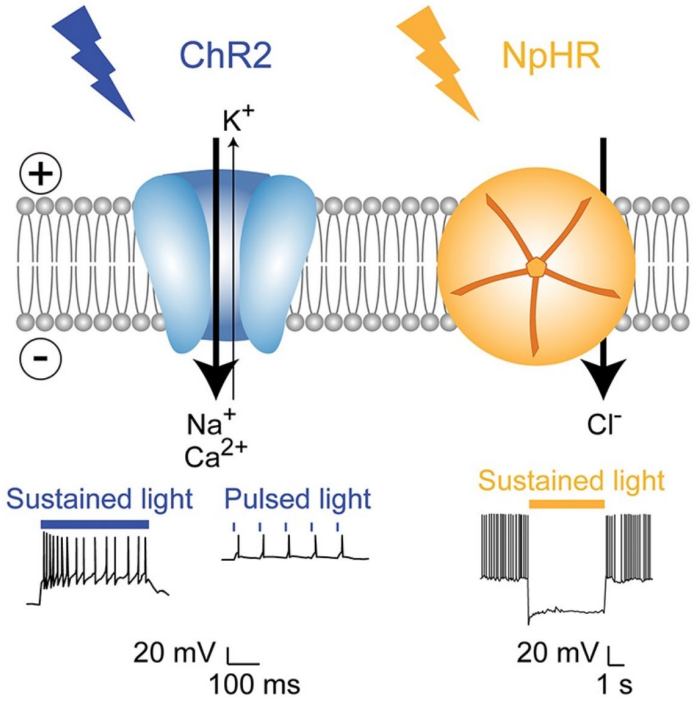

Figure 4. Optogenetic technology. *Light-gated ion channels and pumps allow us to modulate cellular activity with millisecond precision. In the figure, the two most widely used optogenetic tools, Channelrhodopsin2, an excitatory light-gated ion channel, and Halorhodopsin, an inhibitory light-gated pump, as well as the corresponding increase or decrease in single-cell current in response to their activation, are shown. Figure adapted with permission from*[137].

Just like with any other technique, however, it is necessary to be aware of its caveats. It is important to keep in mind that optogenetic tools drive cell activation in an unphysiological way, sometimes producing unnatural or overly strong behaviors[121,138]. In addition, the presence of exogenic membrane-bound proteins may alter the properties of the cell membrane[139] and even interfere with endogenous neurotransmitter release[140]. Furthermore, studies have shown that certain inhibitory opsins can cause rebound excitation, leading to an increase, rather than decrease, in cell activity[134,141]. Finally, while it is possible to express opsins under specific cell-defined promoters, the majority of the optogenetic studies uses rather generally expressed opsins, which synchronously excite or inhibit large cell populations. In such cases, it is impossible to disentangle the contribution of specific neuronal subpopulations to the observed behavior. Nevertheless, while these limitations need to be considered when interpreting behavioral results, optogenetics still represents one of the best-suited molecular tools for spatially, temporally and genetically-defined control of neuronal activity.

1.3.4 Fiber Photometry

While optogenetics is an indispensable tool for accurately controlled perturbation of neural activity, complete characterization of neural circuits that underlie behavior demands real-time measurement of neural activity in awake, freely moving animals. One of the main techniques used for this purpose is calcium imaging, which employs genetically encoded calcium indicators (GECI) to measure change in neuronal activity[142]. The basic principle of this technique relies on our understanding that the depolarization of a neuronal membrane leads to a rapid influx of calcium, causing neurotransmitter release (**Figure 5a**)[143]. The main representatives of the GECI class are the members of the GCaMP family[144], which, upon binding calcium ions, emit a fluorescence signal that can be recorded and used to quantify neuronal activity (**Figure 5b**). This technique, however, has two major drawbacks: firstly, GCaMP proteins possess relatively slow temporal dynamics, with signal half-rise time requiring tens of milliseconds[145], making them unsuitable to represent precise neuronal activity happening on a millisecond time scale. Secondly, since calcium sensors act via binding the intracellular calcium rather than measuring direct electrical activity, they are an indirect proxy, rather than a precise measure of neuronal activity[146]. Nevertheless, calcium imaging has proven to be incredibly useful in gaining insight into neuronal activity of awake, behaving animals. Most commonly, calcium imaging is employed in combination with epifluorescence or two-photon microscopy imaging, done in awake, but head-fixed mice[147,148], or in a one-, two- or even multi-photon system, using head-mounted miniature endomicroscopes (miniscopes) in freely moving mice[149]. However, these systems have limitations due to their cost, weight and complexity of experimental execution, as well as relatively small fields of view. A much simpler to apply alternative is fiber photometry (FP). As opposed to calcium imaging microscopy techniques, which can resolve population or single-cell activity, FP is used to record bulk activity from a large, genetically defined neuronal population[150,151]. Instead of heavy and restraining tools mentioned above, FP relies on chronically implanted optic fibers, which deliver light and collect the overall fluorescence emitted by the GECI expressed in the target region (**Figure 5c**). This renders FP highly useful as it only minorly affects the animal's ability to move and explore its environment, allowing for more natural behavior. However, FP has two major limitations: firstly, it cannot differentiate between potentially diverse functions of cells within the recorded population unless transgenic mouse models are employed. Secondly, even when FP is employed in transgenic mouse lines, it cannot provide single-cell

resolution, making the study of single-unit or population level activity within a specific subpopulation impossible.

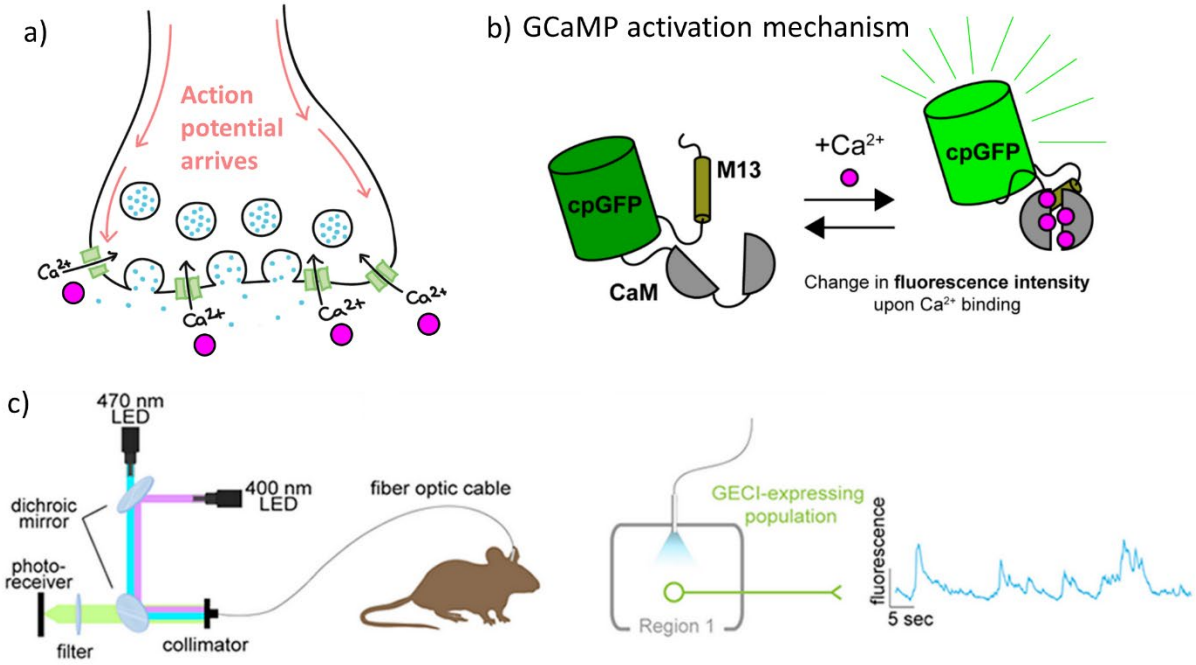

Figure 5. GECI activation mechanism and fiber photometry setup. a) *Arrival of an action potential to the axonal terminal triggers Ca^{2+} influx responsible for consequent neurotransmitter release.* ***b)*** *Ca^{2+} binds to the calmodulin (CaM) subunit on a GCaMP molecule, causing conformational change and fluorescence change.* ***c)*** *Standard fiber photometry setup. Light from GECI and isosbestic channels is delivered through a single optic fiber using dichroic mirrors to combine them into a single path. The optic cable is attached to the animal via a chronically implanted ferrule through which an optic fiber is implanted above the region of interest. A small and light cable allows easy and unimpeded behavior. Light is delivered, and emitted fluorescence measured, through a single fiber. The signal is recorded from either somata or axons as bulk fluorescence over time. Adapted with permission from*[152,153].

1.3.5 Axonal anterograde viral tracing

When characterizing brain circuits, it is important to not only measure or perturb their activity, but to also visualize their structural connectivity. To this end, scientist have developed recombinant adeno-associated viral vectors (AAV) used to deliver genetic material of interest into specific cell populations. AAV vectors are single-stranded DNA molecules derived from a defective human parvovirus. They are usually equipped with a fluorescent protein, such as GFP or eYFP, that allow their visualization in injected cells. One of their major benefits, compared to, for example, rabies viruses, is their safety, as they cannot replicate without a

helper virus. Additional benefits include low toxicity, as well as long-term and stable expression of the gene they carry[154,155]. AAV vectors can deliver genetic material in a promoter-dependent manner; the use of the CaMKII promoter will result in fluorophore expression in all excitatory neurons, whereas the use of a Cre-dependent AAV will result in the expression of the fluorophore only within very specific cell populations that contain Cre-recombinase. When an AAV virus infects the cells, it fills them fully, including the cell body, axon and axonal terminals, but does not jump the synapse, remaining contained to the infected cells[154,155]. Upon successful expression, the brains of the animals injected with the virus can be imaged and the number of cells and anterograde axonal projections expressing the virus quantified. In this study, AAV-CaMKII viruses were used to deliver optogenetic and calcium imaging tools in wild-type mice, and Cre-dependent AAV viruses were used to trace neuronal subpopulations and deliver calcium-imaging tools in transgenic, Cre driver mouse lines.

1.4 Aims of the study

While AIC is a highly complex region, human studies have convincingly demonstrated that one of its main roles is the detection of salient stimuli, used to inform appropriate switching between large-scale brain networks and guide flexible behavior. However, due to the aforementioned technical limitations of human imaging tools, causal involvement of the AIC in behavioral switching has not been proven. Furthermore, we lack understanding of specific neuronal subpopulations within the AIC that may contribute to salience detection and behavior switching. While in-so-far conducted rodent studies suggest that rodent IC possesses necessary functional attributes to encode stimulus salience and potentially govern flexible behavior, to date, no study has explored the role of rodent AIC in salience detection or behavior switching in freely moving mice.

Therefore, the first aim of my dissertation was to study **the role of AIC in flexible behavior and behavior switching in freely moving mice**. To this end, I designed a novel behavioral paradigm, called Multimaze, that allowed freely moving animals to switch between multiple behaviors at their own volition, and combined it with optogenetic perturbation to investigate the effect of AIC stimulation or inhibition on flexible behavior.

The second aim was to explore **the role of AIC in salience detection** and to further characterize its natural activity patterns during flexible behavior. Towards this goal, I employed fiber photometry to measure neuronal activity in excitatory neurons in the AIC, while the animals freely explored the Multimaze, or were exposed to an array of stimuli of different valence and saliency.

The third aim was to explore **AIC sub-circuitry that may play a role in behavioral switching and salience detection**. To this end, we performed AAV tracings in three transgenic mouse lines to characterize their brain-wide projection patterns. Using fiber photometry, I further examined the activity patterns of one of these subpopulations, to further characterize the properties of genetically-labelled neuronal subpopulations within the AIC.

2. MATERIALS AND METHODS

2.1 Animals

All animal experiments were carried out in accordance with the regulations imposed by the government of Upper Bavaria. Male C57BL/6NRj mice were obtained from the in-house breeding facility (Max-Planck-Institute of Neurobiology/Biochemistry). All experimental procedures were performed on 3-6 months old mice kept on an inversed 12h light-cycle (lights off at 10:00 AM). All mice were pair-housed and provided with *ad libitum* access to food (standard chow diet) and water.

2.2 Viral constructs

In vivo optogenetic experiments were conducted using the following viruses: inhibitory AAV9-CaMKIIa-eNpHR3.0-eYFP (2.4 x 10^{13} particles ml^{-1}, viral preparation #v66768), was obtained from Addgene. Excitatory rAAV5-CaMKIIa-hChR2-(H134R)-EYFP-WPRE-PA (6.2 x 10^{12} particles ml^{-1}) and control rAAV5-CaMKIIa-EYFP-WPRE-PA (4.3 × 10^{12} viral genomes (vg) ml^{-1}) were both obtained from the UNC Vector Core (Gene Therapy Center, University of North Carolina at Chapel Hill, USA). Fiber photometry experiments were conducted using pGP-AAV9-CaMKIIa-GCaMP7f (2.5 x 10^{13} vg ml^{-1}, viral preparation #v119052) for wild-type, and pGP-AAV-syn-FLEX-jGCaMP7f-WPRE (2.7 x 10^{13} vg ml^{-1}, viral preparation #v37577) for transgenic mouse lines, both coming from Addgene. Anterograde AAV tracings in transgenic mouse lines were conducted using AAV5-Efla-DIO-mCherry (7.3 x 10^{12} vg ml^{-1}), obtained from the UNC Vector Core (Gene Therapy Center, University of North Carolina at Chapel Hill, USA). All adeno-associated viruses purchased from the UNC Vector Core were obtained under an MTA agreement with the University of North Carolina.

2.3 Stereotactic surgeries

For peri-operative analgesia, the analgesic Metamizol (Hexal, 200mg/kg body weight, s.c.) was administered subcutaneously 30 minutes prior to the start of the surgery. To initiate anesthesia, the mouse was placed in a chamber flooded with 5% isoflurane in oxygen-enriched air. After the anesthesia was established (confirmed by testing for the loss of reflexes) the mouse was positioned in the stereotaxic frame (Stoelting) and placed on a heating pad to maintain its body temperature at 37°C. To protect the eyes, eye ointment (Bepanthen, Bayer), was applied. For viral injections, glass-pipettes (B100-50-10, Sutter Instruments) were pulled and attached to a microliter syringe (5 µL Model 75RN, Hamilton) using glass needle compression fittings (#55750-01, Hamilton). The syringe was inserted into the holder on a syringe pump (UMP3, WPI) fitted to the stereotaxic frame, controlled by a microcontroller (micro4, WPI). Before skull trepanations, lidocaine was topically administered at the drilling site. The following coordinates were used to target the AIC (all distances from Bregma): wild-type animals: AP: +1.9 mm, ML: ±2.7 mm, DV: -3.1 mm; transgenic GENSAT mice: AP: +1.7 mm, ML: ± 2.5 mm, DV: -3.4 mm. At the end of the surgery, Carprofen (Rimadyl, Pfizer, 5 mg/kg bodyweight) was administered intraperitoneally as post-operative pain care. The animals were closely monitored for a minimum of three days post-surgery. To ensure full recovery as well as adequate virus expression in the brain, the experiments started between three (fiber photometry) and four (optogenetics) weeks after the surgery.

Optogenetic experiments: two symmetric skull trepanations, one in each hemisphere, were made above the AIC using the above coordinates, until the skull was just penetrated. 130 nL of virus were injected at a rate of 80 nL/min into the AIC at DV: -3.1. Custom made optic fibers (200 µm core diameter, 0.22 NA, secured into 1.25 mm zirconia ferrules, Thorlabs) were tested before implantation for transmission (≥ 80%) of the input light. The fibers were disinfected in 80% alcohol, placed 0.4 mm above the injection site, and secured with acrylic glue (Ultra Gel, Pattex). To further secure the fibers and to prevent light emission from the skull, an additional layer of black dental cement (Super Bond C&B, Génerique International) was added on top of the superglue.

Fiber photometry experiments: a single skull trepanation was performed above the left AIC and 130 nL of the virus were injected at a rate of 80nL/min. Custom made optic fibers (200 µm

core diameter, 0.48 NA, secured into 1.25 mm zirconia ferrules, Thorlabs) were tested for transmission (≥ 80%) of the input light. As described above, the fiber was disinfected, lowered to 0.2 mm above the injection site and secured with acrylic glue (Ultra Gel, Pattex) and dental cement (Super Bond C&B, Génerique International).

Axonal AAV tracings in transgenic animals: a single skull trepanation was performed above the left AIC and 350 nL of the virus were injected at a rate of 80nL/min. The trepanation was sealed using bone wax and the skin sutured. After four weeks the animals were sacrificed.

2.4 Behavioral experiments

Prior to the start of any experiment, mice were handled by the experimenter for 5-10 minutes per day, for five days in a row. The animals were habituated to being tethered to the optic cables during the handling protocol. All experiments were performed during the dark phase of the light cycle between 10 AM and 7 PM.

2.4.1 Multimaze behavior box

To be able to assess the effect of AIC perturbation on flexible behavior, I designed a novel behavioral paradigm, called Multimaze (**Figure 6a**). The Multimaze behavior box was made from white Plexiglas that was sanded down to prevent light reflections from the walls and the floor. The box was 50 cm long, 30 cm wide with 30 cm tall outer walls. Three of the corners were turned into 10 cm x 15 cm large rectangular chambers, called behavior zones, with 4 cm wide entrances, surrounded by 10 cm tall inner walls. The fourth corner contained a social interaction zone, which consisted of a circular segment separated from the larger intermediate area by a 10 cm x 10 cm barred-fence. Given that the experiments could last up to one hour at a time, the box contained a water bottle holder with a spout reaching into the interior of the behavior box. Furthermore, each of the small rectangular chambers could be blocked off by a custom-made entrance cover, to allow for further modification of the paradigm.

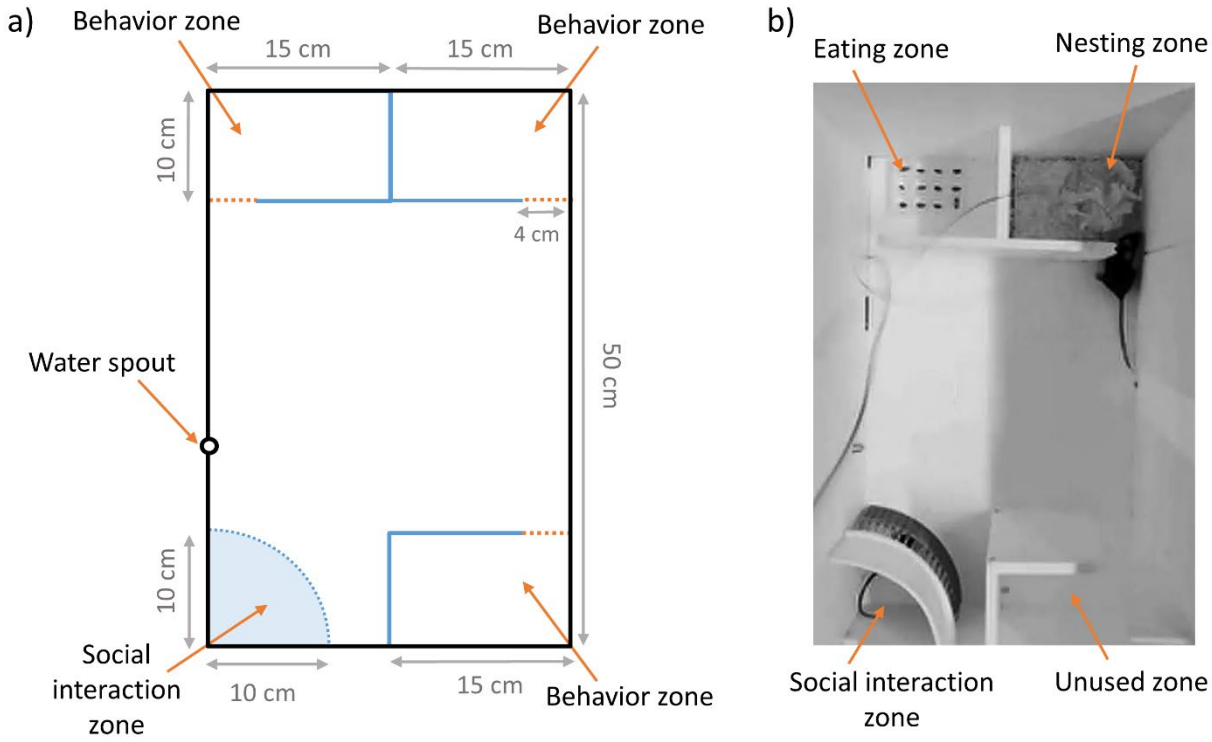

Figure 6: Multimaze behavior box. a) *A schematic of the Multimaze behavior box. Three of the four corners contained 10 cm x 15 cm x 10 cm large rectangular chambers that could be equipped with the contents of an experimenter's choice. Each of the zones contained a 4 cm wide entry that could be, if desired, closed off, thus modifying the number of used zones. One of the corners contained a 10 cm x 10 cm circular sector surrounded by a 10 cm tall barred fence. The box also contained a water bottle to ensure the animals would not go thirsty over longer experimental sessions.* ***b)*** *A picture of the experimental setup used in this study. Two of the three rectangular chambers were used as eating and nesting zones and social interaction zone contained an adult male conspecific. The third behavior zone was closed off and could not be visited by the experimental animals.*

For experiments described in this work, the following behaviors were characterized (**Figure 6b**):

1. Nesting: a small piece of artificial white grass was cut to size and placed on the floor of one of the small rectangular chambers. In addition, nesting material of the same type as the mice would normally receive in the home cage was available.

2. Eating: one 24-well tissue culture plate (VWR) was cut into symmetric halves using a laser cutter. One half containing 12 wells (each 1.7 cm x 1.7 cm x 1.7 cm), was glued to the bottom of another rectangular corner chamber. A single unshelled sunflower seed was placed in each of the wells. To initiate feeding, animals had to reach inside the well to retrieve the seed and shell it before consumption. Two days before the start of the experiments, mice were given sunflower seeds in their home cage to become accustomed to them.

3. Social interaction: Social interaction took place in the semi-circular zone. Before the start of the experiment, an adult (4 months old) male conspecific was placed in a semi-circular enclosure, which was covered with a custom-built Plexiglas cover. The barred-fence enclosing the zone assured that while the mice were unable to physically interact (apart from very brief touching), visual, auditory and olfactory stimuli could travel unobstructed. Each day, a different male conspecific was introduced to a particular experimental animal to prevent loss of interest.

On top of the above behaviors, the Multimaze also allowed me to measure other voluntary behaviors, such as grooming, as well as the number of transitions between the zones, acting as a proxy for behavioral switching, and locomotion.

2.4.2 Behavior with optogenetic manipulation

Before the start of experiment, the implants on the animals' head were connected to a yellow (593.5 nm wavelength) or blue (473 nm wavelength) laser source via fiber-optic patch cables and a rotary joint (0.22 NA, Doric Lenses, Canada), allowing the animal to move freely in the Multimaze. The laser intensity at the tip of the patch cables was set to 3-5 mW for the blue and 10-12 mW for the yellow laser. The lasers were synchronized to, and triggered by, ANYmaze software (Stoelting) via TTL pulses. The animals were placed in the Multimaze behavior box for five consecutive days, 1 hour per day. Each experiment was divided into four 15-minute segments. During the first and third 15-minute segments, the laser light was switched off. During the second and fourth 15-minute segments, the light was switched on to stimulate or inhibit the AIC. For AIC excitation, blue light was delivered in 1 s on, 4 s off cycle, at 10 Hz frequency and with each pulse delivered at 10% duty cycle. For AIC inhibition, light was delivered continuously for the duration of the 15-minute segment. Videos were collected using webcams (Logitech) and animal tracking was performed using DeepLabCut[156] (optogenetic stimulation experiment) or ANYmaze (optogenetic inhibition experiment).

2.4.3 Data extraction and behavioral analysis

Optogenetic stimulation cohort: raw videos were collected and processed using a custom-written Python script through the Scientific Computing Cluster (SCC) of the Gesellschaft für wissenschaftliche Datenverarbeitung mbH Göttingen (GWDG), shared corporate facility of Georg-August-Universität Göttingen and the Max Planck Society. Raw videos were trimmed, masked and cropped. Following pre-processing, a subset of video frames (1290 frames from four videos) were labelled with 13 mouse body parts (snout, ears, sides, back, paws, tail base, tail mid and tail tip) in DeepLabCut. The network was trained on a subset of this data, corrected and iterated until the improvements were no longer measurable. The final average error of the network was 7.59 px with a p-cutoff value of 0.85. To acquire behaviorally meaningful data, I manually drew behavioral zones on the video to determine the coordinates and thus acquire the data about where the mouse was present at any given moment. For the final analysis, the center point of the mouse's body was used. The data were pre-processed and analyzed using custom-written scripts in Python and R.
Optogenetic inhibition cohort: all videos were collected and tracked with ANYmaze. Datasheets for individual animals were exported and pre-processed in R, using a custom-written script. Pre-processed data were analyzed in plotted using custom-written scripts in R.

2.5 Fiber photometry recordings

2.5.1 Photometric signal acquisition

Fiber photometry recordings measure bulk fluorescence through a single optical fiber that simultaneously delivers excitatory light and collects emitted fluorescence. In my experiments, I measured bulk fluorescence from neurons expressing GCaMP7f using a commercial fiber photometry system (one side, two colors, Doric Lenses) with two excitation wavelengths: 405 nm (isosbestic point for GCaMP fluorescence signal, measuring background fluorescence) and 465 nm (GCaMP signal). Before the start of the experiment, excitation light intensity was measured at the end of the patch cords (~20 µW for 564 nm and ~7 µW for 405 nm wavelength). A mouse was tethered to the low-autofluorescence fiber-optic patch cables (0.48 NA) (Doric

Lenses, Canada). The fiber photometry system was synchronized to the ANYmaze software using TTL pulses. GCaMP signal was recorded at 12 kHz, demodulated, and downsampled to 30 Hz.

2.5.2 Behavior with fiber photometry

Wild-type animals: The experiments were performed in Multimaze in two cohorts, the first containing five and the second containing four mice. The experiments were conducted in four sessions: the first three sessions were conducted in the first cohort and the fourth session in the second cohort. The first three sessions were performed on three consecutive days. Each day, the fluorescence signal was first recorded in the home cage for 5 minutes, to let the signal stabilize and to establish a baseline measurement. On the first two days, the animals were then immediately transferred into the Multimaze for 30 minutes with the arena being arranged in the same way as described in section 2.4.1. On day 3, after the initial 5-minute stabilization period, the animals were placed in a fear conditioning box (Ugo Basile, Italy) and administered six electric foot shocks of 0.4 mA strength and 1 second duration spread across a 6-minute window. The inter-shock-interval ranged between 30-90 seconds. Afterwards, the mice were transferred to the Multimaze and allowed to explore freely for an additional 30 minutes. In the fourth session, conducted in a separate cohort, food was removed from all cages with experimental animals for 24 hours preceding the experiment. The following day, the same protocol was used as for sessions 1 and 2. Videos were collected using webcams (Logitech) and animal behavior was manually scored. Social interaction was labeled when physical, nose-to-nose interaction between the mice, as well as close proximity, with the experimental mouse being directly turned towards the social interaction partner, was present. Eating was labeled from the moment a seed was carried to the mouse's mouth, until the eating episode was finished. Grooming was labelled for the duration of the grooming episode, with only the episodes lasting at least 3 seconds included in the analysis. For foot shocks, the 3 seconds following the shock delivery were analyzed. For tail suspension, the entire episode, lasting from the moment the mouse was picked off the ground to the time it was placed on the ground, was labeled.

Transgenic animals: For the results shown for fiber photometry in the GENSAT animals two cohorts of three mice were used. The first cohort underwent the same experiment as described

in the section above, with a 5-minute habituation period followed by a 30-minute recording in the Multimaze. The arena was set in the same way as described in section 2.4.1. The second cohort, also comprising of three animals, was performed in a custom-made circular open field made of transparent Plexiglas, with a 30 cm diameter. There, the mice first underwent a 5-minute habituation period, followed by a sequence of six 1 second long air puffs delivered in 60-second intervals. All videos were collected using webcams (Logitech) and animal behavior was manually scored. Eating, grooming and social interaction were labelled the same was as described above. For air puffs, the 3 seconds following the air puff delivery were analyzed.

2.5.3 Photometric signal analysis

All fiber photometry data was analyzed using custom-written Python scripts. The first 30 seconds of the signal were excluded and the data were smoothed using a second-order Savitzky-Golay filter. To reduce bleaching and motion artefacts, a least-squares linear fit was used on the 405 nm signal which was then aligned to the 465 nm signal using a procedure developed by Lerner et al. (https://github.com/talialerner/Photometry-Analysis-Shared/blob/master/Dropbox/MATLAB/Shared%20photometry%20code/controlFit.m). The change in fluorescence (ΔF/F) was calculated as ΔF/F = (465-nm signal - fitted 405-nm signal)/fitted 405-nm signal. The signal was further Z-scored using the median of the overall signal trace. To calculate the average response for any specific behavior, the signal was normalized by subtracting the median of the 3 seconds preceding behavior onset and the mean and SEM calculated.

2.6 AAV tracings in transgenic animals

For AAV tracings in GENSAT animals, the surgery was performed in the same way as described in section 2.3. Coronal sections of axonal AAV tracings were acquired on a Leica SP5 confocal microscope and stitched and visually adjusted using Fiji software. The images of coronal sections were visually examined for projection patterns and compared to Franklin & Paxinos mouse brain atlas (4^{th} edition). Detailed cell counting and quantification were not performed.

2.7 Histology

At the end of experimental protocol, animals were anesthetized with a mixture of Ketamine and Xylazine (100 mg/kg and 20 mg/kg bodyweight, respectively, Serumwerk Bernburg) and trans-cardially perfused with 4% paraformaldehyde (PFA) in phosphate buffered saline (PBS). Brains were fixed in PFA for another 24-48 hours at 4°C. Coronal sections were cut at 70 µm with a VT1000S vibratome (Leica Biosystems). To visualize fiber implantations, as well as the whole spread of the virus, all sections between +2.5 mm and +1.0 mm from Bregma were collected and mounted onto glass slides using custom-made mounting medium containing Mowiol 4-88 (Roth, Germany) with 0.2 mg/mL DAPI (Sigma-Aldrich, MO). Sections were visualized under an epifluorescence microscope (Leica DFC7000 T). The spread of the virus and fiber placement were confirmed using the Franklin & Paxinos mouse brain atlas (4^{th} edition). Only animals with correct viral injection as well as fiber placement sites were included in the analysis and are reported in this study.

2.8 Statistical analysis

All statistical analyses were performed with GraphPad Prism (GraphPad Software, version 9) or custom-written R code. Group comparisons were done using standard two-way ANOVA, repeated-measures two-way ANOVA or mixed-effects analysis followed by post-hoc multiple t-tests with Bonferroni correction. Single variable comparisons were done using two-tailed paired or unpaired t-tests. The identity of the test used in particular analyses is specified in individual figure legends. Sample sizes were determined using power analysis tests. All mice with poor fiber placement or implant loss during any stage of experiments were excluded from the study. During optogenetic experiments, littermates were randomly assigned to the experimental or control groups. Data collection and analysis were not performed with blinding to the conditions.

3. RESULTS

3.1 Establishment of a novel behavioral paradigm

The initial step of the project was the establishment of a behavioral paradigm that would allow me to explore the role of rodent AIC in behavioral switching during flexible behavior. To this end, we designed a novel paradigm, called Multimaze, that allowed observation of behavioral switching which occurs spontaneously in freely behaving animals. The paradigm consisted of a 30 cm x 50 cm rectangular box made of white Plexiglas, that contained three small rectangular chambers and one semi-circular enclosure (**Figure 7a**). Each of the three small chambers could be equipped with the contents of the experimenter's choice, thus allowing an introduction of multiple versatile behaviors. The semi-circular enclosure was designed to house a conspecific (see Methods section for details). Each of the three corner chambers could be closed off with a designated gate, making the arena easily modifiable.

As mentioned previously, the AIC has been shown to act as a switch between large-scale brain networks, specifically the DMN and CEN. While probing such function is challenging without whole-brain imaging techniques, I attempted to approach that by introducing behaviors that would act as a proxy for the functions of the relevant networks. In one of the zones, I placed a dish with twelve small circular wells (1.7 cm x 1.7 cm x 1.7 cm), each of which contained a single unshelled sunflower seed. To procure a seed, the animals had to reach into a small well, grab the seed, bring it to the surface and shell it before consumption could be initiated. This is a non-trivial task in which animals often accidentally drop the seed and have to repeat the action. Since this required focus and outwardly directed attention, seed eating served as a proxy for CEN engagement. In another chamber, I placed ground cover and fresh nesting material, the same type as used in the animals' home cage. This zone aimed to represent a safe environment in which a mouse could rest and relax, thus acting as a proxy for DMN activity. Finally, I chose to introduce social behavior, as it has previously been reported engage the AIC and represent a salient stimulus in rats[102].

To quantify the behavioral patterns, I measured time the animals spent in the specific zones. Measurements were collected for the following four zones: eating zone, social interaction zone, nesting zone and interzone, which acted as a transition zone between the first three zones (**Figure 7a**). When placed in the Multimaze, the animals were allowed to freely explore the novel environment, transitioning between the zones at their own volition. Mice voluntarily engaged with each of the respective behaviors (**Figure 7d**), confirming that Multimaze can be used as a paradigm to examine flexible behavioral switching in freely moving mice.

3.2 Optogenetics during flexible behavior

3.2.1 Optogenetic stimulation of the AIC

To examine whether the AIC plays a role in behavioral switching, I first chose to employ optogenetic stimulation of the AIC. To achieve this, excitatory pyramidal neurons in the AIC were bilaterally infected with an AAV coding for Channelrhodopsin under the CaMKII promoter (AAV2/5-CaMKIIa-ChR2.0), and an optic fiber was implanted above the injection site (**Figure 7b**). As a control condition, the littermates of the experimental mice were injected and implanted in the same way, with the only difference being that the AVV only encoded a fluorophore rather than an excitatory opsin (AAV2/5-CaMKIIa-eYFP). The animals were placed into the Multimaze for 60 minutes per day, five days in a row, and optogenetic stimulation was delivered during the second (Q2) and fourth (Q4) 15-minute segment of the experiment on all experimental days (**Figure 7c**) to allow the comparison of behavior during, and outside of, AIC stimulation. The light was delivered at 10 Hz in a 1 second on, 4 seconds off cycle. This specific protocol was used to avoid overstimulation, which can, based on previous experience gathered in the lab, impair movement and sometimes even result in seizures.

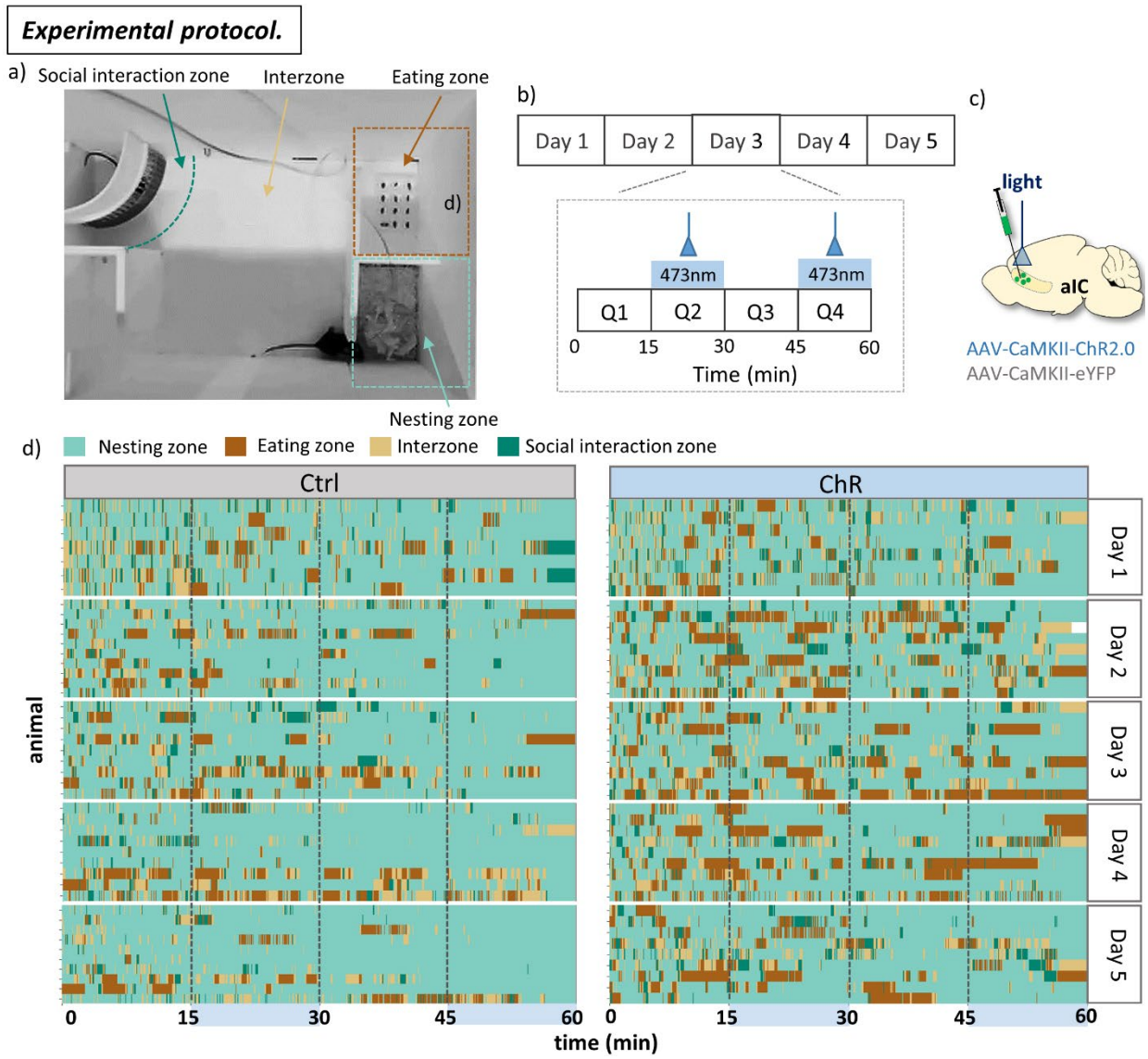

Figure 7. Multimaze behavioral paradigm and the experimental protocol. a) *Top-down picture of the Multimaze behavioral paradigm designed to assess flexible behavior in freely moving mice. The boundaries of the three zones are marked in their respective colors: Social interaction zone (dark green), Eating zone (brown) and Nesting zone (teal). Interzone is marked with a yellow arrow.* ***b)*** *Experimental protocol used in the optogenetic experiment. Animals were placed into the Multimaze for 60 minutes per day, for 5 days in a row. Optogenetic stimulation was delivered during the second (Q2) and fourth (Q4) 15-minute interval.* ***c)*** *Virus injection and optic fiber placement above the AIC.* ***d)*** *Representative raster plots of the two experimental groups, showing the time each individual animal spent in each of the zones during a 60-minute experimental session on each day. Each row represents a single animal on a given day.*

Since AIC has been shown to act as a switch between large-scale brain networks, the alteration of which may affect the frequency of behavior switching, I first decided to explore whether the perturbation of its activity affected the number of times the animals transitioned between the zones, which acted as a proxy for altered behavior switching. A high number of transitions is

associated with increased exploratory drive, which is normally observed when animals are placed into novel environments. As such, I hypothesized that AIC stimulation would predominantly exert its effect at later time points both within and across days, as animals became habituated to the environment, leading to lower novelty and lower salience, and thus fewer transitions.

To observe the change in the number of transitions across days, data was normalized to day 1 to compensate for the baseline difference between the groups. My analysis showed that AIC stimulation led to a significant difference in the number of transitions between the two groups (**Figure 8b**), while this effect was not observed in the absence of AIC stimulation (**Figure 8a**). Since increased transitioning between the zones could occur due to stimulation-induced increase in locomotion, I next compared locomotor activity across days. Similar to the number of transitions, optogenetic stimulation resulted in a significant difference in locomotion between the two groups which was not observed during Laser OFF periods(**Figure 8c,d**). To test whether AIC stimulation caused a generalized increase in locomotion, possibly through driving excessive motor activity, I performed an additional open field experiment in a separate cohort of optogenetic animals. This experiment revealed no difference in the overall locomotion (**Figure 8e,f**), suggesting that AIC stimulation does not drive excess motor activity. Rather, these data suggest that AIC stimulation leads to a reduced decrease in exploratory drive, possibly through a prevention of salience decrease that normally accompanies habituation to novel environments.

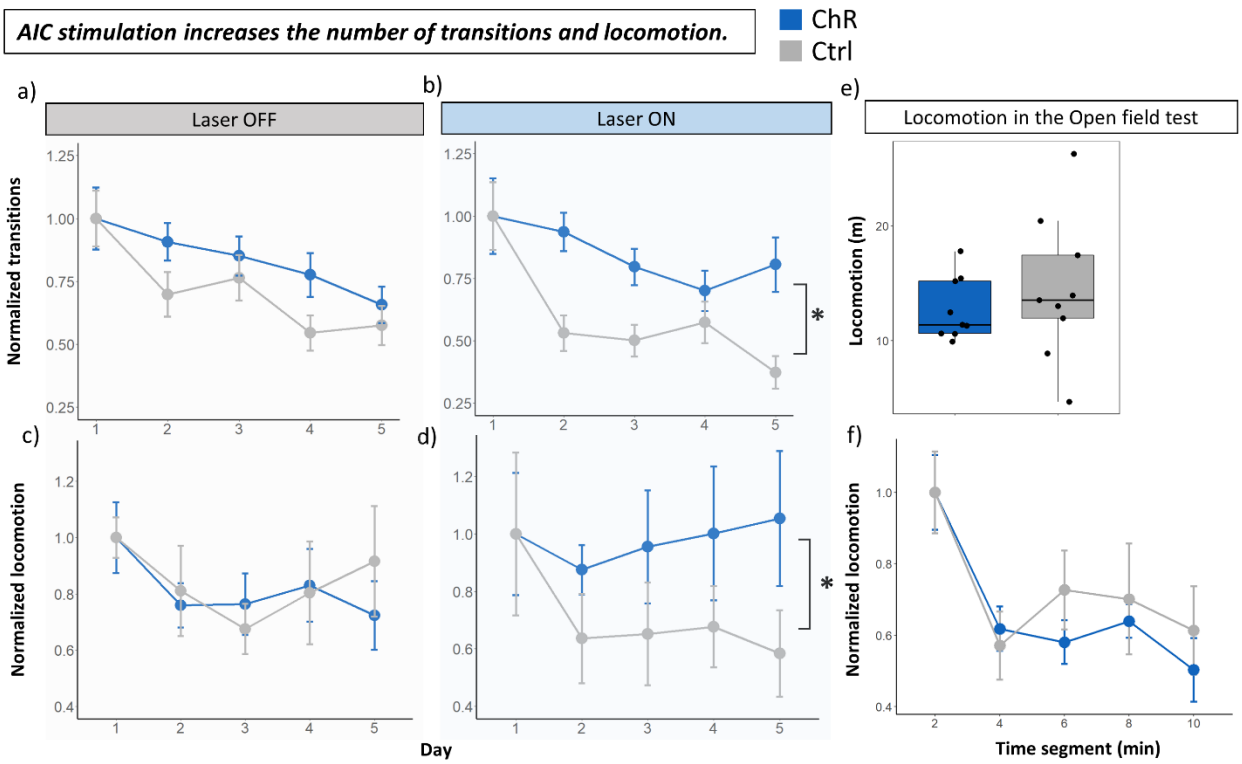

Figure 8: AIC stimulation prevents a time-dependent decrease in the number of transitions and locomotion. *(N = 8 ChR2.0, N = 10 eYFP, Mixed-effects analysis of number of transitions and locomotion).* ***a)*** *Number of transitions for Laser OFF segments. Group (opsin) effect: F(1, 16) = 2.404, p = 0.141; day effect: F(2.5, 35.83) = 4.177, p* = 0.0168; Group x day effect: F(3, 43) = 0.7, p = 0.557.* ***b)*** *Number of transitions for Laser ON segments. Group (opsin) effect: F(1, 16) = 8.119,* ***p* = 0.0116****; day effect: F(1.338, 34.22) = 0.91, p = 0.427; Group x day effect: F(3, 43) = 0.562, p = 0.643* ***c)*** *Change in locomotion across days for Laser OFF segments. Group (opsin) effect: F(1, 16) = 0.106, p = 0.750; day effect: F(2.754, 36.72) = 0.236, p = 0.855; Group x day effect: F(3, 40) = 0.434, p = 0.730* ***d)*** *Change in locomotion across days for Laser ON segments. Group (opsin) effect: F(1, 16) = 4.743,* ***p* = 0.0447****; day effect: F(2.618, 36.65) = 0.175, p = 0.891; Group x day effect: F(3, 42) = 0.182, p = 0.908.* ***e-f)*** *AIC stimulation has no effect on overall locomotion in an open field test (N = 9 ChR2.0, N = 9 eYFP).* ***e)*** *AIC had no effect on cumulative locomotion over 10 minutes (two-tailed non-paired t-test: t=0.7510, df=16, p = 0.464).* ***f)*** *AIC stimulation had no effect on locomotion when segmented into 2-minute bins (two-way RM ANOVA of locomotion). Group (opsin) effect F(1, 16) = 0.677, p = 0.423; Time effect: F(3.153, 50.45) = 13.84, p**** < 0.0001; Group x time effect: F(4 ,64) = 0.658, p = 0.623.*

Having observed the effect of optogenetic stimulation on the number of transitions across days, I next addressed whether the difference could be observed in an acute, within-experiment, manner. While novelty, and thus salience, decreases over days, it also decreases within a 60-minute-long experimental session. As such, AIC stimulation should have a stronger effect on the number of transitions during the later time-points of each experimental session, compared to the earlier ones. To test this hypothesis, I compared the cumulative number of transitions during the first (Q1) and the last (Q4) 15-minute segments of the experiment. Indeed, ChR

animals showed a significantly higher number of transitions in Q4 compared to controls, yet no such difference was observed in Q1 (**Figure 9a**). Interestingly, no difference in the number of transitions was observed on day 1 (**Supplementary Figure 1**). This could be due to the fact, that salience is at its maximum during the initial stages of the experiment and AIC stimulation cannot increase it any further. Alternatively, it is possible that AIC stimulation at the intensity and frequency used in this protocol needs to be delivered across a longer time window before its effect can be measured. When the number of transitions was examined within individual zones, analysis revealed that the main difference in the number of transitions occurred in the interzone and the social interaction zone (**Figure 9b**). It should be noted that while not significant, there was also a trend towards a higher number of entries of ChR animals into the eating zone. However, no difference was observed in the nesting zone. Overall, these data revealed that AIC stimulation prevents a decrease in the number of transitions between the zones, which is accompanied by a significantly smaller decrease in locomotion across days. Furthermore, such effect can also be observed in a within-experiment manner, revealing that AIC stimulation results in a significantly higher number of zone transitions in the last, but not the first, 15-minute segment of the experiment. Overall, the above data support the hypothesis that AIC stimulation may prevent habituation-induced salience decrease, which consequently leads to an increase in behavior switching.

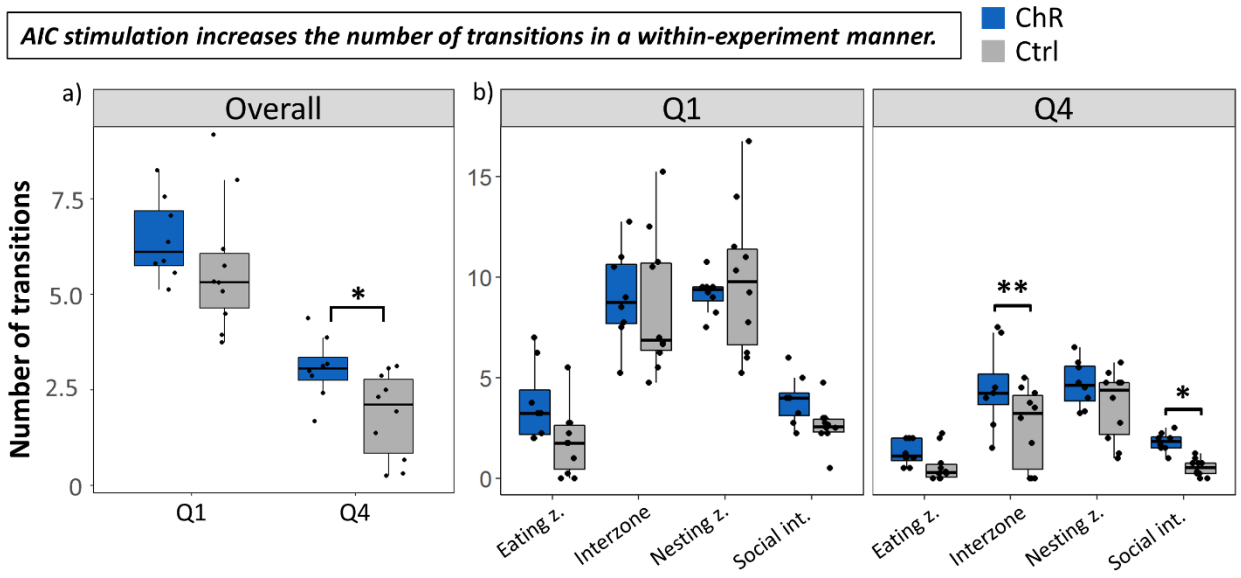

Figure 9: AIC stimulation increases the number of zone transitions within the experiment. *(N = 8 ChR2.0, N = 10 eYFP).* ***a)*** *Two-tailed unpaired t-test revealed that AIC stimulation results in a significantly higher number of transitions in the last 15-min segment of the experiment (t = 2.67, df = 15.9,* ***p* = 0.0168****).* ***b)*** *Number of transitions is significantly*

increased in interzone and social interaction zone during the last 15-min segment of the experiment. Two-way ANOVA of a number of transitions. ***Q1:*** *Group (opsin) effect: F(1, 64) = 1.846, p = 0.179; zone effect: F(3, 64) = 41.693, p < 0.0001; group x zone effect: F(3, 64) = 1.020, p = 0.39.* ***Q4:*** *Group (opsin) effect: F(1, 64) = 15.072,* ***p*** = 0.000248****; *zone effect: F(3, 64) = 26.646, p < 0.0001; group x zone effect: F(3, 64) = 0.696, p = 0.558. Bonferroni post-hoc test: Interzone:* ***p** = 0.00351****; *Social interaction zone:* ***p* = 0.0488****.*

I next examined whether AIC stimulation would also affect the relative amount of time the animals spent in individual zones. If the AIC truly contributes to appropriate switching between brain networks that contribute to internally or externally focused behaviors, its perturbation may result in animals preferentially engaging with more externally focused (eating, social interaction) or internally focused (resting, nesting) behaviors. To explore this, I first chose to examine time spent in the zones across and within days, as this is where I could already observe the effects of AIC stimulation on transitions and locomotion. Across days, optogenetic stimulation significantly increased the amount of time ChR animals spent in the eating zone, and significantly decreased the amount of time they spent in the nesting zone. A small but statistically significant difference was also observed in the social interaction zone, showing that optogenetic stimulation increased the amount of time the animals spent there (**Figure 10a,b**). While a statistically significant effect was already observed when all four experimental segments (Q1 to Q4) were pooled, additional analysis revealed that AIC stimulation effect was confined exclusively to Laser ON (Q2 + Q4) periods (**Supplementary Figure 2**). Interestingly, similar to the number of transitions, no significant effect was observed on day 1, with the stimulation effect only starting from day 2 onwards (**Figure 10a,b**). Furthermore, it is interesting to observe that the effect of the stimulation did not continue to increase continuously across the subsequent days; rather, it peaked on day 2 for both eating and social interaction zones, remaining relatively stable thereafter (**Figure 10a,b**). As mentioned before, it is possible that salience is so high on day 1 that AIC stimulation cannot lead to a further increase. However, in this case, given that salience is linked to novelty, and novelty is expected to decrease across a 60-minute experimental session, one would expect to observe a difference between the two groups during Q4 on the first experimental day, which was not found (**Supplementary Figure 3**). As such, two other possible explanations should be considered. The first is that AIC stimulation must be delivered across a long enough time window to induce downstream changes in plasticity of either the AIC, its downstream structures, or both. This consequently results in a baseline activity increase of the affected structures, leading to a persistent behavioral effect that is, thereafter, insensitive to further AIC stimulation. In this

case, from day 2 onwards, I would expect to measure a stable behavioral effect within a single experimental session with little difference in behavior between early and late time points (Q1 vs. Q4). Conversely, it is possible that while stimulation needs to be delivered across a long enough time window to sensitize the downstream structures which are, thereafter, more receptive to AIC stimulation, it does not result in baseline activity increase. In this case, one would expect, that the stimulation effect wears off during the night, is not observed during Q1 on the following day when stimulation is absent, and is then reinstated with consequent stimulation during Q2 the following day.

To explore this, I compared time in the zones for the first (Q1) and last (Q4) 15-minute segments of the experiments. Given that no effect was observed on day 1, I chose to average the behavioral data across days 2-5. In Q1, a significant difference between the groups was observed in the nesting zone (**Figure 10c**), but not in any other zone. Comparatively, in Q4, a significant difference was observed for both eating and nesting zones, with the nesting zone difference being much larger compared to Q1 (**Figure 10c**). It is important to notice that while not significant, there is a trend towards ChR animals spending more time in the eating zone already in Q1. This suggests that there are two components to the time-dependent effect of the AIC stimulation: after stimulation is delivered over a long-enough time window for its effect to be measured, it seems to change the baseline activity of the relevant structures, as its behavioral effect is already observed during Q1 on the following day, when stimulation is not yet present. However, once additional stimulation is introduced in Q2, there is a significant increase in the observed effect, suggesting that acute stimulation further augments the pre-existing behavioral effect (**Figure 10c**). It is interesting to note that there is no increase in behavioral difference between subsequent Q1 sessions when plotted across subsequent days (**Supplementary Figure 3**), suggesting that the AIC stimulation effect returns to a pre-existing, albeit already augmented, baseline between the end of one and beginning of the next experimental session.

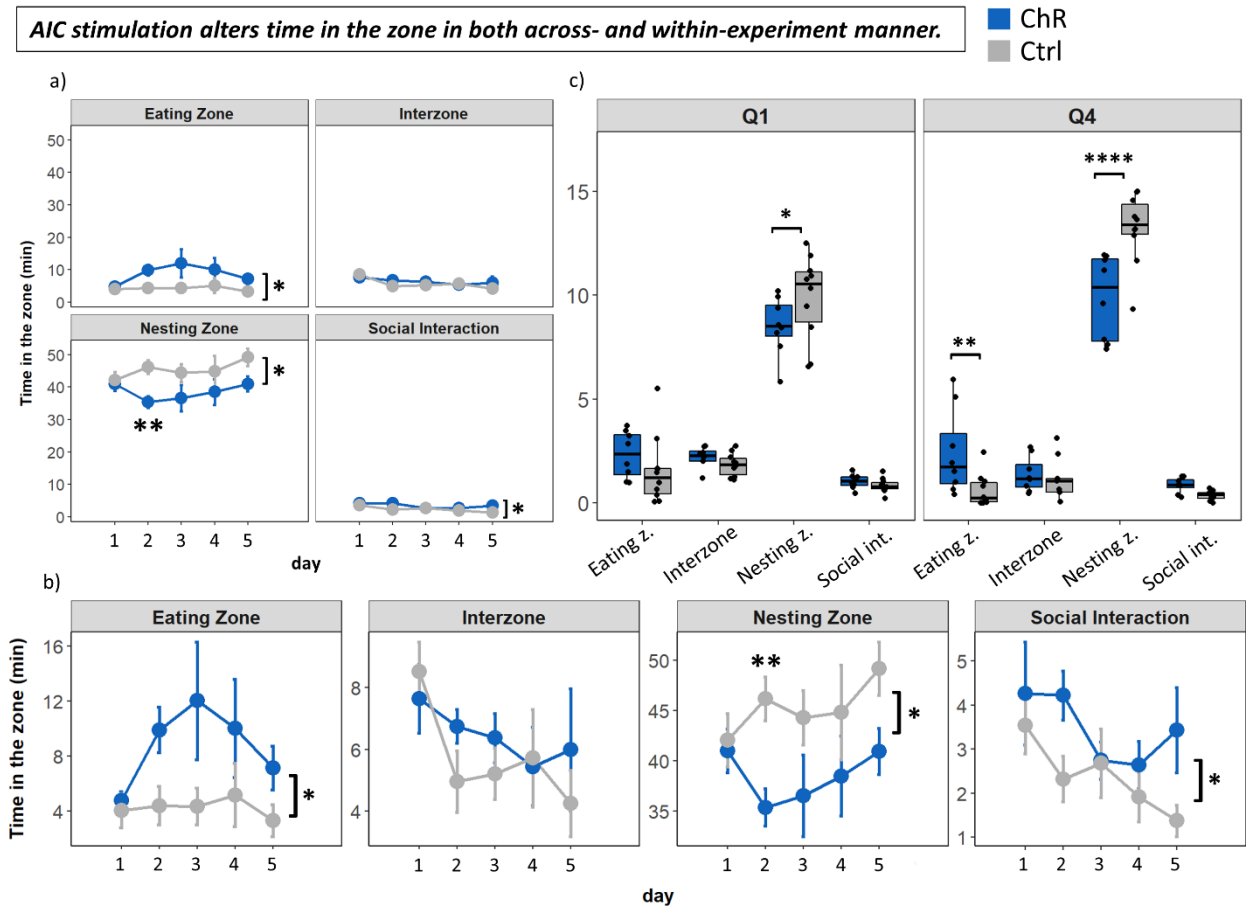

Figure 10: Optogenetic stimulation shows a time-dependent effect both across and within days. a) *Observing the development of the AIC stimulation effect across days reveals that optogenetic stimulation significantly increases the amount of time animals spend in the eating and social interaction zones, and decreases the amount of time they spend in the nesting zone (N = 8 ChR2.0, N = 10 eYFP, Mixed-effects analysis of time spent in the zone).* ***Eating zone:*** *Group (opsin) effect: F(1, 16) = 6.400,* ***p* = 0.02;*** *day effect: F(2.295, 32.89) = 0.613, p = 0.569; group x day interaction effect: F(3, 43) = 0.282, p = 0.838.* ***Interzone:*** *Group (opsin) effect: F(1, 16) = 6.400, p = 0.347; day effect: F(2.442, 34.19) = 0.935, p = 0.419; group x day interaction effect: F(3, 42) = 0.376, p = 0.77.* ***Nesting zone:*** *Group (opsin) effect: F(1, 16) = 7.522,* ***p* = 0.0145****; day effect: F(2.325, 33.33) = 1.09, p = 0.356; group x day interaction effect: F(3, 43) = 0.189, p = 0.903. Bonferroni post-hoc test; day 2****: p** = 0.0064****, Social interaction zone:*** *Group (opsin) effect: F(1, 16) = 4.789,* ***p* = 0.0438****; day effect: F(2.753, 39.46) = 1.518, p = 0.227; group x day interaction effect: F(3, 43) = 1.569, p = 0.2108.* ***b)*** *The same as in a) but on a free axis for easier visualization.* ***c)*** *Stimulation effect shows a cumulative effect within days. (N = 8 ChR2.0, N = 10 eYFP, Two-way ANOVA of time spent in the zone).* ***Q1:*** *Group (opsin) effect: F(1, 64) = 0.000216, p = 0.988; zone effect: F(3, 64) = 179.48, p**** < 0.0001; group x zone interaction effect: F(3, 64) = 2.729, p = 0.051.* ***p* = 0.0192*** *for Nesting zone.* ***Q4:*** *Group (opsin) effect: F(1, 62) = 0.0379, p = 0.541; zone effect: F(3, 62) = 285.13, p**** < 0.0001; group x zone interaction effect: F(3, 62) = 12.600,* ***p**** < 0.0001****. Bonferroni post-hoc test ChR vs control:* ***p** = 0.0049*** *for Eating zone,* ***p**** < 0.0001*** *for Nesting zone.*

Having observed both across- and within-day effect of the AIC stimulation, I finally wanted to examine whether the overall effect of AIC stimulation on time spent in the zone could be observed. To this end, I pooled the data collected on days 2-5 and plotted them separated by the presence or absence of optogenetic stimulation (**Figure 11a**), as well as cumulatively (**Figure 11b**). The comparison of the average time in the zone during AIC stimulation periods (Laser ON: Q2 + Q4) and light off periods (Laser OFF: Q1 + Q3) revealed that a much greater effect – increased time in the eating zone and decreased time in the nesting zone – was observed during Laser ON periods. In line with the effect represented in **Figure 10**, however, a significant nesting zone effect was still observed in the absence of stimulation (**Figure 11a**). It is also important to note that while the effect in the eating zone was not significant, a trend towards ChR animals spending more time there remained ($p = 0.075$, **Figure 11a**). This confirms that stimulation effect is carried over into the periods where AIC stimulation is absent, further confirming that the effect of AIC stimulation is not solely limited to stimulation-ON periods. The overall comparison of the time spent in the zones between days 2-5 (**Figure 11b**) thus succinctly summarizes the main effect of the optogenetic treatment: AIC stimulation significantly increased the amount of time the animals spent in the eating zone and significantly decreased the amount of time the animals spent in the nesting zone. When observed across days, AIC stimulation also increased time in social interaction zone (**Figure 10a,b, Supplementary Figure 2**). Furthermore, the above analysis reveals that stimulation effect occurs over time, and is only measurable from day 2 onwards (**Figure 10a,b**). Thereafter, a relatively small stimulation effect can already be measured during the stimulation-free Q1 period on each subsequent experimental day. However, additional optogenetic treatment significantly reinforces the already existing effect (**Figure 10c**).

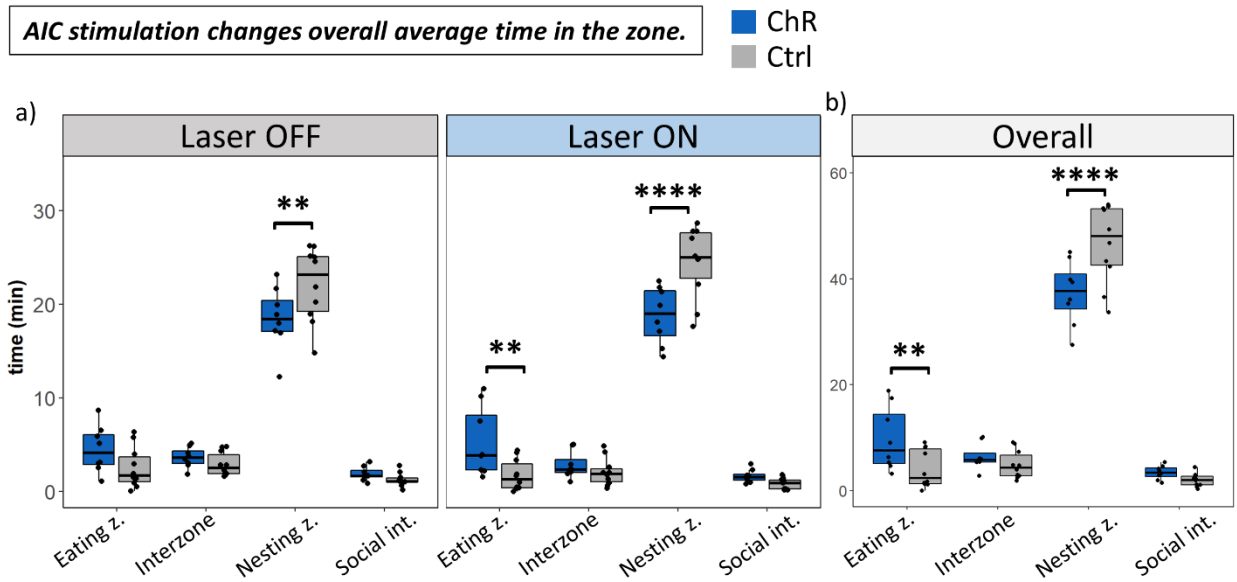

Figure 11: Optogenetic stimulation alters the amount of time animals spend in the zones in a non-acute manner. a) *AIC stimulation causes the animals to spend more time in the Eating zone and less time in the Nesting zone (N = 8 ChR2.0, N = 10 eYFP, two-way ANOVA of time spent in the zone.* ***Laser OFF (Q1 + Q3):*** *Group (opsin) effect: F(1, 64) = 0.014, p = 0.907; zone effect: F(3, 64) = 262.05, p**** < 0.0001; group x zone interaction effect: F(3, 64) = 5.015, p** < 0.003. Bonferroni post-hoc test ChR vs control:* ***p** = 0.001*** *for Nesting zone.* ***Laser ON (Q2 + Q4):*** *Group (opsin) effect: F(1, 64) = 0.059, p = 0.907; zone effect: F(3, 64) = 296.08, p**** < 0.0001; group x zone interaction effect: F(3, 64) = 12.16,* ***p**** < 0.0001****. Bonferroni post-hoc test ChR vs control:* ***p** = 0.00239*** *for Eating zone,* ***p**** < 0.0001*** *for Nesting zone.* ***b)*** *Overall average time spent in the zone between days 2-5. Group (opsin) effect: F(1, 64) = 0.027, p = 0.869; zone effect: F(3, 64) = 311.06, p* < 0.0001; group x zone interaction effect: F(3, 64) = 9.27,* ***p**** < 0.0001****. Bonferroni post-hoc test ChR vs control:* ***p** = 0.00913*** *for Eating zone,* ***p**** = 0.000038*** *for Nesting zone.*

Overall, the above data show that AIC stimulation prevents a reduction in the number of transitions and locomotion, suggesting it may prevent habituation-driven salience decrease. Furthermore, the data show that AIC greatly increases time spent in the eating zone, and marginally increases the amount of time the animals spend in social interaction zone, both of which acted as proxy for the CEN. In addition, AIC stimulation decreases the amount of time in the nesting zone, a proxy for the DMN. My data thus support the hypothesis that AIC stimulation shifts the balance between internally and externally focused behaviors, increasing the amount of time the animals spend engaged with externally focused at the expense of internally focused behaviors. This in turn, indirectly suggests that AIC stimulation may indeed disrupt the natural balance in switching between large-scale brain networks.

3.2.2 Optogenetic inhibition of the AIC

Our initial experiment suggests that AIC stimulations alters behavioral switching and perturbs flexible mouse behavior. However, as ChR-driven AIC stimulation is non-physiological, this does not yet confirm that AIC activity is necessary for normal behavioral switching per se. As such, I decided to inhibit AIC activity to examine its necessity for behavioral switching. To this end, I prepared another cohort where I transfected excitatory pyramidal neurons of the AIC with an AAV carrying an inhibitory opsin (AAV2/5-CaMKII-eNpHR3.0). Similar to the optogenetic cohort, control animals were littermates transfected with the same virus only carrying a fluorophore (AAV2/5-CaMKII-eYFP) (**Figure 12a**). The experimental protocol was the same as described in **Figure 7c**, with 60-minute sessions carried out on five consecutive days, with inhibition being continuously delivered during the second (Q2) and fourth (Q4) 15-min segment (**Figure 12b**). As opposed to the ChR stimulation, yellow light was delivered continuously, for the duration of the 15-minute window, as, in my experience, longer-term inhibition does not lead to any unwanted side effects, such as altered locomotion or seizures.

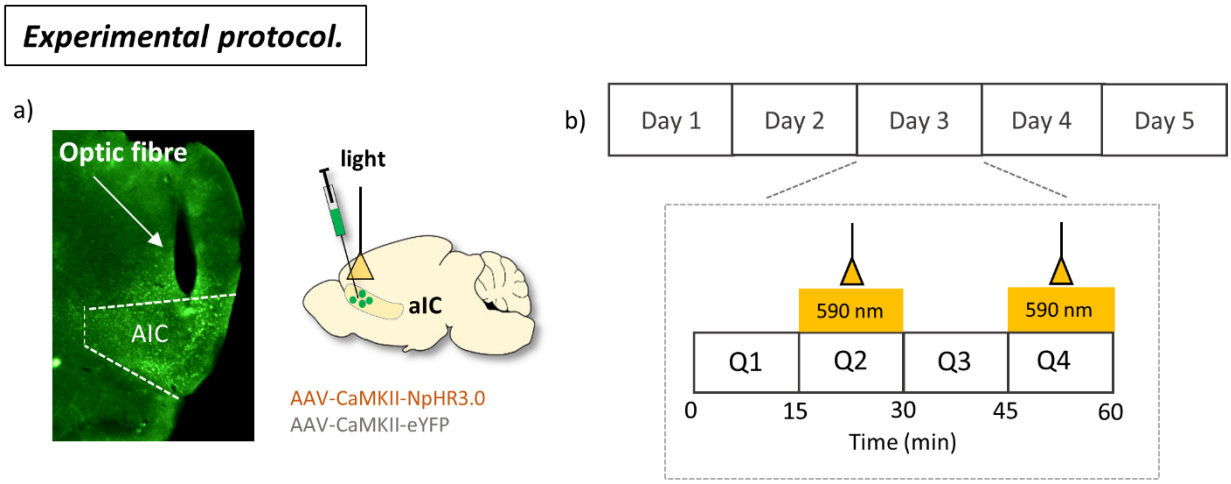

Figure 12: Experimental protocol used to assess the effect of AIC inhibition on flexible behavior. a) *Representative injection site in the AIC (left) and visual representation of injection and implantation site above the AIC.* ***b)*** *Time-course of the experiments and timing of optogenetic inhibition.*

In order to investigate the effects of AIC inhibition, I first analyzed the data in a manner analogous to that of the stimulation experiments, characterizing the number of transitions and locomotion across days. However, as opposed to stimulation experiments, AIC inhibition had

no effect on either number of transitions (**Figure 13a,b**) or locomotion across days (**Figure 13c,d**).

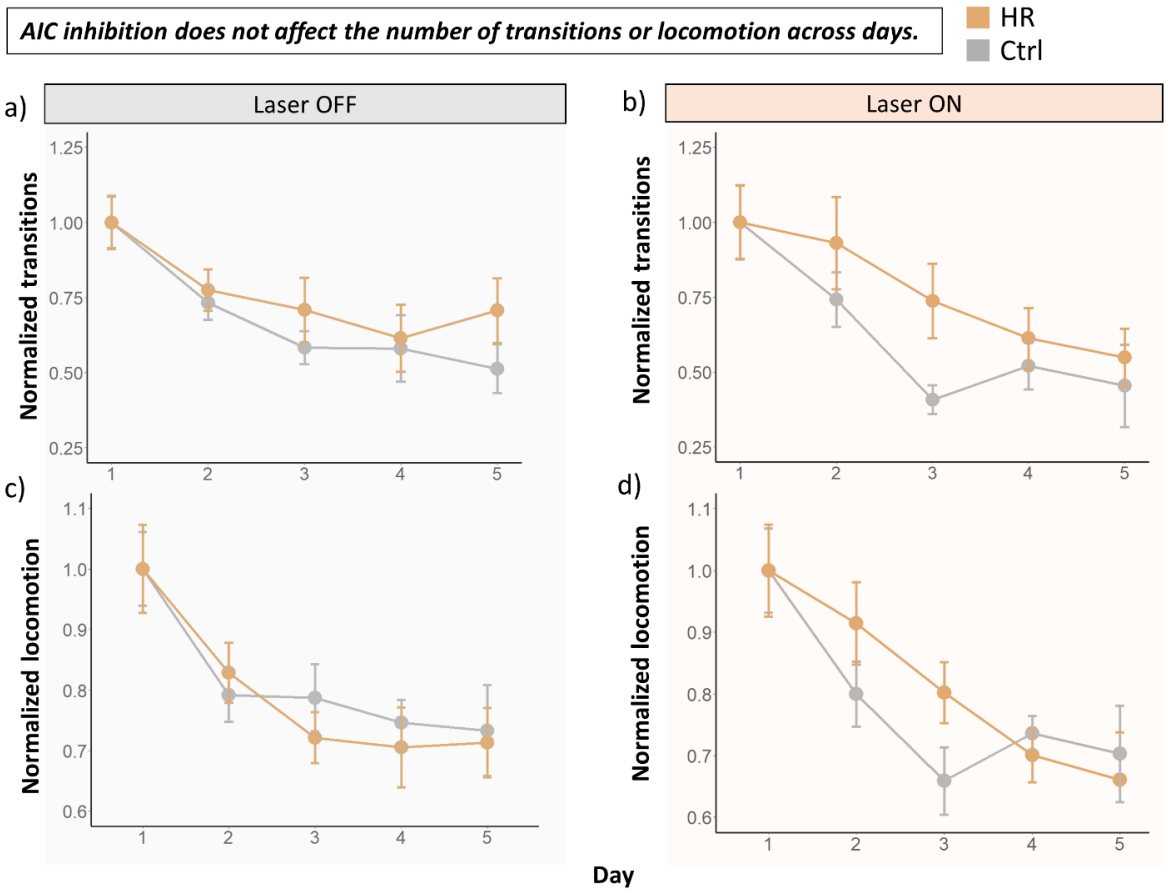

Figure 13: AIC inhibition does not affect the number of transitions and locomotion across days. *(N = 10 eNpHR3.0, N = 10 eYFP. a-b) Change in the number of transitions across days, two-way RM ANOVA of transitions and locomotion.* ***a) Laser OFF:*** *Group (opsin) effect: F(1, 18) = 2.948, p = 0.103; day effect: F(2.431, 43.77) = 5.029, p** = 0.0068; group x day interaction effect: F(3, 54) = 0.722, p = 0.543.* ***b) Laser ON:*** *Group (opsin) effect: F(1, 18) = 0.818, p = 0.378; day effect: F(3.068, 55.22) = 10.55, p < 0.0001; group x day interaction effect: F(4, 72) = 0.5847, p = 0.675. c-d) Change in locomotion across days, two-way RM ANOVA of transitions and locomotion.* ***c) Laser OFF:*** *Group (opsin) effect: F(1, 18) = 1.019, p = 0.326; day effect: F(2.305, 37.96) = 3.927, p = 0.113; group x day interaction effect: F(3, 54) = 0.630, p = 0.599.* ***d) Laser ON:*** *Group (opsin) effect: F(1, 18) = 0.837, p = 0.373; day effect: F(2.109, 41.50) = 2.236, p*= 0.0263; group x day interaction effect: F(3, 54) = 1.613, p = 0.197.*

Having observed no difference in the effect of AIC inhibition on the number of transitions or locomotion, I next examined whether it affected the relative amount of time that animals spent in the zones. However, similar to the number of transitions and locomotion, AIC inhibition had no effect on the amount of time the animals spent in any of the zones across days (**Figure**

14a,b). Likewise, no difference was observed when the data were examined in a within-experiment manner, comparing the first and the last 15-minute segments (**Figure 14c**).

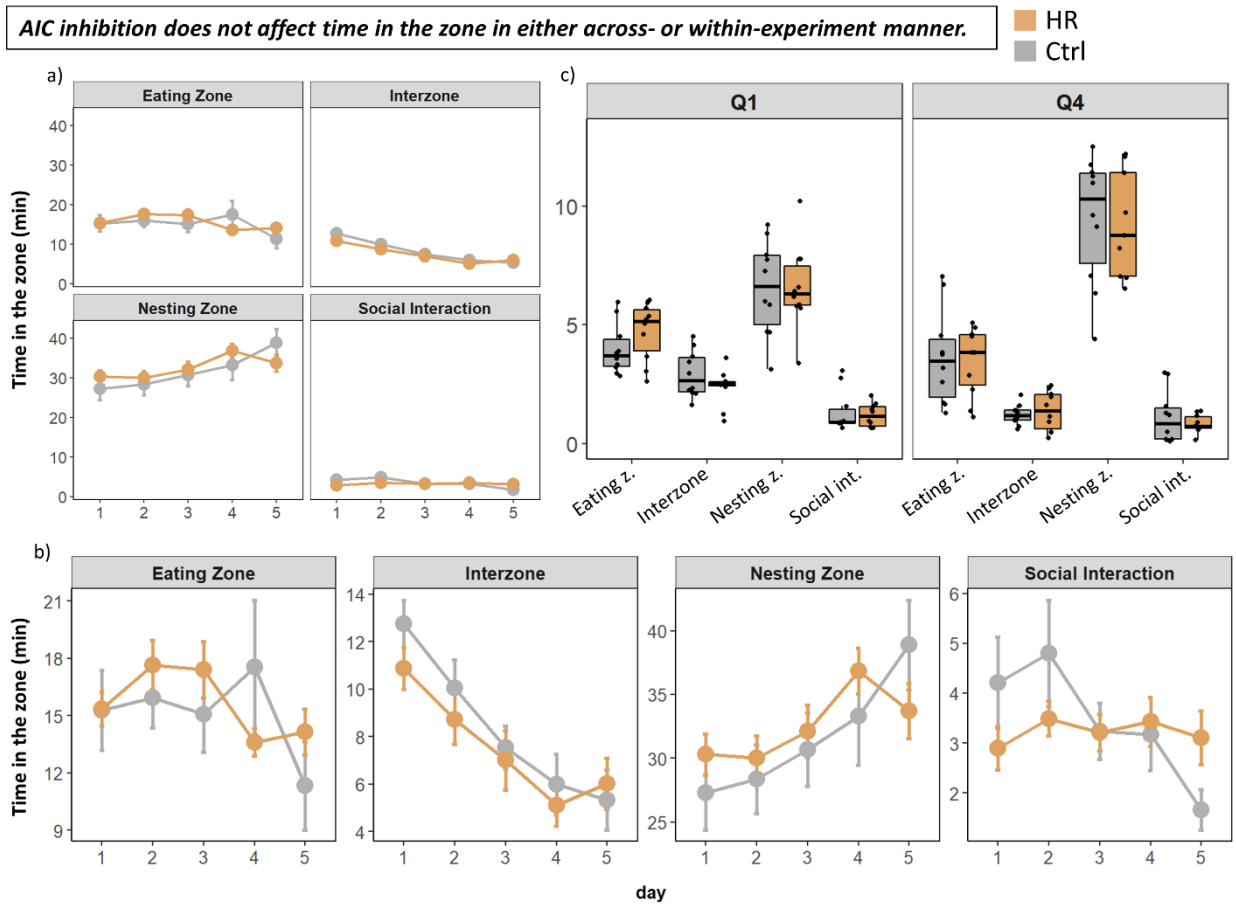

Figure 14: AIC inhibition does not affect time in the zone in either across- or within-experiment manner. *(N = 10 eNpHR3.0, N = 10 eYFP)* ***a-b)*** *AIC inhibition has little to no effect on amount of time animals spend in the zone across days (2-way RM ANOVA or Mixed-effects analysis of time spent in the zone).* ***Eating zone****: Group (opsin) effect: F(1, 18) = 0.102, p = 0.732; day effect: F(4, 72) = 2.249, p = 0.072; group x day interaction effect: F(4, 72) = 1.723, p = 0.154.* ***Interzone****: Group (opsin) effect: F(1, 18) = 0.632, p = 0.437; day effect: F(3.221, 56.37) = 16.49, p**** < 0.0001; group x day interaction effect: F(4, 70) = 0.609, p = 0.658.* ***Nesting zone****: Group (opsin) effect: F(1, 18) = 0.107, p = 0.748; day effect: F(2.778, 50.00) = 5.912, p** < 0.002; group x day interaction effect: F(4, 72) = 1.569, p = 0.192.* ***Social interaction zone****: Group (opsin) effect: F(1, 18) = 0.102, p = 0.753; day effect: F(2.991, 53.83) = 3.031, p** < 0.003; group x day interaction effect: F(4, 72) = 2.507, p* = 0.0494.* ***c)*** *AIC inhibition has no within-experiment effect on time spent in the zones (two-way ANOVA of time spent in the zone).* ***Q1****: Group (opsin) effect: F(1, 72) = 0.006, p = 0.940; zone effect: F(3, 72) = 102.670, p**** < 0.0001; group x zone effect: F(3, 72) = 1.173, p = 0.326.* ***Q4****: Group (opsin) effect: F(1, 72) = 0.018, p = 0.894; zone effect: F(3, 72) = 135.333, p**** < 0.0001; group x zone effect: F(3, 72) = 0.246, p = 0.864.*

As expected, the analysis of the average overall time in the zone during or outside of optogenetic inhibition (**Figure 15a**) confirmed that AIC inhibition had no effect on the average

overall time in the zone. Furthermore, no effect was observed when cumulative average time in the zone was compared between the two groups (**Figure 15b**).

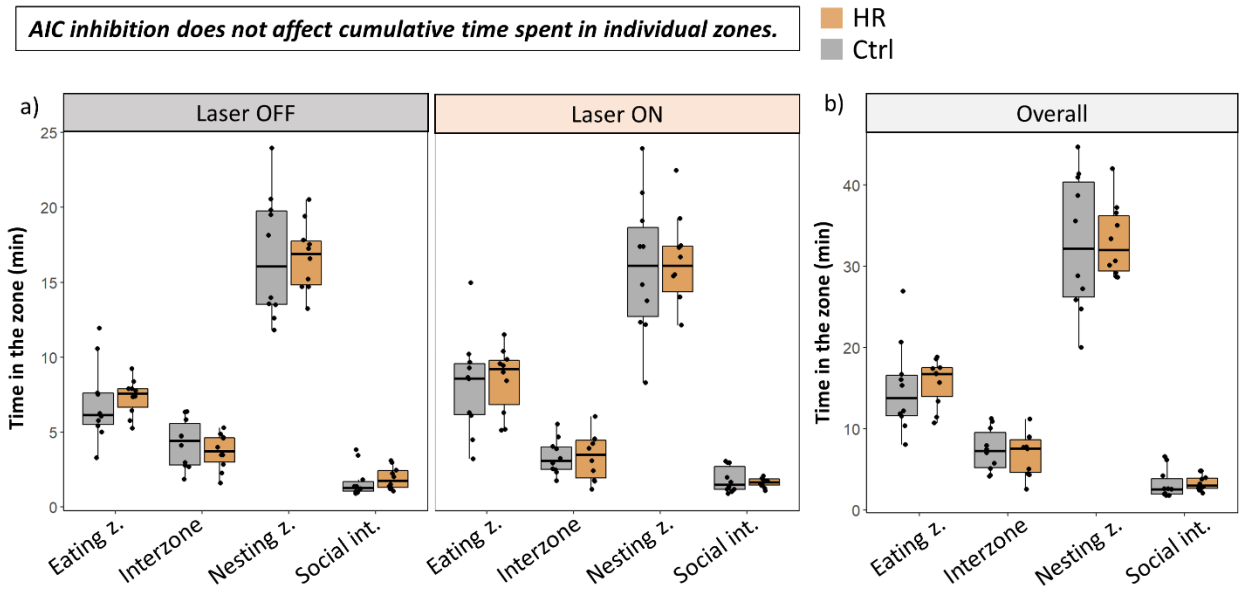

Figure 15**: **AIC inhibition has no effect on the amount of time animals spend in the zones** (N = 10 eNpHR3.0, N = 10 eYFP). **a)** AIC inhibition has no effect on time in the zone in either Laser ON or Laser OFF condition (two-way ANOVA of time spent in the zone). **Laser ON:** Group (opsin) effect: F(1, 72) = 0.002, p = 0.964; zone effect: F(3, 72) = 185.372, p* < 0.0001; group x zone effect: F(3, 72) = 0.0841, p = 0.969. **Laser OFF:** Group (opsin) effect: F(1, 72) = 0.00000582, p = 0.998; zone effect: F(3, 72) = 221.842, p**** < 0.0001; group x zone effect: F(3, 72) = 0.853, p = 0.853. **b)** AIC inhibition does not affect overall time the animals spent in the zone (two-way ANOVA of time spent in the zone). Group (opsin) effect: F(1, 72) = 0.020, p = 0.888; zone effect: F(3, 72) = 205.027, p**** < 0.0001; group x zone effect: F(3, 72) = 0.191, p = 0.902.*

The above analysis revealed no effect of the AIC inhibition on either number of transitions, locomotion or time in the zone. However, it is important to keep in mind that if AIC is truly important for salience detection and switching between large-scale brain networks, the effects of stimulation and inhibition may need to be examined at different time points. Since the effect of the stimulation is observed in the later stages of the experiment, when novelty and thus salience of the environment are the lowest, AIC inhibition should exhibit the most potent effect when saliency is the highest. As such, I would expect to see the strongest effect when the animals are not yet habituated to the arena. This should occur on the first experimental day, as well as in the initial time points of each session. As such, I hypothesized that the AIC inhibition effect may be observed if I examine the change in the above metrics across the 4 time-segments of the experiments (Q1 to Q4). However, such analysis revealed no difference in either time in

the zone, number of transitions or locomotion between the two groups (**Figure 16a-c**). Furthermore, no effect was observed when only day 1, when the salience of the environment should be the highest, was examined (**Supplementary Figure 4**).

Overall, AIC inhibition had no effect on the number of transitions between the zones, locomotion or time in the zone in either across- or within-experiment manner. Furthermore, no effect was observed when presumably the most salient time points of the experiment were examined, leading to the conclusion that AIC inhibition does not affect flexible behavior and behavior switching under these specific conditions.

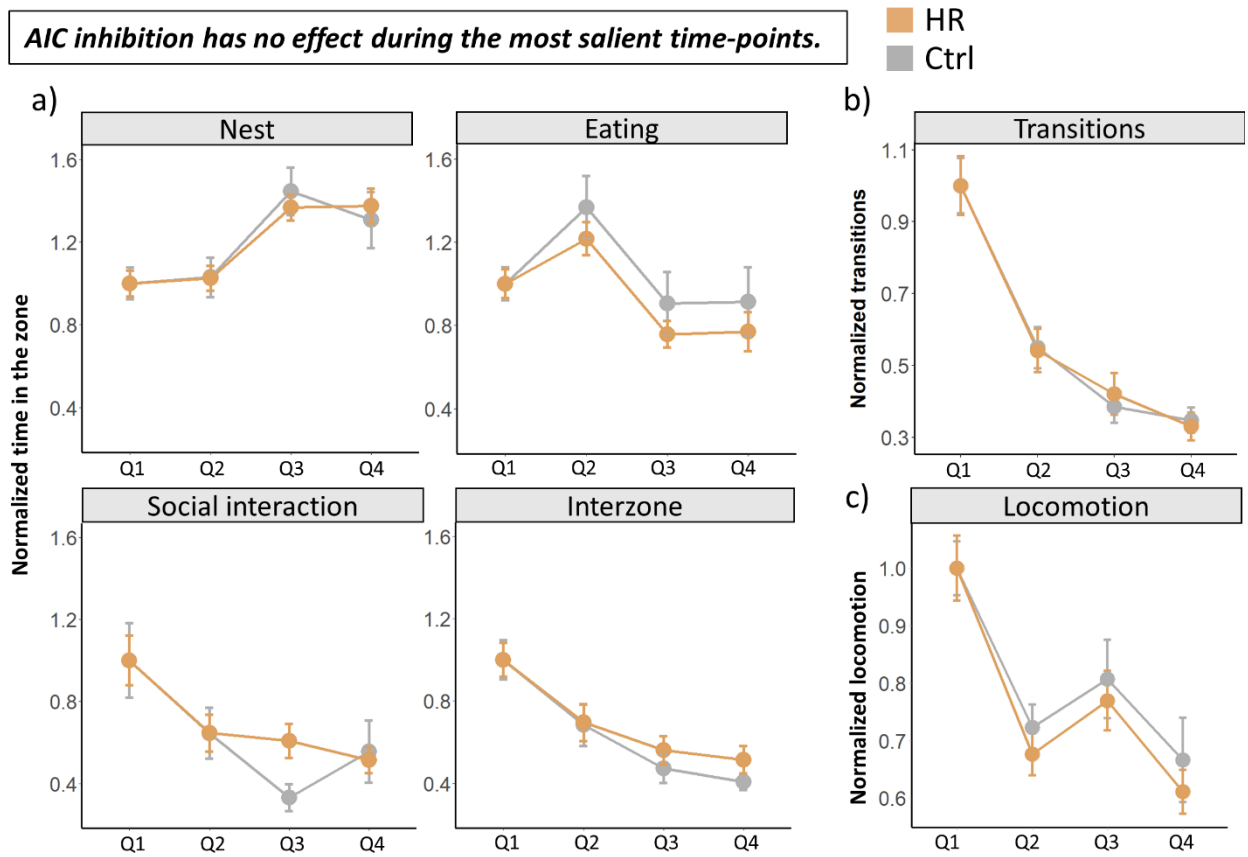

Figure 16: AIC inhibition has no within-experiment effect on time in the zone, transitions or locomotion. *(N = 10 eNpHR3.0, N = 10 eYFP)* ***a)*** *2-way RM ANOVA of time in the zone.* ***Nesting zone****: Group (opsin) effect: F(1, 18) = 0.238, p = 0.632; period effect: F(2.224, 40.03) = 11.69, , p**** < 0.0001; group x period interaction effect: F(3, 54) = 1.454, p = 0.237.* ***Interzone****: Group (opsin) effect: F(1, 18) = 0.354, p = 0.559; period effect: F(2.353, 42.35) = 37.63, p*** < 0.0001; group x period interaction effect: F(3, 54) = 0.458, p = 0.713.* ***Eating zone****: Group (opsin) effect: F(1, 18) = 0.754, p = 0.397; period effect: F(2.772, 49.00) = 14.73, p*** < 0.0001; group x period interaction effect: F(3, 54) = 0.438, p = 0.727.* ***Social interaction zone****: Group (opsin) effect: F(1, 18) = 0.258, p = 0.618; period effect: F(2.266, 40.78) = 12.14, p*** < 0.0001; group x period interaction effect: F(3, 54) = 1.145, p = 0.339.* ***b)*** *2-way RM ANOVA of transitions between the zones. Group (opsin) effect: F(1, 18) =*

*0.00124, p = 0.973; period effect: F(2.107, 37.93) = 22.35, p*** < 0.0001; group x period interaction effect: F(3, 54) = 0.133, p = 0.940.* ***c)*** *2-way RM ANOVA of locomotion. Group (opsin) effect: F(1, 18) = 0.532, p = 0.475; period effect: F(2.239, 40.31) = 117.80, p*** < 0.0001; group x period interaction effect: F(3, 54) = 0.174, p = 0.913.*

3.3 Fiber photometry during flexible behavior

While aIC stimulation had clear impact on behavioral switching, I failed to observe any effects upon aIC inhibition, which may have several reasons (see discussion). To further understand the possible role of aIC I turned to fiber photometry (FP) which allows bulk neural activity recordings using genetically-encoded calcium indicators. My FP experiments had two major aims. Firstly, I wanted to characterize AIC activity during complex behavior, to examine whether AIC activity increases or decreases during the behaviors affected by optogenetic stimulation. Secondly, given the hypothesized role of the AIC as salience detector in human imaging studies, I wanted to establish whether rodent AIC plays a similar role.

To explore the above questions, I transfected excitatory pyramidal neurons of the AIC with an AAV virus carrying a genetically-encoded calcium indicator GCaMP7f under the CaMKII promoter. Similarly to optogenetics, I implanted an optic fiber through which both light delivery and fluorescence detection were carried out (**Figure 17a,b**) and collected data in two different experimental cohorts. The following protocol was used to examine the role of AIC in flexible behavior and salience detection: the first cohort, containing five animals, underwent three recording sessions carried out on three consecutive days. During sessions 1 and 2, mice were first placed in the home cage for 5 minutes to establish the baseline fluorescence signal. Afterwards, they were immediately placed into the Multimaze, which was equipped in the same way as described in the optogenetic experiments, with nesting, eating and social interaction zones (**Figure 7a**). On day 3, the protocol was the same as on days 1 and 2, with the only difference being that the animals received six 1-second foot shocks following home cage recording, and prior to being placed into the Multimaze **(Figure 17c).** Foot shocks, allowing us to study AIC response to adverse stimuli, were delivered in a separate fear-conditioning box, so that no association was formed between the Multimaze and the aversive event. In the fourth session, conducted in a separate experimental cohort consisting of 4 mice, the animals were acutely food-deprived for 24 hours prior to the experiment, to facilitate increased salience of

the sunflower seeds available in the arena **(Figure 17c).** For each behavioral episode, a single trace signifying change in fluorescence was recorded, which allowed the comparison of the AIC signal between multiple episodes of a single behavior (**Figure 17e,f**).

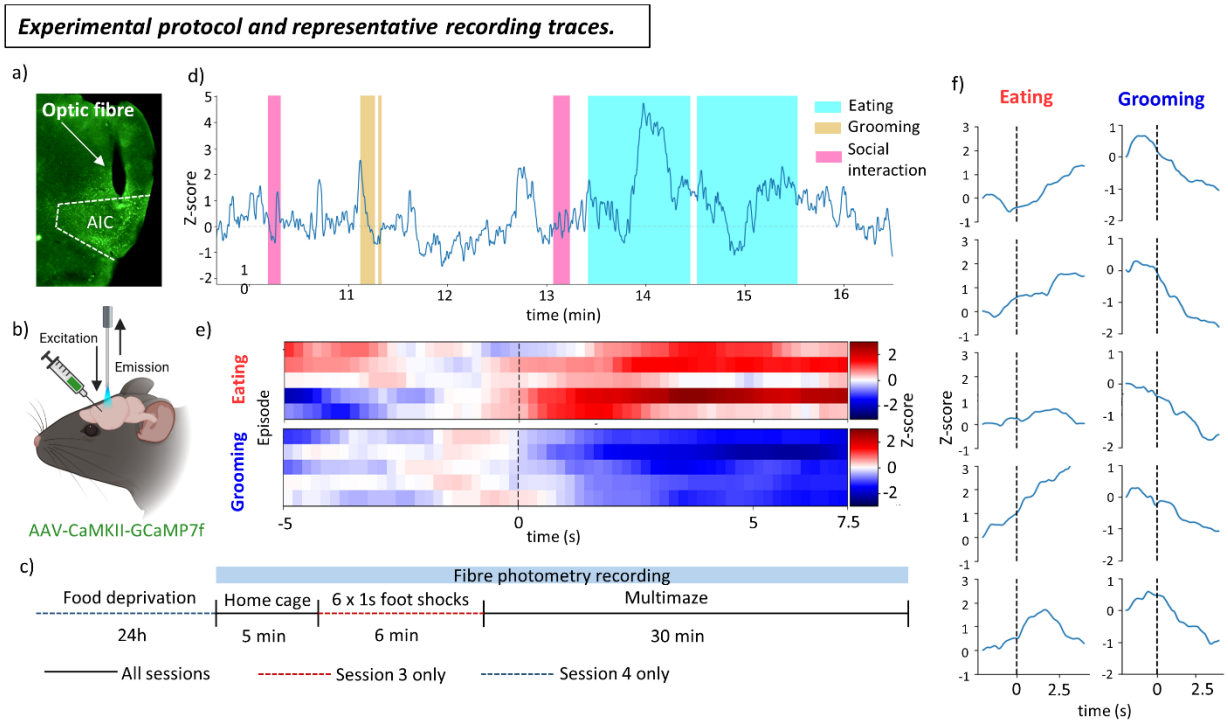

Figure 17: Experimental protocol and sample recording traces from fiber photometry recording. a) *A representative coronal slice demonstrating viral expression and correct fiber positioning within the AIC.* ***b)*** *Virus injection and optic fiber placement above the AIC.* ***c)*** *The experimental protocol, which consisted of 4 recording sessions; the first two consisted of a 5-minute habituation period followed by a 30-minute recording session (black lines). In the third session, habituation was followed by exposure to six foot shocks (red dotted line) and the fourth session was preceded by 24 hours of food deprivation (blue dotted line).* ***d)*** *Example GCaMP7f trace from a single mouse during one of the Multimaze sessions.* ***e)*** *A selection of five events from two of the measured behaviors displayed using peri-event time histogram. Each row represents a single event. Each trace is normalized to a three second window preceding the start of the behavior (time-point 0).* ***f)*** *The same events as displayed in e) shown as individual 3-second-long Z-scored signal traces, displaying varying magnitudes and time-courses of the two behaviors.*

Compared to optogenetics, fiber photometry allows an experimenter to collect larger amounts of data in fewer animals, with standard cohort sizes of approximately five animals[157,158]. Given the lower number of experimental animals, as well as shorter experiment duration compared to optogenetic experiments, I decided to perform a much more complete analysis. To achieve this, all videos were manually scored to conduct detailed behavioral analysis where specific behaviors, rather than just time spent in the zones, were measured. The following behaviors and stimuli were annotated and their corresponding AIC activity analyzed: **eating**, where

precise times when the animal began and stopped eating a seed were recorded; **social interaction**, where nose-to-nose interactions, as well as close proximity during which the experimental animal directly faced the social interaction partner were marked. Furthermore, I examined **grooming**, **foot shocks** and **tail suspension** during the animal's transfer from the home cage to the Multimaze. Such selection of stimuli provided me with a possibility to study the activity of the AIC during behaviors and stimuli of different valence and salience to reveal whether AIC responds primarily to appetitive/aversive conditions or rather to all salient behaviors and stimuli regardless of their valence. Specifically, eating and social interaction served as positively-valenced conditions, while tail suspension and foot shocks served as negatively-valenced conditions (**Figure 18a,b**). In addition, I also wanted to examine behaviors and stimuli that would engage the CEN, SN and DMN in different ways. It was relatively easy to find behaviors and stimuli that would direct the animals' attention outwards, representing activation of the SN and CEN: eating, which required focus to procure and shell the seed, as well as foot shocks and tail suspension, both shifting the mouse's attention to the external environment in order to respond to a potentially threatening situation. It was, however, much harder to incentivize and recognize behaviors that would represent internally-focused role of the DMN. Here, I decided to examine grooming, since it may represent one of a few clearly self-focused behaviors that can be observed in a mouse (**Figure 18c**). This is further supported by a study which showed that grooming in rats resulted in increased local field potential gamma-band oscillations, known to accompany DMN activation[159]. Fascinatingly, the study showed that the increase was greater during grooming than during periods of quiet wakefulness, suggesting that grooming engages the DMN especially strongly, and may thus represent a great candidate behavior to serve as a proxy of DMN activation.

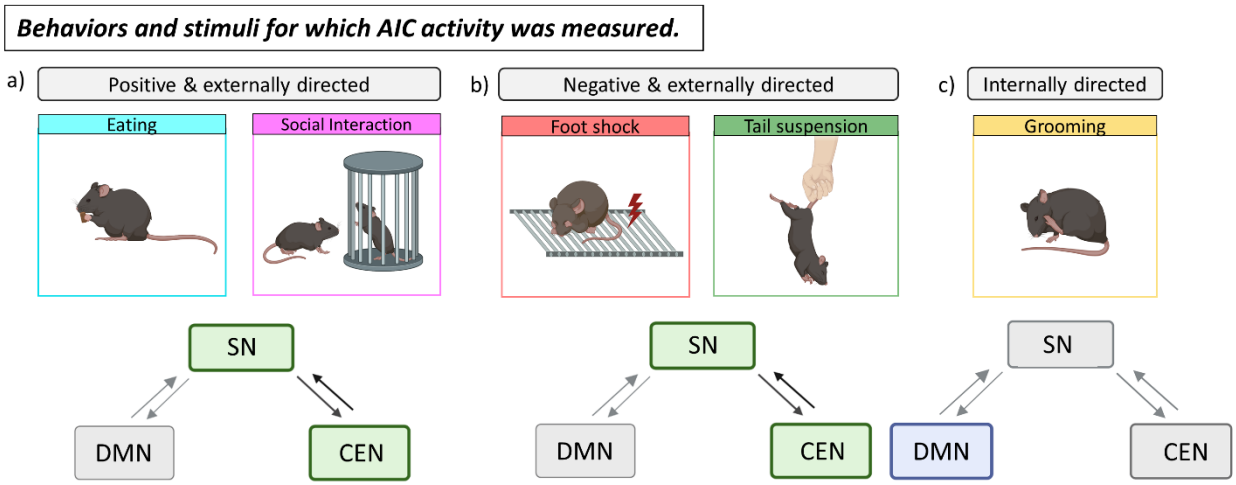

Figure 18: Illustration of stimuli and behaviors for which AIC activity was measured. a) *Eating and social interaction were chosen as the two behaviors of positive valence that required external focus and thus concomitant SN and CEN engagement.* ***b)*** *Foot shock and tail suspension were chosen as the stimuli of negative valence that elicited external focus and concomitant SN and CEN engagement.* ***c)*** *Grooming was chosen as an internally focused behavior that would be expected to engage the DMN but not the SN or the CEN. Abbreviations: SN: salience network; DMN: default mode network; CEN: central executive network.*

Examination of the AIC responses to various behaviors revealed that AIC responds to salient stimuli across different valences. AIC responded especially strongly during eating and tail suspension, both of which evoked strong and significant increase in the AIC activity (**Figure 19a,d**). Furthermore, AIC responded with a smaller and less consistent increase during foot shocks (**Figure 19c**), which was surprising, given that the insular cortex is known to be involved in perception of pain[160]. It is possible, however, that the effect would become more significant with a larger number of collected traces. Furthermore, it is important to note that AIC activity decrease in some cases could be due to unexamined freezing behavior, since it has been previously shown that freezing results in decreased IC activity[105]. AIC response during social interaction was weaker and less consistent, with a trend towards activity increase (**Figure 19b**). As can be observed from the corresponding peri-event time histogram and box plot, there was a relatively large level of diversity in AIC responses, with an increase in some and decrease in other cases (**Figure 19b**). It is possible that the extent of AIC activation depends on the extent of interaction between the two mice which is difficult to assess precisely. Finally, I examined grooming behavior, which, to my knowledge, does not hold any particular valence under given experimental conditions, but was chosen as an internally-focused behavior which should engage the DMN. Interestingly, grooming elicited a remarkable decrease in AIC activity (**Figure 19e**), despite its strong sensory-motor component. This is particularly fascinating, as

human studies have established that AIC activity in humans is inversely correlated with the activity in the DMN[9,35] – if rodent AIC serves a similar function, I would thus expect to see corresponding activity decrease in behaviors that engage the DMN. Furthermore, it is interesting to notice that there is an increase in AIC activity during externally focused behaviors supposed to engage the CEN such as eating, foot shock, social interaction and tail suspension, and a decrease during grooming, and internally focused behavior assumed to engage the DMN.

Another interesting observation in my data was the presence of an anticipatory signal during eating. As it can be observed from the mean trace and the peri-event time histogram (PETH), the AIC signal began to increase before the actual onset of eating behavior (**Figure 19a**, left dotted line). This suggests that rather than encoding only appetitive and/or gustatory components of the stimulus, AIC neurons also encode anticipation for the upcoming behavior. Such an increase was not observed preceding any other behavior, suggesting that it requires the animal to engage in the behavior voluntarily, which is not the case during foot shock or tail suspension. As such, the observed increase likely represents an anticipatory signal during the time window between the animal making the decision to engage in a behavior, and the actual start of the behavior.

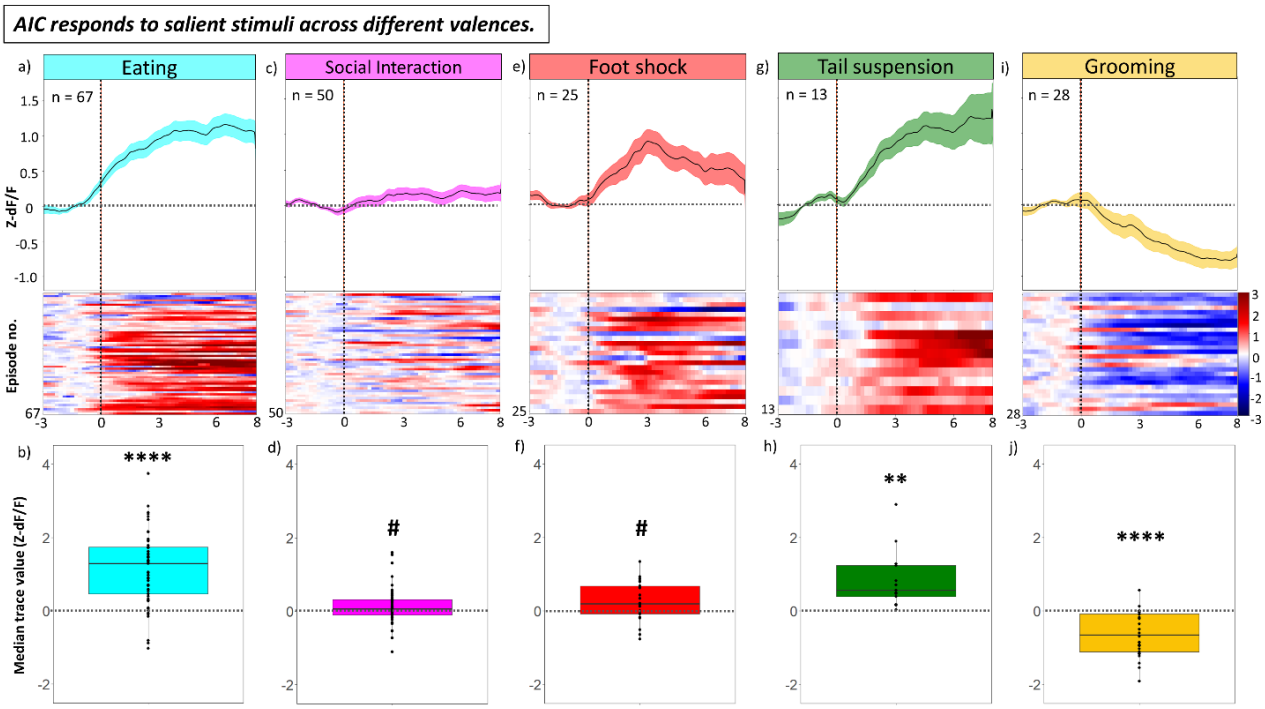

Figure 19: AIC responds to salient stimuli regardless of their valence *(N = 5).* ***a-e) Top:*** *Mean + SEM traces for each of the five examined behaviors, normalized to the 3 second time-window prior to the onset of behavior (time-point 0).* ***Middle:*** *Peri-event time histogram*

showing individual traces for the corresponding behaviors. Each trace is normalized to the 3 second window prior to the onset of behavior. All behaviors are plotted on the same scale for easier comparison. ***Bottom:*** *A box plot representing relative change in Z-scored amplitude from the baseline (3 seconds prior to the onset of behavior) for each of the five behaviors. Each of the points represents a median value for the whole episode trace from the onset of behavior to the end of the episode. Significance was determined using a two-tailed paired t-test. Eating: t = -8.6508, df = 56.0,* ***p**** < 0.0001****; Social Interaction: t = -1.8302, df = 49.0,* $\boldsymbol{p^{\#} = 0.073}$*; Foot shock: t = -2.0073, df = 24.0,* $\boldsymbol{p^{\#} = 0.056}$*; Tail suspension: t = - 3.8098, df = 12.0,* ***p** < 0.0025****; Grooming: t = 5.537, df = 27.0,* ***p**** < 0.0001.**

In the above experiments, I confirmed the role of the AIC in salience detection through examining its activity during a number of different stimuli. To further confirm its role in salience encoding, I performed an additional experiment where I increased the salience of an already examined stimulus. This would serve as an additional control that would affirm that the observed response is not due to certain sensory properties of varying stimuli and motor properties of different behavioral responses. In order to do that, I food deprived a separate cohort of four animals for 24 hours prior to the experimental session and then exposed them to sunflower seeds in the same context as in the original, non-food deprived experiment. The AIC signal in food deprived animals displayed significantly higher amplitude compared to the sated animals (**Figure 20a,c,d**). Furthermore, the signal increased much more sharply, which can be observed in a significant difference between signal slopes (**Figure 20a,b,d**). Interestingly, however, I could observe that in food deprived animals the anticipatory signal that could be observed in sated state is no longer present (**Figure 20a,d**), but that AIC signal increases sharply and quickly with the onset of eating.

Overall, my fiber photometry experiments provide evidence that similar to humans, rodent AIC encodes salient stimuli across different valences. Furthermore, AIC activity increases with an increased stimulus salience when the animals' homeostatic state shifts. This suggests that rodent AIC may indeed play a role as a salience detector, adjusting its response to a shift in an organism's homeostatic needs.

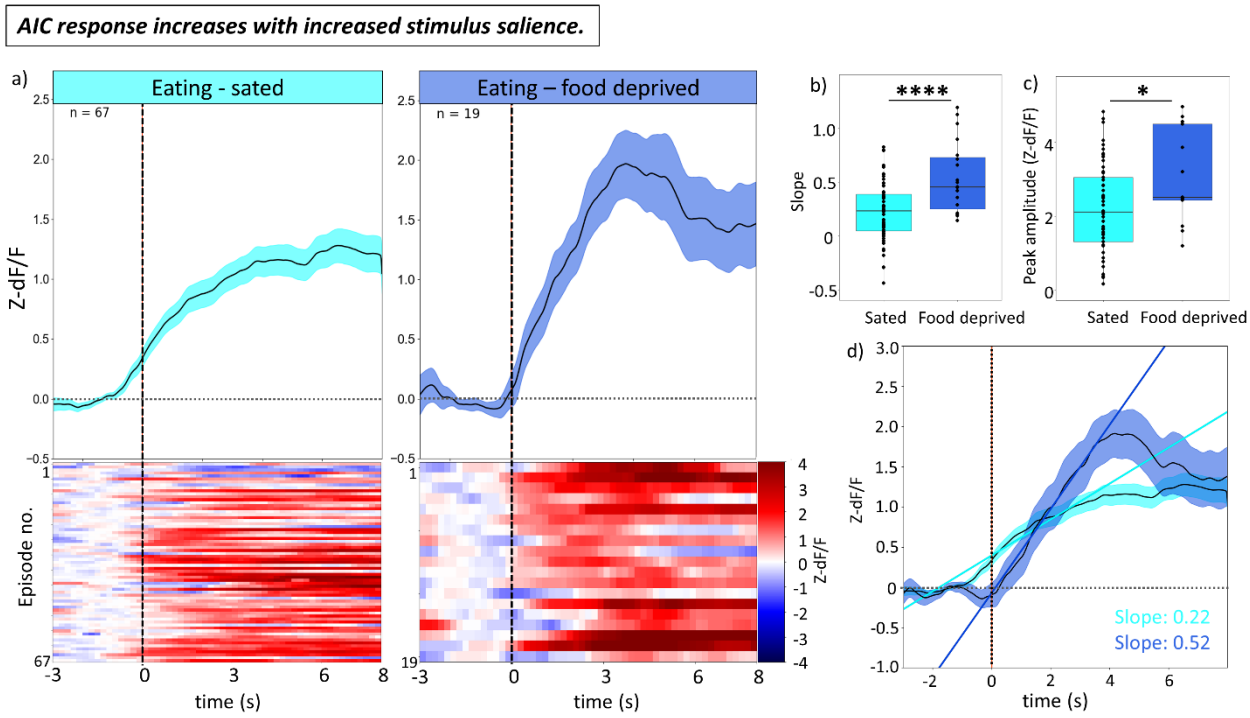

Figure 20: AIC response increases with increased salience of a stimulus *(N = 5 for sated and N = 4 for food-deprived animals).* ***a) Top****: Mean + SEM traces of AIC response to eating in sated (left) or food-deprived (right) animals normalized to the 3 second time window prior to behavior onset.* ***Bottom****: Peri-event time histogram showing individual traces for the corresponding behaviors. Each trace is normalized to the 3 second window prior to the onset of behavior. Both behaviors are plotted on the same scale.* ***b)*** *Comparison of the signal slope for individual eating episodes (two-tailed t-test, t = 4.3144, df = 84,* ***p**** **** < 0.0001****).* ***c)*** *Comparison of peak signal values for individual eating episodes (two-tailed t-test, t = -2.4192, df = 68,* ***p* = 0.01823****).* ***d)*** *A comparative plot of the mean AIC signal in sated and food deprived mice during an eating episode. A comparison of mean slope values reveals a steeper and larger increase in AIC response in food-deprived animals.*

3.4 Circuit probing in the AIC

3.4.1 Structural characterization of AIC neuronal subpopulations

Having shown the involvement of the AIC in salience detection and flexible behavior, I finally wanted to probe the involvement of specific neuronal circuits that may contribute to the above observations. To this end, I decided to explore structural and functional properties of three different, so far unexamined, AIC neuronal subpopulations in transgenic mouse lines. To do so, I used three transgenic BAC-Cre recombinase driver lines from the gene expression nervous

system atlas (GENSAT) project of Rockefeller University, which generates transgenic lines that allow for cell-specific gene manipulations in the mouse central nervous system[161,162]. We obtained three mouse lines with strong Cre expression within specific neuronal populations that, as observed in the GENSAT *in situ* hybridization library, were localized almost exclusively in the AIC. The three lines expressed Cre-recombinase under Sim1, Rgs14 and GRP promoters, respectively. Since the choice of the lines was based on their expression pattern rather than the known functions of the promoter genes, a discussion of their in-so-far known functional roles is outside the scope of this project.

First, I wanted to characterize the output pattern of the three subpopulations. To this end, the animals were unilaterally injected with a Cre-dependent AAV carrying an mCherry fluorophore into the AIC (**Figure 21a,b**). First, I examined the spatial location of the infected AIC output cell bodies to investigate whether their localization displays similar or diverse pattern. Interestingly, the examination of the infected cell body placement revealed distinct localization patterns for the three lines. GRP-Cre cells were predominantly located in cortical layers II and III, Rgs14-Cre cells almost exclusively in layer III, and Sim1-Cre cells primarily in cortical layer V (**Figure 21c**).

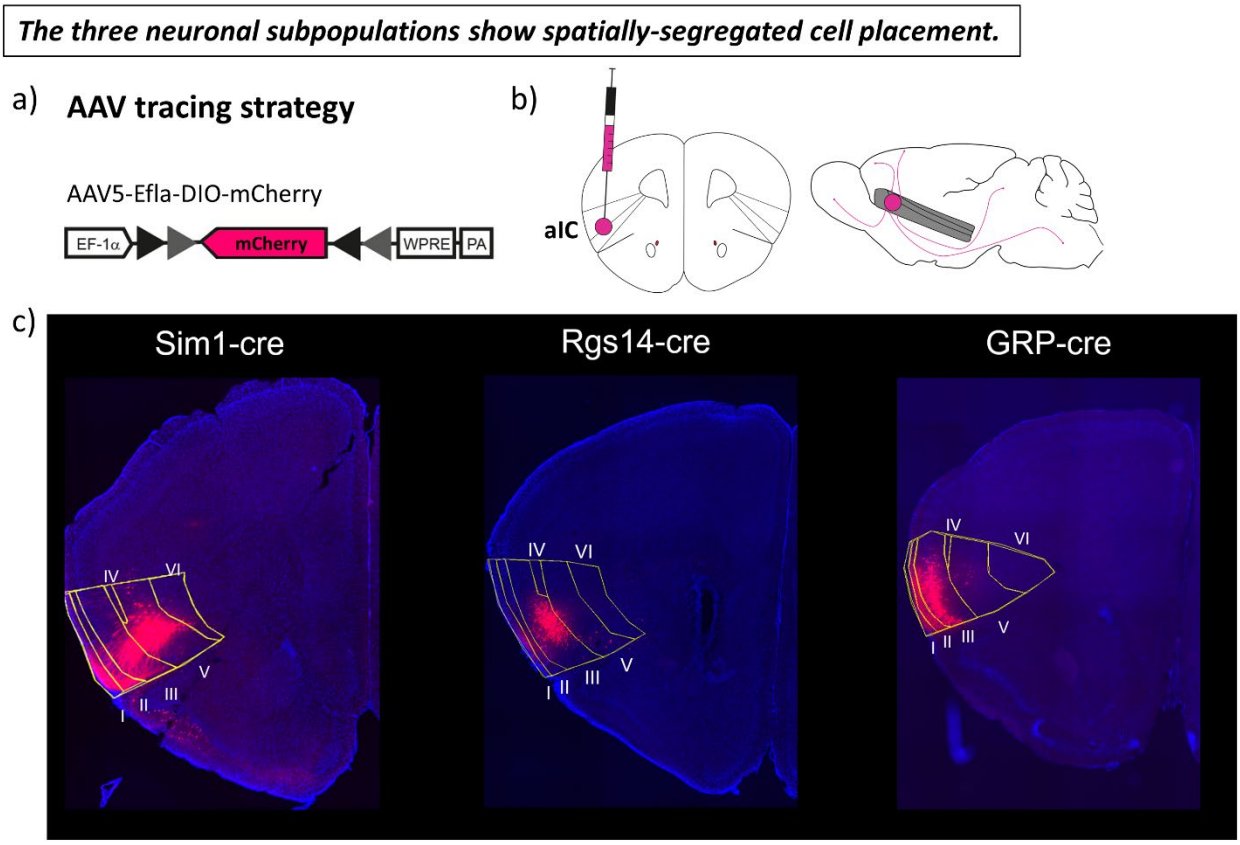

Figure 21: Spatial segregation of the infected cell bodies in three transgenic lines. *(N = 3 Rgs14-Cre, N= 3 Sim1-Cre, N= 3 GRP-Cre)* ***a)*** *AAV tracing strategy used to identify the output pattern of the three neuronal subpopulations.* ***b)*** *Visual representation of an injection site for the three lines.* ***c)*** *Visualization of the starter cell population for each of the three transgenic lines. Note the different placement of the starter cells within the AIC. Surgeries and imaging were done with help from Eunjae Cho.*

I next went on to characterize neuronal output pattern of the three subpopulations. While I did not precisely quantify projection density and cell number, I here present preliminary qualitative characterization of the subpopulations' projection patterns. Upon the examination of coronal brain slices across the whole brain, I identified five main antero-posterior levels at which strong projections from two or more populations could be observed: striatum, extended amygdala, amygdala, posterior cortical and subcortical regions and locus coeruleus (**Figure 22**, top to bottom). At the level of the striatum, Sim1-Cre neurons projected predominantly to the ventro-lateral caudate putamen (CPu) (**Figure 22a**, first row), whereas Rgs14-Cre neurons projected to ventro-lateral CPu and strongly to the core region of the nucleus accumbens (AcbC) (**Figure 22b**, first row). Weak overall CPu labelling was observed also in the GRP-Cre line, with stronger labelling observed in the anterior commissure (**Figure 22c**, first row). At the level of the extended amygdala, Sim1-Cre and Rgs14-Cre lines exhibited strong labelling in the

interstitial nucleus of the posterior limb of the anterior commissure (IPAC), whereas the GRP-line exhibited labeling in anterior basolateral amygdala (BLA) (**Figure 22**, second row). At the level of the amygdala, all three lines exhibited strong labelling, however, the expression was localized to different nuclei: whereas Rgs14-Cre neurons projected to both central amygdala (CeA) and BLA, Sim1-Cre neurons projected exclusively to CeA, and GRP-Cre neurons exclusively to the BLA (**Figure 22**, third row). All three regions also projected to posterior brain regions, including cortical as well as subcortical and brainstem regions (**Figure 22**, fourth row). GRP-Cre neurons projected strongly to the entorhinal cortex (ENT) (**Figure 22c**, fourth row), whereas Sim1-Cre and Rgs14-Cre neurons projected weakly to the ENT, but sent projections to a number of other posterior regions including midbrain and brainstem nuclei, hippocampal formation (HPC), as well as visual and retrosplenial cortex (RSP) (**Figure 22a,b**, fourth row). Finally, all three lines projected to locus coeruleus (LC), a primary noradrenergic nucleus of the brain (**Figure 22**, bottom row). Of the three lines, GRP-Cre neurons showed the strongest LC labeling, whereas Rgs-14-Cre and Sim1-Cre neurons exhibited somewhat weaker fluorescence. Overall, my tracing experiment shows that the three neuronal populations are spatially segregated within the AIC layers, and exhibit diverse projection patterns, suggesting different functional properties.

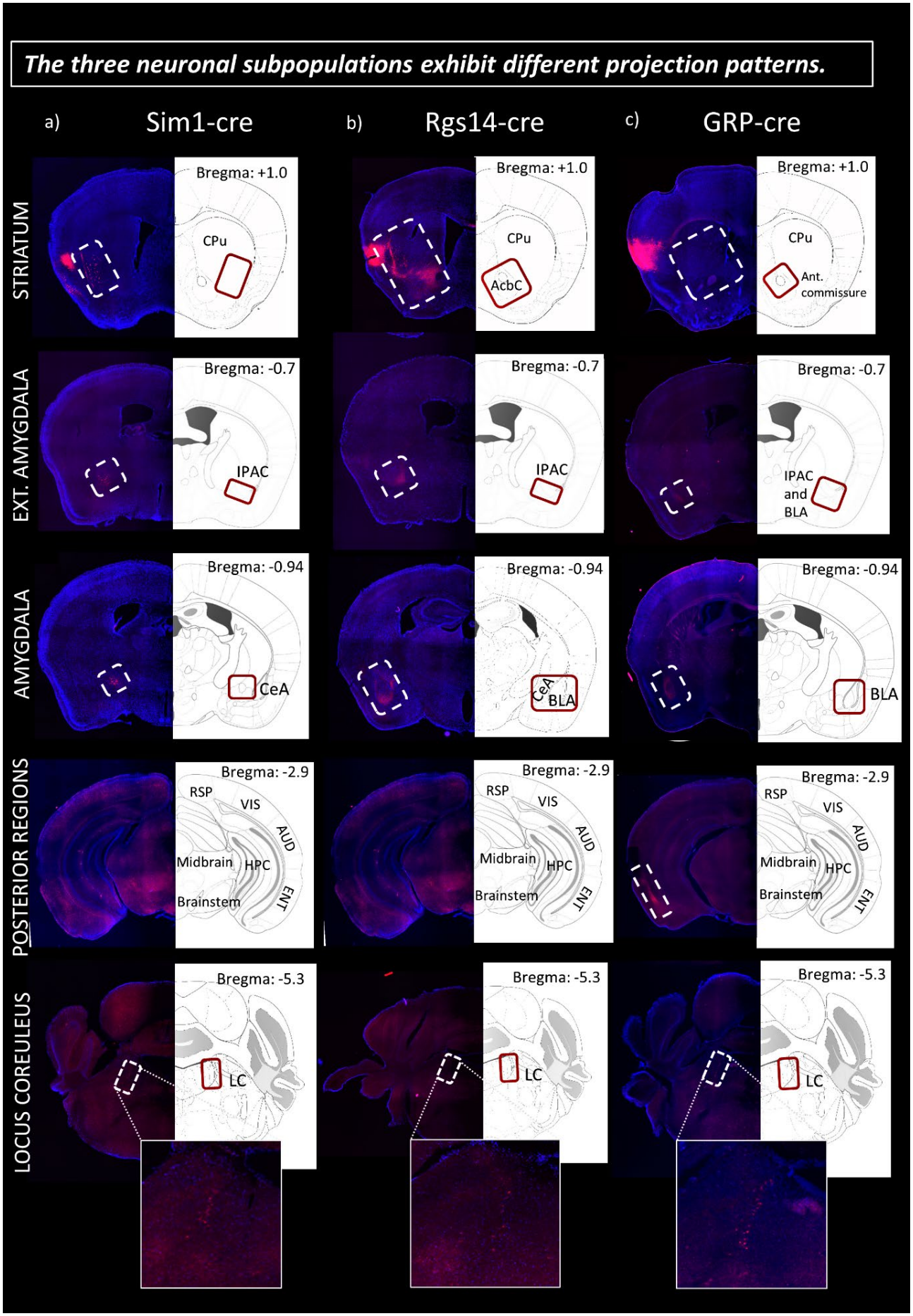
The three neuronal subpopulations exhibit different projection patterns.
a) Sim1-cre
b) Rgs14-cre
c) GRP-cre
STRIATUM
EXT. AMYGDALA
AMYGDALA
POSTERIOR REGIONS
LOCUS COREULEUS
Bregma: +1.0
CPu
AcbC
Ant. commissure
Bregma: -0.7
IPAC
IPAC and BLA
Bregma: -0.94
CeA
BLA
Bregma: -2.9
RSP
VIS
AUD
Midbrain
HPC
Brainstem
ENT
Bregma: -5.3
LC

Figure 22: The three neuronal subpopulations exhibit different projection patterns. *(N = 3 Rgs14-Cre, N= 3 Sim1-Cre, N= 3 GRP-Cre)* ***a-c)*** *Projection patterns for the Sim1-Cre, Rgs14-Cre and GRP-Cre lines at different antero-posterior levels of the brain.* ***Top- to bottom:*** *The three lines have been found to send their projections to five major brain regions: striatum, extended amygdala, amygdala, posterior regions including entorhinal cortex and locus coeruleus.* ***Abbreviations:*** *CPu: Caudate Putamen; AcbC: Nucleus Accumbens core; IPAC: the interstitial nucleus of the posterior limb of the anterior commissure; CeA: central amygdala; ant. BLA: anterior basolateral amygdala; post. BLA: posterior basolateral amygdala; RSP: retrosplenial cortex; VIS: visual cortex; AUD: auditory cortex: ENT: entorhinal cortex; HPC: hippocampal formation, LC: locus coeruleus. Surgeries and imaging were done with help from Eunjae Cho.*

3.4.2 Functional characterization of the GRP-Cre line

The final set of experiments was aimed at characterizing functional properties of the three transgenic lines. To this end, I once again employed fiber photometry to measure bulk activity of the targeted cells. However, due to a low number of cells and their observed non-uniform distribution between male and female mice, targeting turned out to be particularly challenging, and the final throughput very low. As such, I only managed to collect a usable set of data from the GRP-Cre line, the results for which are presented below.

To measure the activity of GRP-Cre neurons, I bilaterally injected a Cre-dependent adeno-associated virus carrying a calcium indicator GCaMP7f into the AIC (**Figure 23b**). As an initial screen, I once again selected an array of behaviors that would allow me to measure AIC activity in response to salient stimuli of different valence. Given the results obtained in wild-type mice, I also measured AIC activity during grooming. Recordings were conducted in two sessions: in the first one, mice were put into the Multimaze following a 5-minute habituation period and allowed to explore the arena for 30 minutes. There, the data for eating, social interaction and grooming behaviors were obtained. In the second session, aimed at assessing AIC response to negatively-valenced stimuli, the animals were placed in an empty circular open field where I delivered 6 air puffs, where a small amount of pressurized air was blown into the mouse's face (**Figure 23c**). The data for tail suspension was also collected; however, due to a low number of trials and noisy recordings the results are not shown.

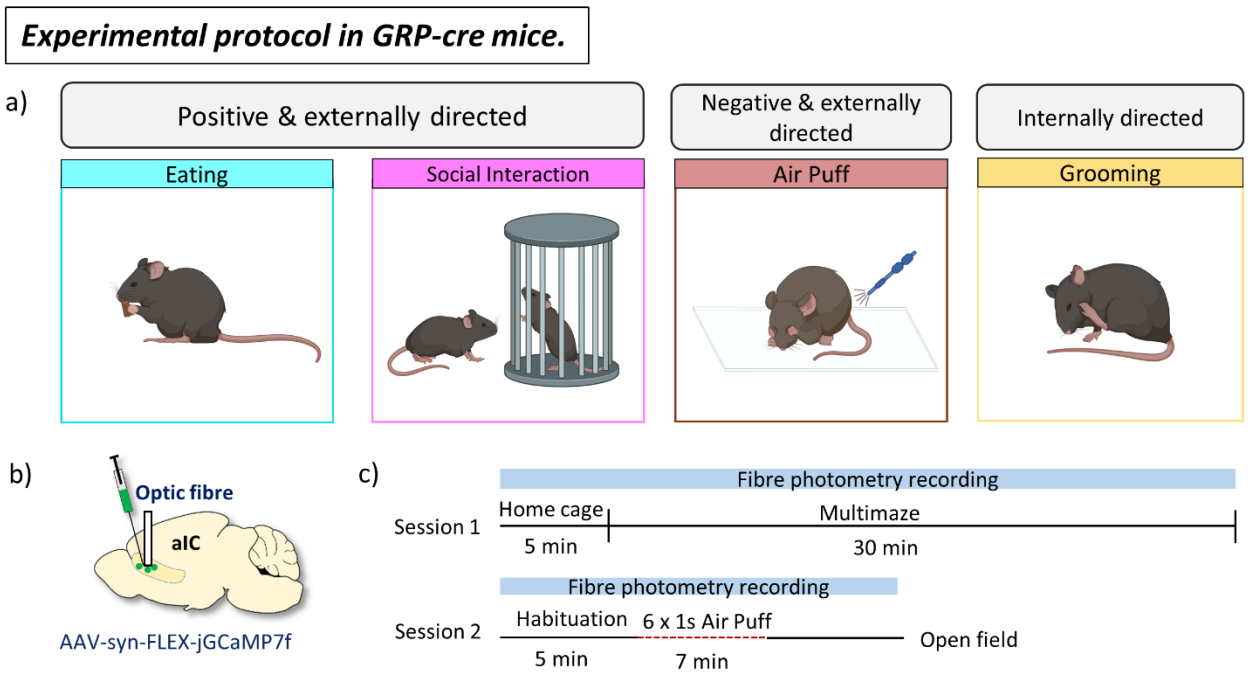

Figure 23: Experimental protocol for characterization of GRP-Cre line. a) *A selection of four behaviors used to assess the activity of the GRP-Cre neurons.* ***b)*** *Visual representation of injection and implantation site in the AIC.* ***c)*** *Experimental time-course. Top: The experiment performed in the Multimaze where eating, social interaction and grooming were measured. Bottom: a separate experiment was performed in an empty open field box to assess the response of GRP-Cre neurons to an air puff, a negatively-valenced stimulus.*

Characterization of the GRP-Cre neuronal activity revealed that this specific neuronal subpopulation responds similarly for some and differently for other behaviors compared to the bulk excitatory AIC activity. Similar to global AIC activity, the neurons showed a significant increase in activity during social interaction (**Figure 24b**), where activity increase was even greater than in wild-type mice. Furthermore, similar to the wild-type mice, GRP-Cre neuronal activity decreased during grooming (**Figure 24c**), with the decrease being smaller and less consistent compared to the wild-type animals. Interestingly, however, GRP-Cre neuronal activity significantly decreased during eating (**Figure 24a**), which is the opposite of what I observed in general excitatory AIC population. Finally, there seemed to be variable responses to the negatively-valenced air puff, with certain air puffs leading to an increase and certain to a decrease in AIC activity (**Figure 24d**). It is important to notice, however, that the signal was very noisy during the session that tested the effect of air puffs on GRP-Cre neuronal activity, which can be observed in highly variable trace and large signal error (**Figure 24d**). As such, it will be important to conduct further experiments to confirm the response of this subpopulation to negatively-valenced stimuli.

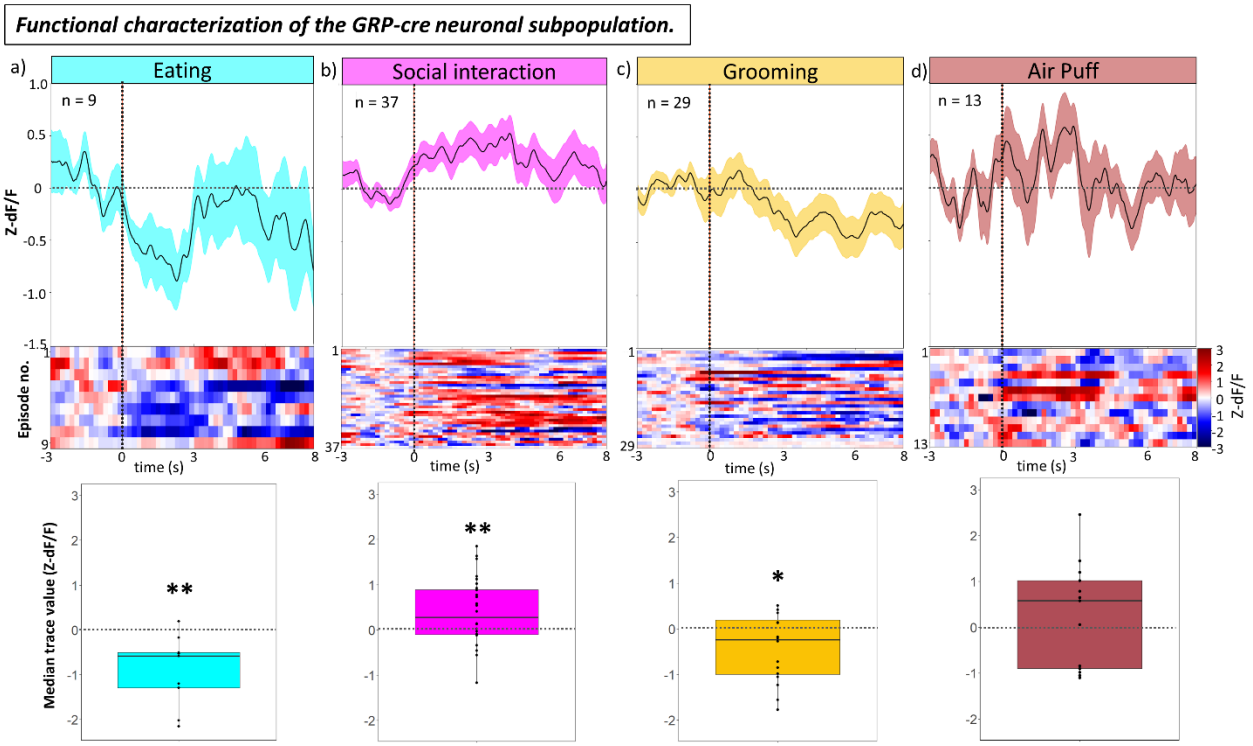

Figure 24: Functional characterization of GRP-Cre neuronal responses *(N = 3).* ***a-e) Top:*** *Mean + SEM traces for each of the four examined behaviors, normalized to the 3s time-window prior to the onset of behavior (time-point 0).* ***Middle:*** *Peri-event time histogram showing individual traces for the corresponding behaviors. Each trace is normalized to the 3 second window prior to the onset of behavior. All behaviors are plotted on the same scale.* ***Bottom:*** *A box plot representing relative change in Z-scored amplitude from the for each of the four behaviors. Each of the points represents a median value for the whole episode trace from the onset of behavior to the end of the behavior episode. Significance was determined using a two-tailed paired t-test. Eating: t = 3.4186, df = 8,* ***p** = 0.0091****; Social Interaction t = -2.8416, df = 27,*** ***p** = 0.00844****; Grooming:*** *t = 2.2408, df = 15,* ***p* = 0.0406****; Air Puff:*** *t = -0.80346, df = 12, p = 0.4373*

Overall, the above data suggest that GRP-Cre neurons exhibit a different activity profile compared to the global AIC. It is particularly interesting to notice that their activity corresponds neither to valence nor salience of the stimuli: they may respond with an increase or decrease in the case of salient and positively-valenced stimuli (eating and social interaction), and, based on my preliminary results, do not respond consistently to salient and negatively-valenced stimuli (air puff). Interestingly, the activity of these neurons also decreases during grooming; given that grooming is complex behavior with strong sensory and motor components, this suggests that in addition to valence and saliency, GRP-Cre neurons also do not encode purely somatosensory or motor information and may, as such, serve a more complex, or more specific role

Overall, the preliminary experiments probing structural and functional properties of genetically-determined AIC neuronal subpopulations reveal that the three subpopulations show diverse starter cell localization as well as projection patterns. Furthermore, based on the preliminary experiments conducted in the GRP-Cre line, my results suggest that different neuronal subpopulations also serve distinct functional roles within the AIC, with some of their responses matching and others differing to those observed in the general excitatory AIC population. While detailed understanding of the three populations will require further functional experiments including both measurements and perturbation of their activity, these preliminary results provide basic characterization of the in-so-far unexamined neuronal subpopulations within the AIC.

4. DISCUSSION

In my PhD thesis, I show that rodent AIC detects salient stimuli across different valences. Furthermore, my work reveals that optogenetic stimulation of the AIC leads to an increase in exploratory drive and behavior switching, suggesting that its stimulation prevents habituation-driven salience decrease. In addition, AIC stimulation led to a shift in behavioral preference towards externally rather than internally focused behaviors. Cumulatively, these findings suggest that similar to humans, rodent AIC plays a role as a salience detector and may contribute to behavior switching during flexible behavior. Finally, this thesis is, to my knowledge, the first piece of work to broadly characterize structural connectivity of the three genetically-determined neuronal subpopulations within the AIC, and to perform broad functional characterization of one of them.

4.1 AIC stimulation promotes behavioral switching and externally-focused behavior

To explore the role of the rodent AIC in behavior switching and flexibility, I designed a novel behavioral paradigm allowing freely moving mice to flexibly switch between three different behaviors while perturbing AIC activity. My results reveal that AIC stimulation significantly affects the animals' behavior, increasing locomotion as well as switching between behavioral zones. Interestingly, an increase in locomotion was observed in the Multimaze, but not in a separate open field test, suggesting that AIC stimulation does not affect locomotion per se. Rather, my results suggest that AIC stimulation may prevent a habituation-driven decrease in exploratory drive, as novelty of the environment decreases. Since novelty and saliency are strongly intertwined, this finding suggests that AIC stimulation may maintain the animals' exploratory drive by preventing salience decrease.

In addition to increased number of transitions and locomotion, I also found that AIC stimulation changed the relative amount of time the animals spent in different behavioral zones. Specifically, AIC stimulation increased the amount of time spent in eating and social

interaction zones and decreased the amount of time in the nesting zone. These results suggest that AIC stimulation shifts the animals' preference towards more externally oriented, executive and active behaviors, at the expense of internally focused behaviors. This is particularly interesting, as it suggests that AIC stimulation drives the balance between large-scale brain networks towards preferential engagement of the CEN, rather than the DMN. While direct confirmation of this hypothesis would require the use of whole-brain imagining techniques such as fMRI or functional ultrasound (fUS) imaging, my results are in line with recent findings showing that AIC stimulation in rats leads to a decoupling of rodent DMN[34]. As such, this study is the first to provide evidence for the role of AIC in behavioral switching in freely moving mice.

An interesting and important finding of this study is also the time-dependent effect of AIC stimulation on behavior. Interestingly, AIC stimulation had no measurable effect on the very first day of the experiment and only became measurable on the second experimental day (**Figure 10a,b**). This is of great importance, as it may suggest that within more complex experimental setups, a one-off experiment may not be sufficient to examine the effect of a certain region on behavior. This likely becomes of increasing importance as neuroscientists attempt to characterize the ever more complex nature of multifunctional higher-order cortical regions. Furthermore, it is also important to notice that while the effect was amplified with additional AIC stimulation on the following days, a smaller lingering effect could be observed during the first, stimulation-free segment, even after a 24 hour break from the stimulation (**Figure 10c**). This raises some important questions: what is the mechanism that underlies the threshold-like nature of its effect? Why does the effect of optogenetic stimulation get carried over into the next day? It is possible that AIC stimulation results in altered plasticity in either target or downstream regions, increasing their baseline activity or activation probability thus increasing the probability of behaviors which they govern? Studies have indeed shown that optogenetic stimulation can alter the balance of postsynaptic AMPA and NMDA receptors, both being known to govern changes in neuronal plasticity[163]. Furthermore, *in vitro* studies have revealed that ChR-mediated stimulation of certain neuronal pathways could lead to pathway-specific LTP induction[164], and multiple *in vivo* studies have shown that optogenetic stimulation can lead to longer-term changes in behavior[165–168]. To fully understand the lingering nature of acute optogenetic stimulation, it would thus be important to examine its effect on whole brain activity using whole-brain imagining (fMRI, fUS) or immediate early gene

staining (e.g. c-fos) techniques, followed by electrophysiological characterization of individual pathways and regions most affected by the perturbation.

4.2 AIC inhibition has no effect on complex behavior under given conditions

In addition to AIC stimulation, I also tested the effect of AIC inhibition on flexible behavior and behavior switching. However, I was unable to detect any effect of AIC inhibition on either the number of transitions between the zones, locomotion, or time spent in the zones. Given the strong effect of AIC stimulation, this is a rather surprising finding. One possibility to explain this observation is that while ChR-mediated artificial stimulation of the AIC alters behavioral switching, normal AIC activity is not necessary for it per se. Instead, AIC stimulation may drive downstream regions which are causally involved in appropriate behavioral switching. One such candidate region may be the AcbC, which is known to display strong connectivity with the IC[47,49]. A particularly interesting study conducted by Rogers-Carter et al. showed that stimulation of the IC-AcbC pathway increases social exploration of juvenile, but not adult, conspecifics[169]. Since mice perceive the company of juvenile conspecifics to be more salient than that of the adult mice, this suggests that IC-AcbC pathway is indeed involved in increasing the exploration of salient stimuli. Multiple other studies have shown that AcbC-mediated changes in behavioral flexibility depend primarily on dopamine (DA) release within ventral striatum[170,171]. As such, combining AIC stimulation with fiber photometry recordings of genetically-encoded DA sensors in the AcbC would allow one to study whether AIC stimulation effects may be mediated by an increase in DA release within AcbC. In addition to AcbC, prefrontal cortical areas are also known to display connectivity with the IC and have been implicated in behavioral flexibility. Studies have revealed that different prefrontal regions, such as orbitofrontal, prelimbic and infralimbic areas differentially affect strategy learning and reversal[172], and whereas other studies have demonstrated that, similar to AcbC, PFC's role in behavioral flexibility depends on DA release[173]. In addition, another study using a set-shifting task that requires animals to update their behavior in response to changing contingencies showed that neural ensembles within rodent PFC encode predicted action outcome as well as post-outcome discrimination activity, to evaluate whether the preformed behavior was successful in generating a reward or whether behavioral adaptation is required[174].

Dorsomedial striatum is another region known to display strong connectivity with the AIC and its perturbation has been shown to impair successful strategy shifting in rats[175]. Interestingly, the contribution of dorsomedial striatum to behavioral flexibility has been shown to depend on acetylcholine (ACh) signaling[176–178]. Given the implication of both DA and ACh in behavioral flexibility, future studies should characterize neuromodulatory properties of the AIC and assess the contribution of different neuromodulatory systems on flexible rodent behavior. It is also important to note, that the vast majority of the above studies examined the role of specific brain regions in behavioral flexibility within highly constrained and outcome-directed tasks, and as such cannot be directly compared to this study. Based on the complexity and variability of the above research, it seems likely that rodent behavioral flexibility is mediated by a number of regions acting in concordance with one another to mediate appropriate behavioral switching.

Given the AIC inhibition results, it is possible that unperturbed AIC activity is not necessary for behavioral switching per se. However, given the strong evidence the role of AIC in behavioral flexibility in humans, as well as my AIC stimulation and fiber photometry results, this seems unlikely. As such, it is important to discuss a few other factors that could contribute to the lack of observed effect. The first possible reason is the limited appropriateness of the given behavioral paradigm to measure the effect of decreased salience. As mentioned above, salience is highly linked to novelty, and would thus be expected to be the highest in the first experimental days and at the start of each experimental session. However, since I did not inhibit the AIC during the first 15-minute segment on each experimental day, I effectively missed the best time window to observe its effect. In previous experiments conducted in our lab, we have also observed that it is more challenging to observe the effect of IC inhibition compared to stimulation during specific tasks. For examine, one of our studies showed that while PIC stimulation produced an increase in anxiety response on a standard EPM test, the effect of PIC inhibition was only observed when the animals' fear state was additionally increased using electric foot shocks prior to the EPM[47]. As such, it is possible that the effect may only become measurable upon the introduction of a paradigm or behavior of higher saliency. A second reason for the lack of observed effect may be the choice of time-window during which inhibition was delivered. Compared to stimulation, optogenetic inhibition is already less potent and this may be especially problematic when illumination is delivered over longer, 15- to 30-minute time windows, as that may lead to engagement of compensatory mechanisms[179]. Indeed, one study examining the role of the hippocampal CA1 in memory recall showed that when optogenetic inhibition was delivered on a time-scale equivalent to that of pharmacological

inhibition (30 minutes or more), no effect was observed, whereas precise, time-locked optogenetic inhibition during the same task and in the same region resulted in a marked disruption in recall[180]. As such, a more appropriate way to examine the effect of AIC inhibition on salience detection would be to use a better behavioral paradigm that would combine increased salience and more precise AIC inhibition. There are a few options to achieve that: one possibility is to induce a more salient behavioral state, such as hunger, and inhibit AIC either throughout the experiment using pharmacogenetic tools such as Designer Receptors Exclusively Activated by Designer Drugs (DREADDs), or precisely when the animal chooses to eat. Another possibility would be to utilize a fear conditioning paradigm, where the animals learn that a sound cue predicts the arrival of a foot shock, a salient aversive stimulus, and inhibit AIC activity during either stimulus presentation or shock arrival. Another possibility would be to perform an oddball paradigm in head-fixed mice, where a deviant salient stimulus is presented to an animal in a stream of continuous stimuli and inhibit AIC upon the presentation of the deviant stimulus. A combination of one of more of these experiments controlled for possible confounding effects, such as disruption in memory formation in a fear conditioning paradigm, could give convincing evidence that AIC activity is necessary for salience detection. However, it is much more challenging to assess the role of AIC inhibition in spontaneous behavioral switching, with the main challenge being a difficulty in detecting the precise moments when behavioral switches occur. While it would be possible to increase the animals' exploration and behavior switching through administration of stimulant drugs such as amphetamines, even in the presence of AIC inhibition effect, it would be difficult to make a claim that it is truly salience of the environment, rather than perhaps interoceptive signals, that are being altered. A more interesting set of experiments in freely moving mice would be to induce a different baseline state such as depression or anxiety, as it has been shown both for humans[17,38,39,42], and mice[18] that this results in altered states of large-scale brain networks. From there, the experimenter could compare the effect of AIC inhibition on behavior to gauge its effect on the switching between large scale brain networks. Another possibility would be to assess spontaneous behavioral switching in head-fixed mice using behaviors such as a burrowing assay and inhibit the AIC as the mouse initiates the switch from ingress to egress and vice versa[181]. Even there, however, the decision to perform a behavior switch and the engagement of the relevant networks would likely precede the behavioral output, making correct timing of inhibition delivery challenging. Thus, to truly confirm the effect of AIC inhibition on network switching, whole-brain imaging techniques combined with optogenetic tools in awake and freely moving animals will be necessary.

Overall, my optogenetic experiments suggest the following role for the AIC in flexible behavior: in its neutral state, mouse AIC facilitates appropriate switching between internally and externally focused behaviors (**Figure 25**, **left**) which likely primarily relies on the mouse's homeostatic needs. However, upon AIC stimulation, this balance is shifted towards increased activity of the CEN, as seen in the animals' preferred engagement with externally focused behaviors at the expense of internally focused behaviors (**Figure 25**, **right**). Such an interpretation is further supported by the recent study showing that AIC stimulation leads to the decoupling of the rodent DMN[34], thus disrupting the naturally present balance between the networks. Under given experimental conditions, however, AIC inhibition is not potent enough to disrupt such balance, leaving behavior intact.

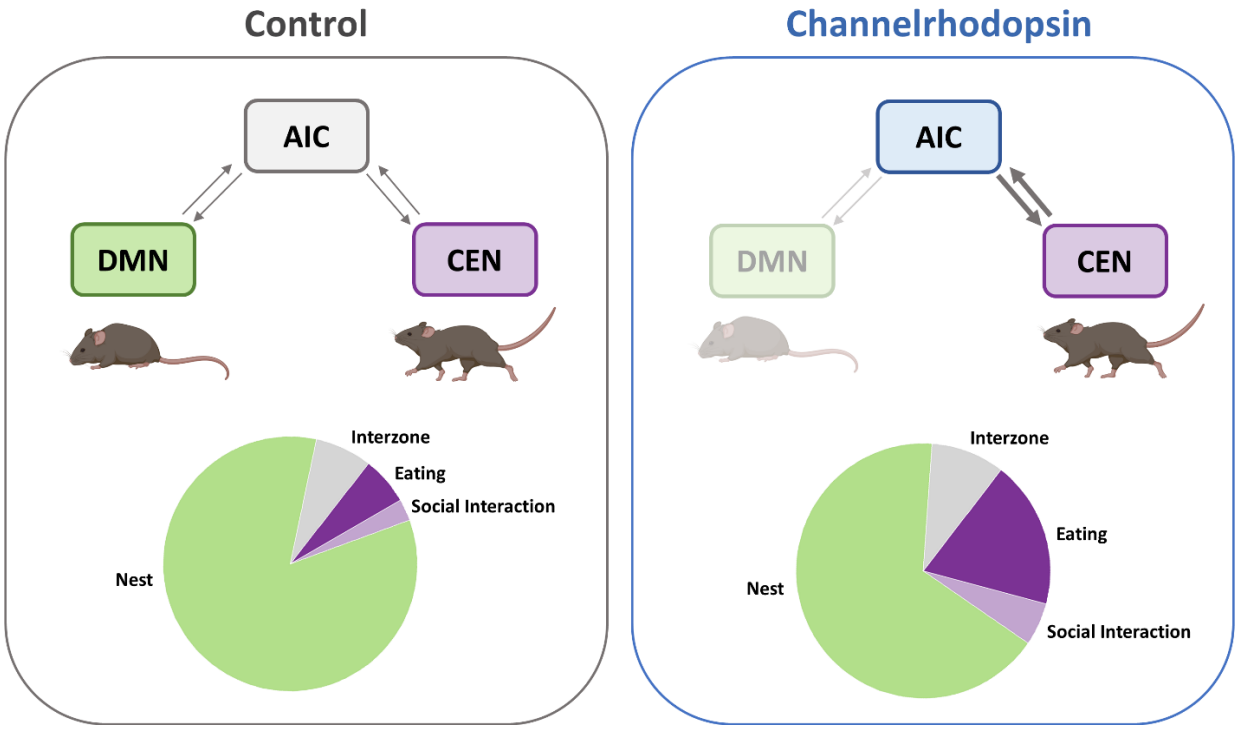

Figure 25: AIC stimulation shifts the balance between large scale brain networks towards preferential engagement of the CEN. *At the level of behavior, this is measurable in increased time the animals spend engaged in externally focused behaviors such as eating and social interaction at the expense of internally-focused behaviors such as nesting. The pie charts represent the proportions of cumulative time the mice spent in each of the zones across the five experimental days.*

4.3 AIC encodes salient stimuli across different valences

In the second part of my PhD project, I measured AIC activity during both flexible behavior and exposure to differently valenced stimuli to explore whether rodent AIC may indeed serve as salience detector. My results convincingly demonstrate that mouse AIC responds to both negatively and positively-valenced salient stimuli, confirming its role in salience detection. Furthermore, I show that when the same stimulus is made more salient by changing the animal's internal state through food deprivation, AIC response increases in both steepness and magnitude (**Figure 20**). My fiber photometry results thus convincingly demonstrate that, similar to humans, rodent AIC encodes salient stimuli regardless of their valence.

A particularly interesting observation was that AIC activity decreased during grooming, since grooming represents one of a few easily recognizable internally focused behaviors in mice. This led us to hypothesize that grooming may engage the DMN. This assumption is further supported by a study done in rats, which showed that grooming resulted in increased local field potential gamma-band oscillations, known to accompany DMN activation[159]. A specifically fascinating finding in that study was that an increase in gamma-band oscillations was even greater during grooming compared to the periods of quiet wakefulness, suggesting that grooming activates the DMN especially strongly. Fascinatingly, in my study, grooming resulted in a highly significant decrease in AIC activity, not observed during any other behavior or stimulus response. This is particularly interesting given the strong sensorimotor nature of grooming, and the IC's well-known involvement in detection of sensory stimuli[50,69,74,160,182]. AIC activity decrease during grooming is in stark contrast to the findings from other studies, which showed that grooming is accompanied by, or relies on, an increase in excitatory neuron signaling not only in the motor cortex but also in regions such as the medial amygdala (MeA)[183,184]. The last study is particularly interesting, as the MeA has been shown to form a part of the rodent DMN[18], further confirming that grooming may indeed represent appropriate behavior to serve as a proxy for the rodent DMN activity.

Our decision to conduct fiber photometry experiments in a complex Multimaze environment rather than to simply expose mice to stimuli of different valences was largely made as I hoped to observe changes in AIC activity at the moment of behavioral switch. However, it has proven

to be exceptionally challenging to detect the precise moment when the animal decides to switch behaviors. Part of the reason is that it is rather difficult to define what precisely a behavior switch even means. Is it the time point when the decision about behavior change is made? Is it the physical change in speed and direction towards the upcoming behavior of choice? Is it detection of a salient external stimulus or an internal state which prompts behavioral switch? The second issue is that either of the above possibilities would likely result in a relatively subtle change on a behavioral level and thus be difficult to observe. It is possible that new, unsupervised behavioral classification tools that are now emerging will be able to detect minute changes in the animals' behavior, thus allowing one to detect a precise moment when behavior switches. However, at this time, I was not able to collect neural data that would reveal how AIC behaves during behavior switching.

An interesting observation from my fiber photometry experiments was an increase in AIC activity preceding the start of eating behavior (**Figure 19**). This confirms that eating-evoked activity increase is not exclusively due to gustatory or appetitive components of the stimulus, but rather represents the anticipation of the upcoming appetitive behavior. Anticipatory signals were not observed before other salient behaviors such as foot shock or tail suspension, suggests that it requires the animal to voluntarily engage with the stimulus. Interestingly, the anticipation signal was no longer observed in food deprived animals. The reason could be that food deprived animals likely make an instant decision to feed in order to meet their homeostatic needs, which results in a much faster transitioning from other behaviors to feeding. This, in turn, shortens the time window between the decision to feed and the execution of eating behavior, during which such an anticipation signal would occur. On the contrary, in sated animals, the decision to feed would be slower and more gradual since there is no pressing homeostatic need to be met. This could be reflected in a slower signal rise, compared to a fast and sharp increase in food deprived animals. A better way to study the development of the anticipatory signal in sated and food deprived animals would be to train mice to associate an auditory cue with stimulus onset and record neuronal activity during the time-window between cue presentation and stimulus onset. A recent study exploring the role of a genetically defined layer V neuronal subpopulation within the AIC showed that these neurons exhibit an anticipatory signal which is significantly greater in thirsty compared to quenched animals[107]. My findings, however, suggest that such anticipatory signal may exhibit different properties in freely moving compared to head-fixed animals, and may actually be harder to detect in food deprived compared to sated animals. Of course, this could also be due to the difference in recorded neuronal populations, since I recorded bulk excitatory neuron activity in the AIC rather than

the specific neuronal subpopulation examined in the aforementioned study. As such, further studies employing more sophisticated recording techniques such as *in vivo* electrophysiology as well as the use of transgenic mouse lines will be needed to further elucidate specific neuronal subpopulations that underlie the anticipatory signal in the AIC.

Overall, my fiber photometry results provide convincing evidence that rodent AIC encodes salient stimuli regardless of their valence. This confirms that rodent AIC indeed possesses the necessary functional attributes to play an important role as a part of rodent salience network.

4.4 A proposed model of information flow through rodent IC

Taking the above results into consideration, this study provides functional evidence for the role of rodent AIC in salience detection and behavior switching. My fiber photometry experiments provide solid evidence that rodent AIC encodes salient stimuli across different valences while my optogenetic stimulation data suggest that an increase in AIC activity leads to an increase in behavior switching, shifting the animals' preference towards externally-focused behaviors such as eating and social interaction at the expense of more internally focused behaviors, such as resting.

Based on my study, as well as other rodent literature investigating the role of the rodent IC, I therefore propose that rodent IC likely plays a similar general role to that proposed for human IC. Rodent PIC has been shown to represent the sensory components of exteroceptive and interoceptive stimuli, as well as their valence and identity[47,49,97,100,103,105,185], while a recent study has also shown that it represents current and predicted physiological states[108]. In comparison, rodent AIC has been shown to be involved in higher-order processes such as social affective processes, risk taking, decision making and adaptive behaviors[102,182,186,187], as well as salience encoding and behavioral switching shown in current study. Based on that, I propose that information flows along rodent IC in a postero-anterior manner: posterior insular regions receive sensory, interoceptive and emotional information, integrating them with stimulus valence and identity to form a neural representation of an organism's unified state in given space and time. This neural representation then is continuously communicated to and updated

in the AIC, which is tasked with recognizing which of the stimuli in the organism's internal or external environment are salient given its current state. When a stimulus is marked as salient, the AIC, acting as a part of the saliency network, recruits other large-scale brain networks, predominantly the CEN, and suppresses the activity of the DMN, shifting the organism's attention to the salient situation at hand and engaging regions required for motor output and outward behavioral change. As such, similar to humans, rodent AIC may act as a gate of executive function, representing the causal outflow hub gating access to attention and working memory, and ultimately guiding appropriate behavioral adaptation in response to inward or outward change.

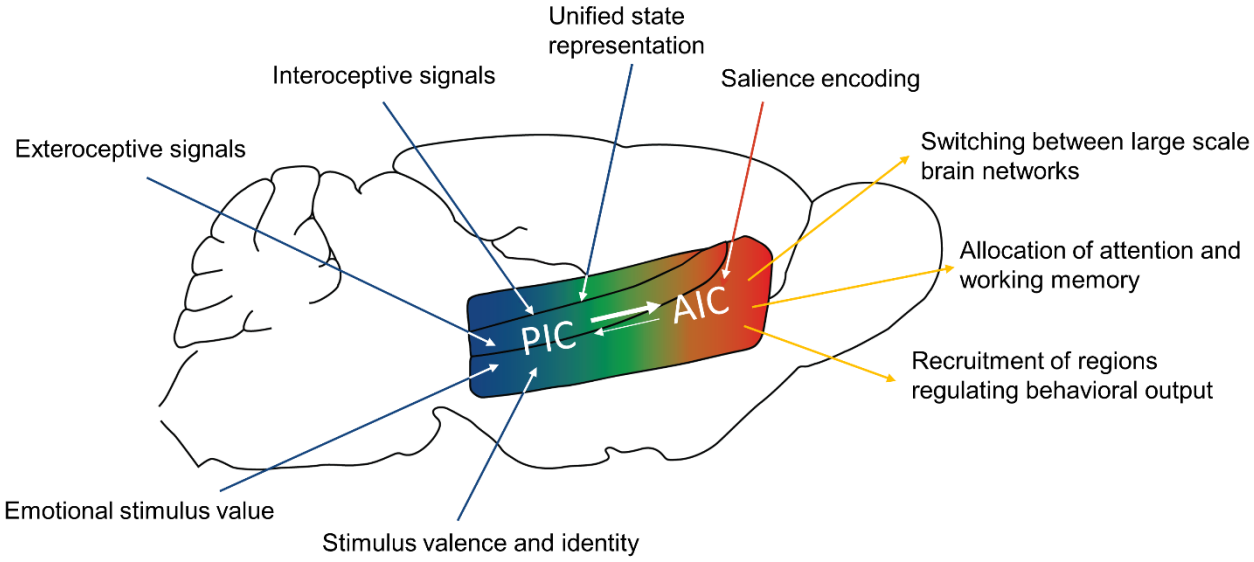

Figure 26: Information flow through rodent IC and proposed role of the AIC. *The studies conducted on the functional role of rodent IC so far suggest that information flow through it may be similar to that in humans. More posterior IC regions receive and integrate sensory, interoceptive, emotional, identity and valence qualities of different incoming stimuli. These are communicated to the AIC as an integrated neural representation of a current organism's state. As salience detector, the role of rodent AIC is to evaluate and identify internal and external stimuli as behaviorally relevant to an organism, and to guide correct behavioral responses by switching between large-scale brain networks, allocating attention and working memory and recruiting regions necessary for correct motor output.*

While it is likely that human AIC is involved in a larger number of more highly sophisticated cognitive functions such as internal dialogue, rumination, complex problem solving, planning and advanced emotion regulation - many of which may be lacking in rodents - the role of AIC in salience detection seems to remain conserved between both organisms. It is likely that, like humans, rodent AIC also plays additional roles in accessing and integrating attention, memory

and other higher-level cognitive processes. Further research is needed to confirm the precise functionality of rodent AIC and the extent of its similarity to humans. As such, it will be exciting to see further progress in the field of rodent large-scale brain networks research, especially as advanced whole-brain imaging techniques begin to be implemented in freely moving animals and combined with neural manipulation tools.

4.5 Structural and functional characterization of genetically determined AIC subpopulations

In the final chapter of this thesis, I present the results of basic structural and functional characterization of genetically determined neuronal subpopulations in the AIC. The three neuronal subpopulations expressed Cre recombinase under specific promoters, Sim1, Rgs14 and GRP. Detailed functions of the three genes are not presented in this work for a simple reason – the three mouse lines were chosen exclusively based on the subpopulations' strong Cre expression within the AIC rather than the known function of the three promoter genes. When examining the infected output cells, I observed that the three subpopulations exhibited spatially segregated starter cell placement within the AIC (**Figure 21**), with Rgs14-Cre and GRP-Cre lines exhibiting starter cell localization in surface layers II and III, and Sim1-Cre line in layer V. In future experiments, it will be important to precisely characterize the antero-posterior spread of the cells within the AIC and to combine *in situ* hybridization techniques with neuronal tracings to examine whether the starter cell populations are completely separate or if any overlap exists. It would also be interesting to perform simultaneous retrograde rabies or Cholera toxin subunit B (CTb) tracings from the core regions innervated by individual subpopulations combined with anterograde tracings or Cre-staining in the AIC, to gain detailed understanding about the percentage of genetically-labelled cells innervating any particular region.

In addition to different infected cell localization, the three lines also exhibited diverse projection patterns (**Figure 27**). None of the lines showed connectivity with the regions exclusively belonging to just one of the three large-scale brain networks: Sim1-Cre neurons also projected to certain regions belonging to all three networks: CeA belonging to the SN, ventral CPu and SNG belonging to the CEN, as well as zona incerta (ZI), retrosplenial cortex

(RSP), hippocampal and peri-hippocampal regions, and visual areas, which are all putative DMN regions (**Figure 27 top**). This is particularly interesting, as direct connectivity between AIC and RSP has so far not been found. Rgs14-Cre line showed strong connectivity with AcbC, CeA and BLA, all of which have been shown to belong to rodent salience network. However, it also projected to the lateral ventral CPu and substantia nigra (SNG), putative CEN regions, as well as visual, hippocampal and peri-hippocampal regions and ZI in the brainstem, which have been shown to belong to the rodent DMN[18] (**Figure 27**, **middle**). Of the three lines, GRP-Cre neurons exhibited the most specific and limited connectivity pattern, with weak fluorescence in the CPu, and a strong projection to the BLA, which represents a part of rodent SN. As opposed to the other two lines, GRP-Cre neurons did not send projections to the general posterior regions encompassing posterior cortical, midbrain and brainstem regions, with their projections localizing almost exclusively to the ENT (**Figure 27**, **bottom**). None of the three neuronal subpopulations projected to core DMN hubs such as prelimbic and anterior medial cortical areas, nor to the major cortical hubs of the CEN, such as primary motor and somatosensory areas, as well as certain thalamic nuclei. In general, the majority of the regions receiving inputs from all three lines belong to a putative rodent SN: AcbC, CeA, BLA and lateral CPu. This observation is in line with studies showing that regions within a specific large-scale network preferentially connect with other regions within the same network[18,32]. It is important to note, however, that axonal tracing experiments like the one presented in this study do not show exact synaptic connectivity, but rather exhibit generalized axonal labeling. As such, some of the structures highlighted here could have the axons simply passing through, rather than forming synaptic connections with, the labelled region. Further retrograde tracing studies from specific regions as well as anterograde tracings combined with synaptic tagging will be necessary to fully elucidate connectivity of the three neuronal subpopulations.

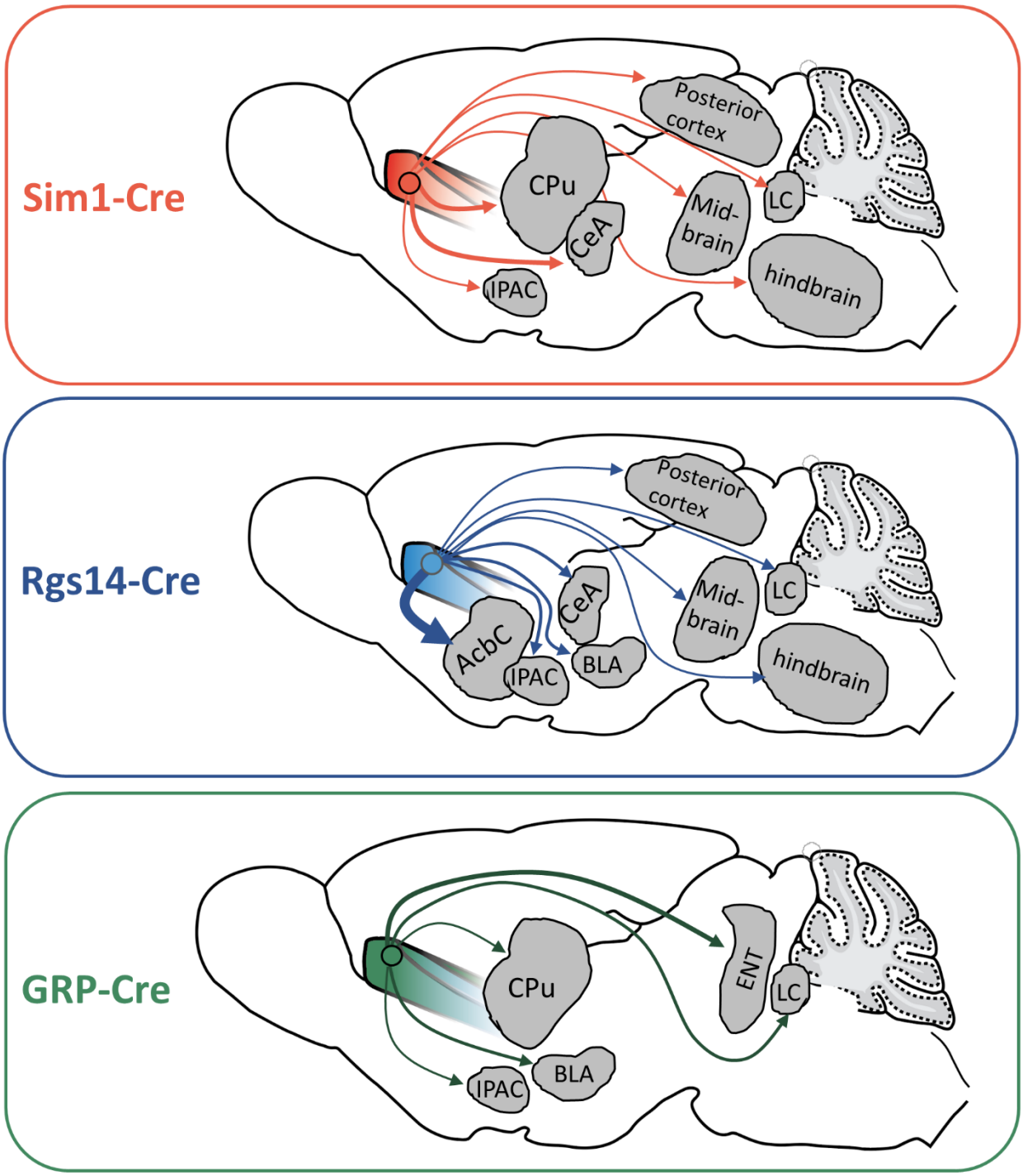

Figure 27. A schematic of output projection patterns for the three neuronal subpopulations. *The three AIC subpopulations exhibited spatially segregated starter cell placement and diverse, yet partially overlapping, projection patterns. The thickness of the arrows indicates putative connection strength based on the preliminary qualitative data analysis. Abbreviations: CPu: Caudate Putamen; AcbC: Nucleus Accumbens core; IPAC: the interstitial nucleus of the posterior limb of the anterior commissure; CeA: central amygdala; BLA: basolateral amygdala; ENT: entorhinal cortex; LC: locus coeruleus.*

In my thesis I also present preliminary functional data for the GRP-Cre neuronal subpopulation. Here I show that functional role of these neurons partially overlaps with and partially

differentiates from that of bulk excitatory AIC activity. Interestingly, GRP-Cre neurons encode neither purely salient nor valence-defined information; neuronal activity increased in response to social interaction but decreased in response to eating, both positively-valenced stimuli. In addition, it showed no consistent response to a negatively-valenced air puff. Similar to the excitatory AIC population, GRP-Cre subpopulation activity also decreased in response to grooming, suggesting it does not primarily process general somatosensory or motor information, given the strong sensorimotor component of grooming. This is an interesting observation, as rat studies have shown that intracerebroventricular administration of GRP results in increased grooming behavior[188,189]. However, the neurons I recorded from have, to my knowledge, never been fully characterized, and while they contain the *Grp* gene, this does not necessarily mean that they also release the GRP neuropeptide. Another interesting observation was a decrease in neuronal activity during eating. IC contains primary gustatory cortex, known to respond to taste information of different identity and valence[98–100,185]. While the gustatory portions of the IC are located more posteriorly, my CaMKII subpopulation recordings showed that the global excitatory subpopulation within the AIC responds strongly during eating. There have, however, been studies that showed that the intraperitoneal injection of certain forms of GRP protein in rats resulted in decreased appetite and increased inter-meal interval, suggesting that GRP plays and important role in regulating appetite and satiety[190–192]. Specifically, a study by Kyrkouli et al. showed that a microinjection of GRP into the amygdala induces an anorexic response in rats[192]. This is particularly interesting, given that my tracing study showed that AIC GRP neurons project to the BLA. BLA has been shown to play a role in processing appetitive information[193], and it contains diverse neuronal sub-circuitry, encoding both appetitive and aversive information[193–196]. As such, it would be interesting to examine precisely which BLA neurons are innervated by the GRP-Cre subpopulation – to achieve that, one could combine trans-synaptic rabies tracings with immunohistochemistry against specific neuronal markers. Another set of experiments to provide insight into the functional properties of the GRP-Cre neuron AIC-BLA projection, as well as other projections of this neuronal subpopulation, would be to use rabies virus-mediated trans-synaptic delivery of calcium indicators and simultaneously record from GRP-Cre starter neurons within the AIC and their target neurons within the BLA using fiber photometry or miniscope imaging.

In this thesis, I present no functional characterization of Rgs14-Cre and Sim1-Cre lines, primarily due to the difficulty of cell targeting with fiber photometry. Despite several attempts, the infected cells within the lines have proven to be distributed in a rather segregated manner, where even small deviations in targeting precision resulted in extremely low or completely

non-existent signal. It is possible, that the use of miniscopes would allow easier data collection given their larger field of view compared to fiber photometry (up to 1.1 by 1.1 mm compared to 200 μm optic fiber diameter), as well as their ability to discern individual cell bodies. While no functional data has been collected for these lines, their structural connectivity may provide some clues. Strong projections to the BLA and AcbC in Rgs14-Cre line suggest its involvement in emotionally salient processes. However, similarly to BLA, AcbC also exhibits complex internal connectivity, where D1- or D2-type medium spiny neurons may participate in either reward or aversion-related processes[197–200]. It would be particularly interesting to examine the AIC-BLA-AcbC circuitry within the Rgs14-Cre line, as it has been shown that certain emotional and motivational behaviors, such as reward seeking, are mediated specifically by a BLA to AcbC projection[201,202]. As such, it would be interesting to understand how a single neuronal subpopulation within the AIC simultaneously influences neuronal activity in both regions. An interesting observation in the Sim1-Cre line was the localization of the infected cells in cortical Layer V suggesting long-range output projections. Sim1-Cre neurons sent projections to the ventral part of CPu, as well as the CeA. A previous study from our lab showed that PIC-CeA projection mediates strong aversive responses[47], whereas other studies have shown it is responsible for encoding bitter taste[100]. As such, it is possible that this neuronal subpopulation may participate in aversive information processing and perhaps even fear, given the CeA's well-established role in fear and anxiety[203]. In addition, given its connectivity with the CPu, an important part of the basal ganglia motor system[204], it is possible that this subpopulation may mediate the transformation of aversive information into a motor response. However, while the examination of projection patterns may provide some clue about its functional role, further studies will be needed to elucidate precise structural and functional properties of the three neuronal subpopulations.

4.6 Limitations of the study

While the present study provides solid evidence for the involvement of rodent AIC in salience detection and behavioral flexibility, there are a few limitations one should be aware of when interpreting the findings. First, a major limitation of my optogenetic experiments is that the animals' behavior is represented as time in the zone rather than exact behaviors. As such, while the nesting zone was intended to represent internally focused behaviors such as wakeful rest,

other behaviors, such as sleep or active nesting, may have occurred. Likewise, there may have been cases where mice chose to lie down and rest in the eating zone. To try and compensate for such events, any experiments where data showed clear outliers were visually examined and any animal that used a specific zone for behaviors meant to be performed elsewhere was excluded. However, the sheer amount of video material (over 100 hours per cohort), made it impossible to manually examine each individual experiment. To deal with the volume of data, I initially attempted to employ pose estimation and behavioral classification algorithms to precisely label animals' behavior. However, while a behavioral classification pipeline was successfully established, my experimental setup proved to be too complex for tools at the time, as it contained and uneven and changeable background and many obstructions in the environment. As new and better pose-estimation and behavioral classification tools are being rapidly developed, future studies will be able to repeat my experiments and characterize the effect of AIC stimulation on flexible behavior with a greater level of precision. It would be particularly exciting if such tools would allow one to precisely define when a switch from one to another behavior happens and link that to activity measurements in the AIC. This would allow one to precisely examine the role of rodent AIC in behavior switching, compared to somewhat rough measurements such as the number of times that the animals transition between the zones.

Another obvious drawback of this study is the lack of techniques that could causally prove the effect of AIC stimulation on the activity of large-scale brain networks. While I can make reasonable assumptions, especially given recent studies showing causal interaction between AIC and the DMN[34,35], this study cannot definitively prove such assumptions without the use of whole-brain imaging techniques. To confirm my claims, one especially promising method is fUS imaging, which can provide insights into real-time whole-brain activity dynamics, and can be even implemented in awake freely moving animals[205,206]. The use of whole-brain imaging techniques will also be important to confirm my assumptions about certain behaviors engaging specific networks: while grooming seems to represent an internally-focused behavior and my observation of concurrent AIC activity decrease seems to supports such an assumption, this study cannot provide causal evidence to confirm that grooming truly engages core regions within the rodent DMN. Linked to this is also a difficulty to correctly interpret animals' behavior – while certain stimuli and behaviors such as electric shock or freezing may easily be interpreted as aversive, other behaviors, such as grooming or social interaction, have a strong contextual component, making them more or less salient, appetitive or aversive, depending on

the situation, which the AIC specifically has been shown to be sensitive to[102]. As such, future studies combining whole-brain imaging with activity perturbation in freely moving mice will be necessary to confirm any claims regarding the involvement of the rodent AIC in large-scale brain networks.

With regards to fiber photometry data collected in wild-type animals, a possible limitation could be the fact that the data comparing feeding-induced AIC activity increase in sated and food deprived animals were collected in two separate cohorts. While the coordinates and virus used for the two cohorts were the same and all the brains were checked for correct virus expression and fiber positioning, it is possible that larger signal amplitude and slope recorded in the second cohort could be due to higher viral expression or slightly different fiber positioning. This, however, seems unlikely, as signal amplitude and slope were consistently higher or lower in all the animals within a single cohort. If there were to be random differences in fiber placement and viral expression, one would expect similar amplitude and slope value distribution in both cohorts given a similar animal number. However, to definitively exclude this possibility, a within-animal control experiment, measuring feeding-evoked AIC activity during sated or food deprived state in the same animal, should be conducted.

Finally, an important limitation needs to be noted for AAV tracings in transgenic lines. While my experiments provide the first ever broad characterization of structural connectivity of three different AIC subpopulations, I performed neither detailed analysis of infected cell position within the AIC, nor axonal fiber counting, thus providing only rough connectivity data. Furthermore, it is important to note that AAV-virus mediated tracings only allow one to examine the number of labelled axonal fibers. As such, it is nearly impossible to determine whether the observed fluorescence is due to the axons passing through a certain structure, or if direct synaptic connectivity between the input neurons and the labelled region truly occurs. To overcome that, one could employ tools that use a fluorescent protein tagged to a synaptic marker such as synaptophysin (for example AAV-DIO-mRuby-T2A-synaptophysin-eGFP)[207] or even apply trans-synaptic transfection with AAV-Cre[208]. Those techniques would allow one to label synaptic terminals of the input cells or identify input-defined postsynaptic neurons and identify the exact regions that the three neuronal subpopulations synapse with.

APPENDICES

Table of figures

Supplementary Figures

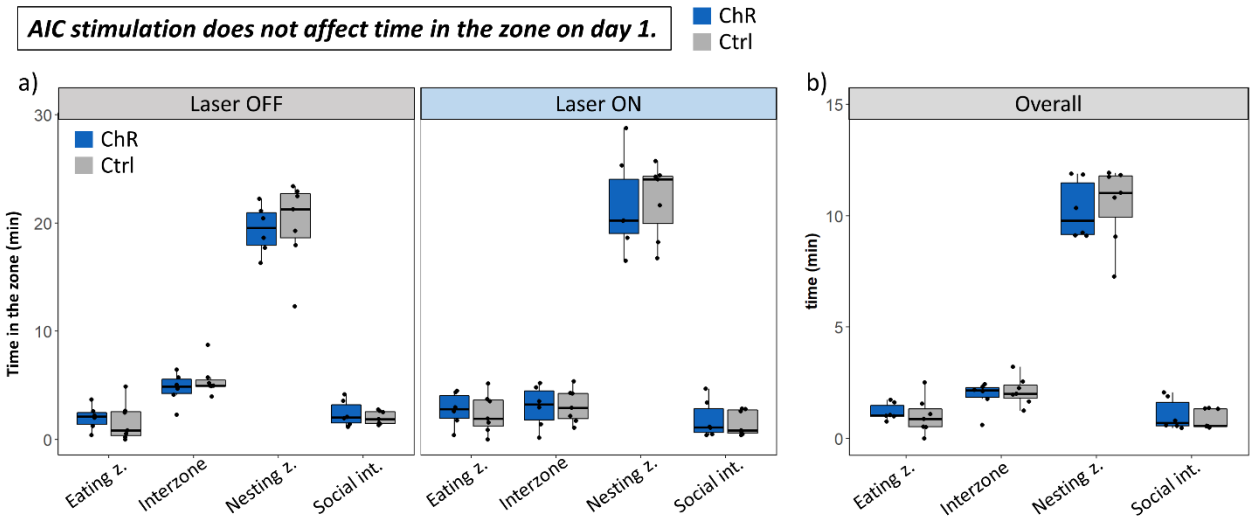

Supplementary Figure 1: Optogenetic stimulation has no effect on the amount of time spent in the zone on day 1 *(N = 6 ChR2.0, N = 10 eYFP, two-way ANOVA of time spent in the zone).* ***a)*** *AIC stimulation had no effect on time in the zone when separated based on absence or presence of AIC stimulation. Laser OFF: Group (opsin) effect: F(1, 44) = 0.065, p = 0.800; zone effect: F(3, 44) = 229.89, p**** < 0.0001; group x zone interaction effect: F(3, 44) = 0.294, p < 0.929. Laser ON: Group (opsin) effect: F(1, 44) = 0.000974, p = 0.975; zone effect: F(3, 44) = 204.83, p**** < 0.0001; group x zone interaction effect: F(3, 44) = 12.16, p < 0.96.* ***b)*** *There was no overall effect of the optogenetic stimulation on the time spent in the zone on day 1 (N = 6 ChR2.0, N = 10 eYFP, two-way ANOVA of time spent in the zone). Group (opsin) effect: F(1, 44) = 0.013, p = 0.911; zone effect: F(3, 44) = 287.89, p**** < 0.0001; group x zone interaction effect: F(3, 44) = 0.212, p < 0.887.*

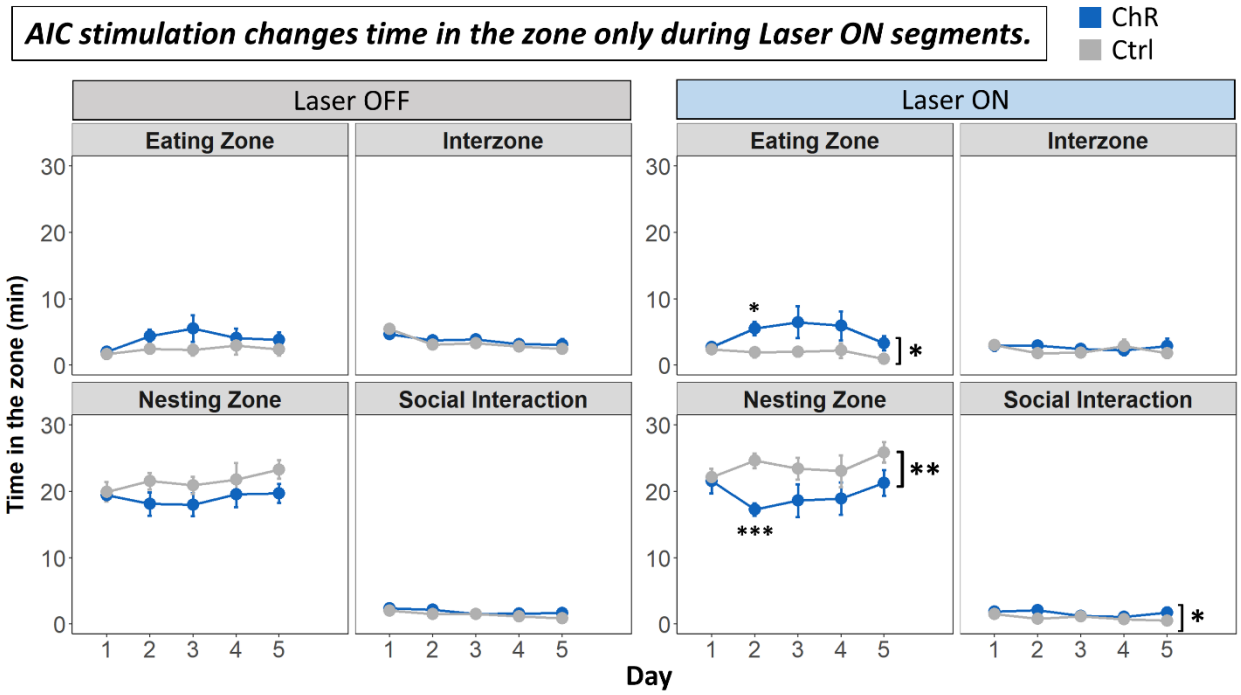

Supplementary Figure 2: The effect of AIC stimulation on time in the zone is confined exclusively to Laser ON (Q2 + Q4) periods *(N = 8 ChR2.0, N = 10 eYFP, Mixed-effects analysis of time in the zone).* ***Laser OFF: Eating zone:*** *Group (opsin) effect: F(1, 16) = 3.304, p = 0.0879; day effect: F (2.465, 35.33) = 0.1177, p = 0.924; group x day interaction effect: F (3, 43) = 0.3484, p = 0.7904.* ***Interzone:*** *Group (opsin) effect: F(1, 16) = 1.357, p = 0.261; day effect: F (1.985, 28.45) = 1.468, p = 0.247; group x day interaction effect: F(3, 43) = 0.0078, p = 0.999.* ***Nesting zone:*** *Group (opsin) effect: F(1, 16) = 3.778, p = 0.07; day effect: F (2.354, 33.75) = 0.7268, p = 0.512; group x day interaction effect: F (3, 43) = 0.1117, p = 0.953.* ***Social interaction zone:*** *Group (opsin) effect: F(1, 16) = 2.413, p = 0.140; day effect: F (2.404, 34.45) = 1.045, p = 0.373; group x day interaction effect: F(3, 43) = 0.465, p = 0.708.* ***Laser ON: Eating zone:*** *Group (opsin) effect: F(1, 16) = 8.044,* ***p* = 0.0119;*** *day effect: F (2.300, 32.97) = 1.403 p = 0.261; group x day interaction effect: F(3, 43) = 0.208, p = 0.891. Bonferroni post-hoc test;* ***day 2: p* = 0.049. Interzone****: Group (opsin) effect: F(1, 16) = 0.353, p = 0.561; day effect: F (2.105, 28.41) = 0.7706, p = 0.478; group x day interaction effect: F (4, 54) = 0.9650, p = 0.434.* ***Nesting zone:*** *Group (opsin) effect: F(1, 16) = 10.40,* ***p** = 0.005****; F (2.694, 38.62) = 1.147, p = 0.339; group x day interaction effect: F(3, 43) = 0.357, p = 0.784. Bonferroni post-hoc test;* ***day 2: p*** = 0.0005****. ***Social interaction zone:*** *Group (opsin) effect: F(1, 16) = 5.249,* ***p* = 0.0359****; day effect: F (2.776, 39.79) = 0.7948, p = 0.496; group x day interaction effect: F (3, 43) = 1.532, p = 0.219.*

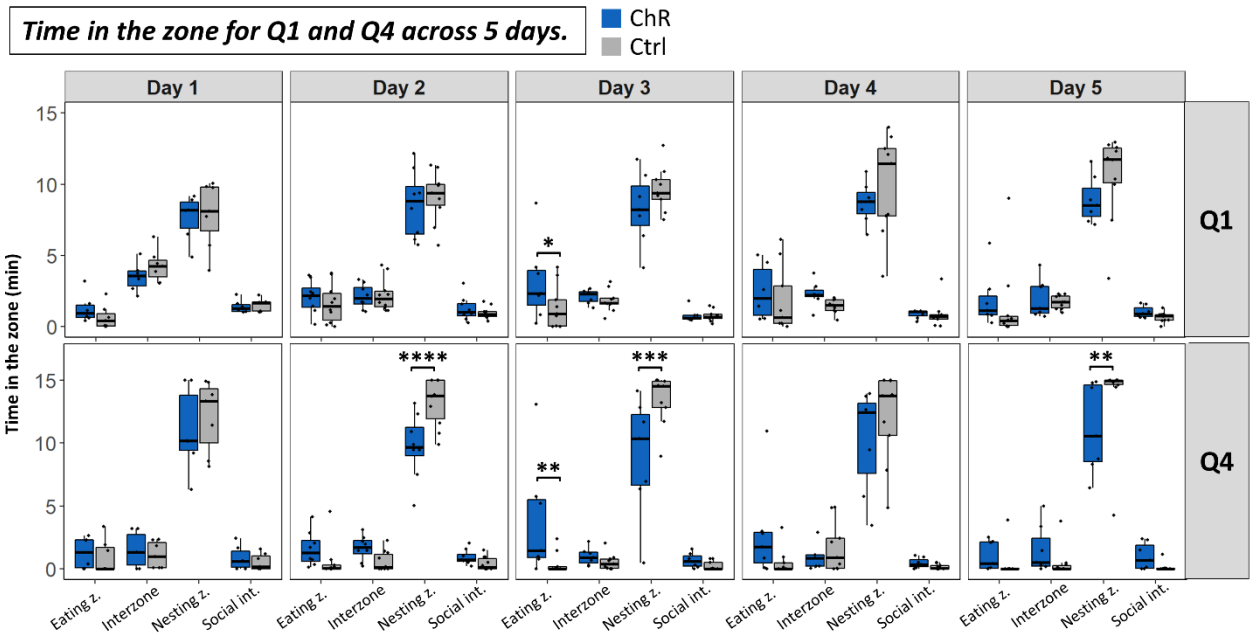

Supplementary Figure 3: Within-experiment time for each zone across all days. *(N = 8 ChR2.0, N = 10 eYFP; Two-way ANOVA of time spent in the zone). AIC stimulation has a significantly stronger effect in Q1 compared to Q4, but no effect is observed on day 1. Notice that the significance of the effect does not increase in Q1 over days, suggesting that stimulation effect returns to a relatively similar baseline between the end of one and the start of next experimental session. Statistical analysis for the plot is provided in* ***Supplementary Table 1****.*

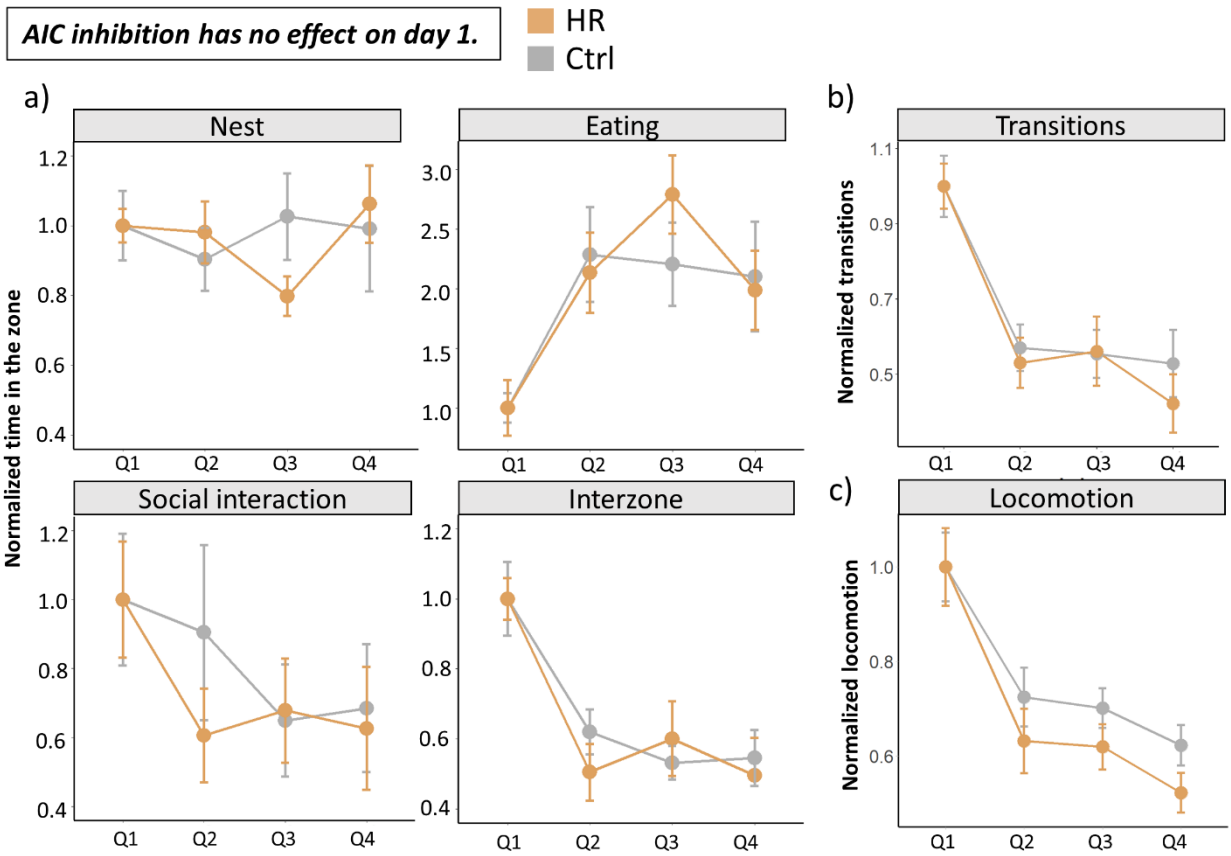

Supplementary Figure 4. AIC inhibition has no within-experiment effect on time in the zone, transitions or locomotion on day 1. *(N = 10 eNpHR3.0, N = 10 eYFP)* ***a)*** *2-way RM ANOVA of time in the zone.* ***Nesting zone:*** *Group (opsin) effect: F(1, 18) = 0.0403, p = 0.843; period effect: F (1.932, 34.77) = 1.112, p = 0.3385; group x period interaction effect: F (2, 36) = 2.407, p = 0.105.* ***Interzone:*** *Group (opsin) effect: F (1, 18) = 0.1254, p=0.7273; period effect: F (2, 36) = 0.2783, P=0.7587; group x period interaction effect F (2, 36) = 0.9484, p=0.3968.* ***Eating zone:*** *Group (opsin) effect: F (1, 18) = 0.1025, p=0.7526; period effect: F (1.929, 34.72) = 0.8518, P=0.4317; group x period interaction effect: F (2, 36) = 0.6989, p=0.5037.* ***Social interaction zone:*** *Group (opsin) effect: F (1, 18) = 0.2853, p=0.5998; period effect F (1.940, 34.92) = 0.3374, p=0.7095; group x period interaction effect: F (2, 36) = 0.8006, p=0.4569* ***b)*** *2-way RM ANOVA of transitions between the zones. Group (opsin) effect: F (1, 18) = 0.2833, p = 0.601; period effect: F (1.956, 35.20) = 1.383, p = 0.264; group x period interaction effect: F (2, 36) = 0.5404, p = 0.587.* ***c)*** *2-way RM ANOVA of locomotion. Group (opsin) effect: F (1, 18) = 2.561, p = 0.127; period effect: F (1.585, 28.54) = 4.074, p* < 0.036; group x period interaction effect: F (2, 36) = 0.02810, p = 0.972.*

Period - Day	Two-way ANOVA	Eating zone	Interzone	Nesting zone	Social interaction zone
Q1 – 1	Group: F (1, 44) = 0.123, p = 0.728 Zone: F(3, 44) = 77.226, p < 0.0001 Group x zone: F(3, 44) = 0.662, p = 0.58	p = 0.386	p = 0.279	p = 0.722	p = 0.902
Q1 – 2	Group: F (1, 64) = 0.014, p = 0.907 Zone: F(3, 64) = 126.33, p < 0.0001 Group x zone: F(3, 64) = 0.474, p = 0.702	p = 0.47	p = 0.876	p = 0.421	p = 0.637
Q1 – 3	Group: F (1, 56) = 0.176, p = 0.6 Zone: F(3, 56) = 90.111, p < 0.0001 Group x zone: F(3, 56) = 2.68, p = 0.056	**p* = 0.0291**	p = 0.734	p = 0.0846	p = 0.990
Q1 – 4	Group: F (1, 55) = 0.012, p = 0.914 Zone: F(3, 55) = 67.479, p < 0.0001 Group x zone: F(3, 55) = 0.971, p = 0.413	p = 0.542	p = 0.369	p = 0.195	p = 0.986
Q1 – 5	Group: F (1, 60) = 0.101, p = 0.752 Zone: F(3, 60) = 82.804, p < 0.0001 Group x zone: F(3, 60) = 1.221, p = 0.310	p = 0.617	p = 0.782	p = 0.0752	p = 0.695
Q4 – 1	Group: F (1, 44) = 0.004, p = 0.949 Zone: F(3, 44) = 104.737, p < 0.0001 Group x zone: F(3, 44) = 0.544, p = 0.655	p = 0.767	p = 0.706	p = 0.262	p = 0.743
Q4 – 2	Group: F (1, 64) = 0.519, p = 0.474 Zone: F(3, 64) = 244.369, p < 0.0001 Group x zone: F(3, 64) = 10.855, **p**** < 0.0001**	p = 0.137	p = 0.125	**p**** < 0.0001**	p = 0.444
Q4 – 3	Group: F (1, 56) = 0.003, p = 0.955 Zone: F(3, 56) = 73.055, p < 0.0001 Group x zone: F(3, 56) = 7.543, **p**** < 0.0001**	**p** = 0.0054**	p = 0.709	**p*** = 0.000435**	p = 0.722
Q4 – 4	Group: F (1, 56) = 0.000187, p = 0.989 Zone: F(3, 56) = 65.03, p < 0.0001 Group x zone: F(3, 56) = 1.91, p = 0.138	p = 0.077	p = 0.512	p = 0.164	p = 0.812
Q4 - 5	Group: F (1, 60) = 0.000134, p = 0.991 Zone: F(3, 60) = 141.807, p < 0.0001 Group x zone: F(3, 60) = 3.227, **p* = 0.029**	p = 0.501	p = 0.277	**p** = 0.0093**	p = 0.377

*Supplementary Table 1: Statistical analysis for **Supplementary Figure 3**.*

References

1. Uddin LQ. Cognitive and behavioural flexibility: neural mechanisms and clinical considerations. Nat Rev Neurosci. 2021;22(3):167–79.
2. Diamond A, Lee K. Interventions shown to aid executive function development in children 4 to 12 years old. Science. 2011;333.
3. Burt KB, Paysnick AA. Resilience in the transition to adulthood. Development and Psychopathology. 2012.
4. Burke SN, Mormino EC, Rogalski EJ, Kawas CH, Willis RJ, Park DC. What are the later life contributions to reserve, resilience, and compensation? Neurobiol Aging. 2019;83.
5. Scott WA. Cognitive Complexity and Cognitive Flexibility. Sociometry. 1962;25(4):405.
6. Brown VJ, Tait DS. Behavioral Flexibility: Attentional Shifting, Rule Switching, and Response Reversal. Encyclopedia of Psychopharmacology. 2015:264–9.
7. Dajani DR, Uddin LQ. Demystifying cognitive flexibility: Implications for clinical and developmental neuroscience. Trends in Neurosciences. 2015;38:571–8.
8. Behavior Rating Inventory of Executive Function, Adult Version. Definitions. 2020.
9. Menon V, Uddin LQ. Saliency, switching, attention and control: a network model of insula function. Brain Struct Funct. 2010
10. Miller EK, Cohen JD. An integrative theory of prefrontal cortex function. Annual Review of Neuroscience. 2001;24:167–202.
11. Müller NG, Knight RT. The functional neuroanatomy of working memory: Contributions of human brain lesion studies. Neuroscience. 2006;139(1).
12. Koechlin E, Summerfield C. An information theoretical approach to prefrontal executive function. Trends Cogn Sci. 2007;11(6):229–35.
13. Binder JR, Desai RH, Graves WW, Conant LL. Where is the semantic system? A critical review and meta-analysis of 120 functional neuroimaging studies. Cerebral Cortex. 2009;19(12).
14. Cabeza R, Prince SE, Daselaar SM, Greenberg DL, Budde M, Dolcos F, et al. Brain activity during episodic retrieval of autobiographical and laboratory events: An fMRI study using a novel photo paradigm. J Cogn Neurosci. 2004;16(9):1583–94.
15. Amodio DM, Frith CD. Meeting of minds: The medial frontal cortex and social cognition. Nature Reviews Neuroscience. 2006;7.
16. Buckner RL, Carroll DC. Self-projection and the brain. Trends Cogn Sci. 2007;11(2).
17. Buckner RL, Andrews-Hanna JR, Schacter DL. The brain's default network: Anatomy, function, and relevance to disease. Annals of the New York Academy of Sciences. 2008;1124:1–38.
18. Mandino F, Vrooman RM, Foo HE, Yeow LY, Bolton TAW, Salvan P, et al. A triple-network organization for the mouse brain. Mol Psychiatry. 2022;27(2):865–872.
19. Zerbi V, Grandjean J, Rudin M, Wenderoth N. Mapping the mouse brain with rs-fMRI: An optimized pipeline for functional network identification. Neuroimage. 2015;123:11–21.
20. Sforazzini F, Schwarz AJ, Galbusera A, Bifone A, Gozzi A. Distributed BOLD and CBV-weighted resting-state networks in the mouse brain. Neuroimage. 2014;87:403–15.
21. Gozzi A, Schwarz AJ. Large-scale functional connectivity networks in the rodent brain. NeuroImage. 2016;127:496–509.
22. Greicius MD, Krasnow B, Reiss AL, Menon V. Functional connectivity in the resting brain: A network analysis of the default mode hypothesis. Proc Natl Acad Sci U S A. 2003;100(1):253–8.
23. Greicius MD, Menon V. Default-mode activity during a passive sensory task: Uncoupled from deactivation but impacting activation. Journal of Cognitive Neuroscience. 2004:1484–92.
24. Uddin LQ, Yeo BTT, Spreng RN. Towards a Universal Taxonomy of Macro-scale Functional Human Brain Networks. Brain Topography. 2019;32.
25. Rudebeck PH, Behrens TE, Kennerley SW, Baxter MG, Buckley MJ, Walton ME, et al. Frontal cortex subregions play distinct roles in choices between actions and stimuli. Journal of Neuroscience. 2008;28(51):13775–85.
26. Vogt BA. Cingulate neurobiology and disease. 1st ed. Cingulate neurobiology and disease. Oxford: Oxford University Press; 2009.
27. Fox MD, Snyder AZ, Vincent JL, Corbetta M, van Essen DC, Raichle ME. The human brain is intrinsically organized into dynamic, anticorrelated functional networks. Proc Natl Acad Sci U S A. 2005;102(27).

28. Nekovarova T, Fajnerova I, Horacek J, Spaniel F. Bridging disparate symptoms of schizophrenia: A triple network dysfunction theory. Front Behav Neurosci. 2014;8(171).
29. Lu H, Zou Q, Gu H, Raichle ME, Stein EA, Yang Y. Rat brains also have a default mode network. Proc Natl Acad Sci U S A. 2012;109(10):3979–84.
30. Tsai PJ, Keeley RJ, Carmack SA, Vendruscolo JCM, Lu H, Gu H, et al. Converging Structural and Functional Evidence for a Rat Salience Network. Biol Psychiatry. 2020;88(11):867–78.
31. Shah D, Blockx I, Keliris GA, Kara F, Jonckers E, Verhoye M, et al. Cholinergic and serotonergic modulations differentially affect large-scale functional networks in the mouse brain. Brain Struct Funct. 2016;221(6):3067–79.
32. Stafford JM, Jarrett BR, Miranda-Dominguez O, Mills BD, Cain N, Mihalas S, et al. Large-scale topology and the default mode network in the mouse connectome. Proc Natl Acad Sci U S A. 2014;111(52):18745–50.
33. Hsu LM, Liang X, Gu H, Brynildsen JK, Stark JA, Ash JA, et al. Constituents and functional implications of the rat default mode network. Proc Natl Acad Sci U S A. 2016;113(31):E4541–7.
34. Menon V, Cerri D, Lee B, Yuan R, Lee SH. Optogenetic stimulation of anterior insular cortex neurons in male rats reveals causal mechanisms underlying suppression of the default mode network by the salience network. Nat Commun. 2023;14(866).
35. Chao THH, Lee B, Hsu LM, Cerri DH, Zhang WT, Wang WW, Ryali S, Menon V. Neuronal dynamics of the default mode network and anterior insular cortex: Intrinsic properties and modulation by salient stimuli. bioRxiv. 2022;9(7).
36. Kurth F, Zilles K, Fox PT, Laird AR, Eickhoff SB. A link between the systems: functional differentiation and integration within the human insula revealed by meta-analysis. Brain Struct Funct. 2010;214(5–6):519–34.
37. Downar J, Blumberger DM, Daskalakis ZJ. The Neural Crossroads of Psychiatric Illness: An Emerging Target for Brain Stimulation. Trends in Cognitive Sciences. 2016;20.
38. Mega MS, Cummings JL. Frontal-subcortical circuits and neuropsychiatric disorders. Journal of Neuropsychiatry and Clinical Neurosciences. 1994;6:358–70.
39. Doll A, Sorg C, Manoliu A, Wöller A, Meng C, Förstl H, et al. Shifted intrinsic connectivity of central executive and salience network in borderline personality disorder. Front Hum Neurosci. 2013;7(727).
40. Feurer C, Jimmy J, Chang F, Langenecker SA, Phan KL, Ajilore O, et al. Resting state functional connectivity correlates of rumination and worry in internalizing psychopathologies. Depress Anxiety. 2021;38(5):488–97.
41. Rotarska-Jagiela A, van de Ven V, Oertel-Knöchel V, Uhlhaas PJ, Vogeley K, Linden DEJ. Resting-state functional network correlates of psychotic symptoms in schizophrenia. Schizophr Res. 2010;117(1):21–30.
42. Whitfield-Gabrieli S, Ford JM. Default mode network activity and connectivity in psychopathology. Annual Review of Clinical Psychology. 2012;8:49–76.
43. Butti C, Hof PR. The insular cortex: a comparative perspective. Brain Struct Funct. 2010;214(5–6).
44. Shi CJ, Cassell MD. Cortical, thalamic, and amygdaloid connections of the anterior and posterior insular cortices. Journal of Comparative Neurology. 1998;399(4):440–68.
45. Mesulam M, Mufson EJ. Insula of the old world monkey. Architectonics in the insulo-orbito-temporal component of the paralimbic brain. Journal of Comparative Neurology. 1982;212(1).
46. Cechetto DF, Saper CB. Evidence for a viscerotopic sensory representation in the cortex and thalamus in the rat. J Comp Neurol. 1987 Aug 1 ;262(1):27–45.
47. Gehrlach DA, Dolensek N, Klein AS, Roy Chowdhury R, Matthys A, Junghänel M, et al. Aversive state processing in the posterior insular cortex. Nat Neurosci. 2019;22(9):1424–37.
48. Allen GV, Saper CB, Hurley KM, Cechetto DF. Organization of visceral and limbic connections in the insular cortex of the rat. Journal of Comparative Neurology. 1991;311(1).
49. Gehrlach DA, Weiand C, Gaitanos TN, Cho E, Klein AS, Hennrich AA, et al. A whole-brain connectivity map of mouse insular cortex. Elife. 2020;9(e55585).
50. Gogolla N. The insular cortex. Curr Biol. 2017 Jun 19;27(12):R580–6.
51. Cechetto DF, Chen SJ. Subcortical sites mediating sympathetic responses from insular cortex in rats. Am J Physiol Regul Integr Comp Physiol. 1990;258(1 27-1).
52. Simmons WK, Avery JA, Barcalow JC, Bodurka J, Drevets WC, Bellgowan P. Keeping the body in mind: Insula functional organization and functional connectivity integrate interoceptive, exteroceptive, and emotional awareness. Hum Brain Mapp. 2013;34(11).
53. Craig AD. How do you feel? Interoception: The sense of the physiological condition of the body. Nat Rev Neurosci. 2002;3(8):655–66.

54. van der Kooy D, Koda LY, McGinty JF, Gerfen CR, Bloom FE. The organization of projections from the cortes, amygdala, and hypothalamus to the nucleus of the solitary tract in rat. Journal of Comparative Neurology. 1984;224(1).
55. Allen D, Fakler B, Maylie J, Adelman JP. Organization and regulation of small conductance Ca2+-activated K+ channel multiprotein complexes. J Neurosci. 2007;
56. Shipley MT. Insular cortex projection to the nucleus of the solitary tract and brainstem visceromotor regions in the mouse. Brain Res Bull. 1982;8(2).
57. Saper CB. Reciprocal parabrachial-cortical connections in the rat. Brain Res. 1982;242(1).
58. Saper CB. Convergence of autonomic and limbic connections in the insular cortex of the rat. Journal of Comparative Neurology. 1982;210(2):163–73.
59. Ruggiero DA, Aovitch S, Granata AR, Anwar M, Reis DJ. A role of insular cortex in cardiovascular function. Journal of Comparative Neurology. 1987;257(2):189–207.
60. Yasui Y, Breder CD, Safer CB, Cechetto DF. Autonomic responses and efferent pathways from the insular cortex in the rat. Journal of Comparative Neurology. 1991;303(3):355–74.
61. Reynolds SM, Zahm DS. Specificity in the projections of prefrontal and insular cortex to ventral striatopallidum and the extended amygdala. Journal of Neuroscience. 2005;25(50).
62. Namburi P, Al-Hasani R, Calhoon GG, Bruchas MR, Tye KM. Architectural Representation of Valence in the Limbic System. Neuropsychopharmacology. 2016;41:697–715.
63. Floresco SB. The nucleus accumbens: An interface between cognition, emotion, and action. Annu Rev Psychol. 2015;66.
64. Jaramillo AA, Agan VE, Makhijani VH, Pedroza S, McElligott ZA, Besheer J. Functional role for suppression of the insular–striatal circuit in modulating interoceptive effects of alcohol. Addiction Biology. 2018;23(5):1020–31.
65. Naqvi NH, Bechara A. The hidden island of addiction: the insula. Trends Neurosci. 2009 Jan 1;32(1):56–67.
66. Mesulam M, Mufson EJ. Insula of the old world monkey. III: Efferent cortical output and comments on function. Journal of Comparative Neurology. 1982;212(1).
67. Flynn FG, Benson DF, Ardila A. Anatomy of the insula - Functional and clinical correlates. Aphasiology. 1999;13:55–78.
68. Gogolla N, Takesian AE, Feng G, Fagiolini M, Hensch TK. Sensory Integration in Mouse Insular Cortex Reflects GABA Circuit Maturation. Neuron. 2014;83(4).
69. Rodgers KM, Benison AM, Klein A, Barth DS. Auditory, somatosensory, and multisensory insular cortex in the rat. Cerebral Cortex. 2008;18(12):2941–51.
70. Qadir H, Krimmel SR, Mu C, Poulopoulos A, Seminowicz DA, Mathur BN. Structural connectivity of the anterior cingulate cortex, claustrum, and the anterior insula of the mouse. Front Neuroanat. 2018;12(100).
71. Science AI for B. Allen Institute for Brain Science (2004). Allen Mouse Brain Atlas. Available from mouse.brain-map.org.
72. Coghill RC, Sang CN, Maisog JM, Iadarola MJ. Pain intensity processing within the human brain: A bilateral, distributed mechanism. J Neurophysiol. 1999;82(4).
73. Hofbauer RK, Rainville P, Duncan GH, Bushnell MC. Cortical representation of the sensory dimension of pain. J Neurophysiol. 2001;86(1):402–11.
74. Craig AD, Chen K, Bandy D, Reiman EM. Thermosensory activation of insular cortex. Nat Neurosci. 2000;3(2).
75. Kupers RC, Gybels JM, Gjedde A. Positron emission tomography study of a chronic pain patient successfully treated with somatosensory thalamic stimulation. Pain. 2000;87(3).
76. Drzezga A, Darsow U, Treede RD, Siebner H, Frisch M, Munz F, et al. Central activation by histamine-induced itch: Analogies to pain processing: A correlational analysis of O-15 H2O positron emission tomography studies. Pain. 2001;92(1–2):295–305.
77. King AB, Menon RS, Hachinski V, Cechetto DF. Human forebrain activation by visceral stimuli. Journal of Comparative Neurology. 1999;413(4):572–82.
78. Williamson JW, McColl R, Mathews D, Ginsburg M, Mitchell JH. Activation of the insular cortex is affected by the intensity of exercise. J Appl Physiol. 1999;87(3):1213–9.
79. Craig AD. How do you feel — now? The anterior insula and human awareness. Nat Rev Neurosci. 2009 Jan 1;10(1):59–70.
80. Winston JS, Strange BA, O'Doherty J, Dolan RJ. Automatic and intentional brain responses during evaluation of trustworthiness of faces. Nat Neurosci. 2002;5(3):277–83.
81. Farrer C, Franck N, Georgieff N, Frith CD, Decety J, Jeannerod M. Modulating the experience of agency: A positron emission tomography study. Neuroimage. 2003;18(2).

82. Tsakiris M, Hesse MD, Boy C, Haggard P, Fink GR. Neural signatures of body ownership: A sensory network for bodily self-consciousness. Cerebral Cortex. 2007;17(10).
83. Barrett LF, Bliss-Moreau E, Quigley KS, Aronson KR. Interoceptive sensitivity and self-reports of emotional experience. J Pers Soc Psychol. 2004;87(5).
84. Livesey AC, Wall MB, Smith AT. Time perception: Manipulation of task difficulty dissociates clock functions from other cognitive demands. Neuropsychologia. 2007;45(2).
85. Mason MF, Norton MI, van Horn JD, Wegner DM, Grafton ST, Macrae CN. Wandering minds: The default network and stimulus-independent thought. Science. 2007;315(5810).
86. Weissman DH, Roberts KC, Visscher KM, Woldorff MG. The neural bases of momentary lapses in attention. Nat Neurosci. 2006;9(7).
87. Singer T, Seymour B, O'Doherty J, Kaube H, Dolan RJ, Frith CD. Empathy for Pain Involves the Affective but not Sensory Components of Pain. Science. 2004;303(5661):1157–62.
88. Huang Z, Tarnal V, Vlisides PE, Janke EL, McKinney AM, Picton P, et al. Anterior insula regulates brain network transitions that gate conscious access. Cell Rep. 2021;35(5):109081.
89. Song A, Jung WH, Jang JH, Kim E, Shim G, Park HY, et al. Disproportionate alterations in the anterior and posterior insular cortices in Obsessive-Compulsive disorder. PLoS One. 2011;6(7):e22361.
90. Nishida S, Narumoto J, Sakai Y, Matsuoka T, Nakamae T, Yamada K, et al. Anterior insular volume is larger in patients with obsessive-compulsive disorder. Prog Neuropsychopharmacol Biol Psychiatry. 2011;35(4):997–1001.
91. Nunn K, Frampton IJ, Gordon I, Lask B. The fault is not in her parents but in her insula - A neurobiological hypothesis of anorexia nervosa. European Eating Disorders Review. 2008;16(5):355–60.
92. Sprengelmeyer R, Steele JD, Mwangi B, Kumar P, Christmas D, Milders M, et al. The insular cortex and the neuroanatomy of major depression. J Affect Disord. 2011;133(1–2):120–7.
93. Shin LM, Liberzon I. The neurocircuitry of fear, stress, and anxiety disorders. Neuropsychopharmacology. 2010;35:169–91.
94. Shi T, Feng S, Wei M, Zhou W. Role of the anterior agranular insular cortex in the modulation of fear and anxiety. Brain Res Bull. 2020;155:174–83.
95. D'Cruz AM, Ragozzino ME, Mosconi MW, Shrestha S, Cook EH, Sweeney JA. Reduced behavioral flexibility in autism spectrum disorders. Neuropsychology. 2013;27(2):152–60.
96. Manoliu A, Meng C, Brandl F, Doll A, Tahmasian M, Scherr M, et al. Insular dysfunction within the salience network is associated with severity of symptoms and aberrant inter-network connectivity in major depressive disorder. Front Hum Neurosci. 2014;7(930).
97. Tan LL, Pelzer P, Heinl C, Tang W, Gangadharan V, Flor H, et al. A pathway from midcingulate cortex to posterior insula gates nociceptive hypersensitivity. Nat Neurosci. 2017;20(11):1591–1601.
98. Wang L, Gillis-Smith S, Peng Y, Zhang J, Chen X, Salzman CD, et al. The coding of valence and identity in the mammalian taste system. Nature. 2018 Jun 30;558(7708):127–31.
99. Chen X, Gabitto M, Peng Y, Ryba NJP, Zuker CS. A Gustotopic Map of Taste Qualities in the Mammalian Brain. Science (1979). 2011 Sep 2;333(6047):1262–6.
100. Peng Y, Gillis-Smith S, Jin H, Tränkner D, Ryba NJP, Zuker CS. Sweet and bitter taste in the brain of awake behaving animals. Nature. 2015;527(7579).
101. Bermudez-Rattoni F, Okuda S, Roozendaal B, McGaugh JL. Insular cortex is involved in consolidation of object recognition memory. Learn Mem. 2005 Sep 1;12(5):447–9.
102. Rogers-Carter MM, Varela JA, Gribbons KB, Pierce AF, McGoey MT, Ritchey M, et al. Insular cortex mediates approach and avoidance responses to social affective stimuli. Nat Neurosci. 2018 Mar 29;21(3):404–14.
103. Contreras M, Ceric F, Torrealba F. Inactivation of the interoceptive insula disrupts drug craving and malaise induced by lithium. Science. 2007 Oct 26;318(5850):655–8.
104. Livneh Y, Ramesh RN, Burgess CR, Levandowski KM, Madara JC, Fenselau H, et al. Homeostatic circuits selectively gate food cue responses in insular cortex. Nature. 2017 Jun 14;546(7660):611–6.
105. Klein AS, Dolensek N, Weiand C, Gogolla N. Fear balance is maintained by bodily feedback to the insular cortex in mice. Science. 2021;374(6570):1010–5.
106. Koren T, Yifa R, Amer M, Krot M, Boshnak N, Ben-Shaanan TL, et al. Insular cortex neurons encode and retrieve specific immune responses. Cell. 2021;184(24).
107. Deng H, Xiao X, Yang T, Ritola K, Hantman A, Li Y, et al. A genetically defined insula-brainstem circuit selectively controls motivational vigor. Cell. 2021;184(26):6344-6360.e18.
108. Livneh Y, Sugden AU, Madara JC, Essner RA, Flores VI, Sugden LA, et al. Estimation of Current and Future Physiological States in Insular Cortex. Neuron. 2020;105(6):1094-1111.e10.
109. Crottaz-Herbette S, Menon V. Where and when the anterior cingulate cortex modulates attentional response: Combined fMRI and ERP evidence. J Cogn Neurosci. 2006;18(5).

110. Downar J, Crawley AP, Mikulis DJ, Davis KD. The effect of task relevance on the cortical response to changes in visual and auditory stimuli: An event-related fMRI study. Neuroimage. 2001;14(6).
111. Linden DEJ, Prvulovic D, Formisano E, Völlinger M, Zanella FE, Goebel R, et al. The functional neuroanatomy of target detection: An fMRI study of visual and auditory/oddball tasks. Cerebral Cortex. 1999;9(8).
112. Downar J, Crawley AP, Mikulis DJ, Davis KD. A multimodal cortical network for the detection of changes in the sensory environment. Nat Neurosci. 2000;3(3):277–283.
113. Downar J, Crawley AP, Mikulis DJ, Davis KD. A cortical network sensitive to stimulus salience in a neutral behavioral context across multiple sensory modalities. J Neurophysiol. 2002;87(1):615–20.
114. Molnar-Szakacs I, Uddin LQ. Anterior insula as a gatekeeper of executive control. Neurosci Biobehav Rev. 2022 Aug 1;139:104736.
115. Logothetis NK. What we can do and what we cannot do with fMRI. Nature. 2008;453.
116. Teegarden S. Behavioral Phenotyping in Rats and Mice. Materials and Methods. 2012;2.
117. Grienberger C, Konnerth A. Imaging Calcium in Neurons. Neuron. 2012;73.
118. Bernstein JG, Boyden ES. Optogenetic tools for analyzing the neural circuits of behavior. Trends in Cognitive Sciences. 2011;15.
119. Homberg JR. Measuring behaviour in rodents: Towards translational neuropsychiatric research. Behavioural Brain Research. 2013;236.
120. Dennis EJ, Hady A el, Michaiel A, Clemens A, Gowan Tervo DR, Voigts J, et al. Systems neuroscience of natural behaviors in rodents. Journal of Neuroscience. 2021.
121. Krakauer JW, Ghazanfar AA, Gomez-Marin A, MacIver MA, Poeppel D. Neuroscience Needs Behavior: Correcting a Reductionist Bias. Neuron. 2017;93.
122. Hoy JL, Yavorska I, Wehr M, Niell CM. Vision Drives Accurate Approach Behavior during Prey Capture in Laboratory Mice. Current Biology. 2016;26(22).
123. Forkosh O, Karamihalev S, Roeh S, Alon U, Anpilov S, Touma C, et al. Identity domains capture individual differences from across the behavioral repertoire. Nat Neurosci. 2019;22(12).
124. Tervo DGR, Kuleshova E, Manakov M, Proskurin M, Karlsson M, Lustig A, et al. The anterior cingulate cortex directs exploration of alternative strategies. Neuron. 2021;109(11).
125. Ragozzino ME, Wilcox C, Raso M, Kesner RP. Involvement of rodent prefrontal cortex subregions in strategy switching. Behavioral Neuroscience. 1999;113(1).
126. Ragozzino ME, Detrick S, Kesner RP. Involvement of the prelimbic-infralimbic areas of the rodent prefrontal cortex in behavioral flexibility for place and response learning. Journal of Neuroscience. 1999;19(11).
127. Hamilton DA, Brigman JL. Behavioral flexibility in rats and mice: Contributions of distinct frontocortical regions. Genes, Brain and Behavior. 2015;14:4–21.
128. Biró S, Lasztóczi B, Klausberger T. A visual two-choice rule-switch task for head-fixed mice. Front Behav Neurosci. 2019;13.
129. Nagy A. Cre recombinase: The universal reagent for genome tailoring. Genesis. 2000;26:99–109.
130. Utomo ARH, Nikitin AY, Lee WH. Temporal, spatial of and cell type-specified control of cre-mediated DNA recombination in transgenic mice. Nat Biotechnol. 1999;17(11):1091–6.
131. Yizhar O, Fenno LE, Davidson TJ, Mogri M, Deisseroth K. Optogenetics in Neural Systems. Neuron. 2011;71.
132. Fenno L, Yizhar O, Deisseroth K. The development and application of optogenetics. Annu Rev Neurosci. 2011;34.
133. Boyden ES, Zhang F, Bamberg E, Nagel G, Deisseroth K. Millisecond-timescale, genetically targeted optical control of neural activity. Nat Neurosci. 2005;8(9):1263–1268.
134. Mattis J, Tye KM, Ferenczi EA, Ramakrishnan C, O'Shea DJ, Prakash R, et al. Principles for applying optogenetic tools derived from direct comparative analysis of microbial opsins. Nat Methods. 2012;9(2):159–72.
135. Gradinaru V, Zhang F, Ramakrishnan C, Mattis J, Prakash R, Diester I, et al. Molecular and Cellular Approaches for Diversifying and Extending Optogenetics. Cell. 2010;141(1):154–65.
136. Zhang F, Gradinaru V, Adamantidis AR, Durand R, Airan RD, de Lecea L, et al. Optogenetic interrogation of neural circuits: Technology for probing mammalian brain structures. Nature Protocols. 2010;5.
137. Shirai F, Hayashi-Takagi A. Optogenetics: Applications in psychiatric research. Psychiatry Clin Neurosci. 2017;71(6):363–72.
138. Häusser M. Optogenetics: The age of light. Nat Methods. 2014;11(10):1012–1014.
139. Zimmermann D, Zhou A, Kiesel M, Feldbauer K, Terpitz U, Haase W, et al. Effects on capacitance by overexpression of membrane proteins. Biochem Biophys Res Commun. 2008;369(4):1022–6.

140. Liu L, Ito W, Morozov A. Overexpression of channelrhodopsin-2 interferes with the GABAb receptor-mediated depression of GABA release from the somatostatin-containing interneurons of the prefrontal cortex. Neurophotonics. 2018;5(02):1.
141. Kravitz AV, Bonci A. Optogenetics, physiology, and emotions. Front Behav Neurosci. 2013;7.
142. Tank DW, Sugimori M, Connor JA, Llinás RR. Spatially resolved calcium dynamics of mammalian Purkinje cells in cerebellar slice. Science. 1988;242(4879):773–7.
143. Baker PF, Hodgkin AL, Ridgway EB. Depolarization and calcium entry in squid giant axons. J Physiol. 1971;218(3):709–55.
144. Chen TW, Wardill TJ, Sun Y, Pulver SR, Renninger SL, Baohan A, et al. Ultrasensitive fluorescent proteins for imaging neuronal activity. Nature. 2013;499(7458):295–300.
145. Dana H, Sun Y, Mohar B, Hulse BK, Kerlin AM, Hasseman JP, et al. High-performance calcium sensors for imaging activity in neuronal populations and microcompartments. Nat Methods. 2019;16(7):649–57.
146. Inoue M. Genetically encoded calcium indicators to probe complex brain circuit dynamics in vivo. Neuroscience Research. 2021;169:2–8.
147. Helmchen F, Denk W. Deep tissue two-photon microscopy. Nature Methods. 2005;2:932–40.
148. Ericson MB, Simonsson C, Guldbrand S, Ljungblad C, Paoli J, Smedh M. Two-photon laser-scanning fluorescence microscopy applied for studies of human skin. J Biophotonics. 2008;1(4):320–30.
149. Aharoni D, Hoogland TM. Circuit investigations with open-source miniaturized microscopes: Past, present and future. Frontiers in Cellular Neuroscience. 2019;13.
150. Gunaydin LA, Grosenick L, Finkelstein JC, Kauvar I v., Fenno LE, Adhikari A, et al. Natural neural projection dynamics underlying social behavior. Cell. 2014;157(7):1535–51.
151. Cui G, Jun SB, Jin X, Pham MD, Vogel SS, Lovinger DM, et al. Concurrent activation of striatal direct and indirect pathways during action initiation. Nature. 2013;494(7436):238–42.
152. Siciliano CA, Tye KM. Leveraging calcium imaging to illuminate circuit dysfunction in addiction. Alcohol. 2018
153. Zhou X, Belavek KJ, Miller EW. Origins of Ca2+Imaging with Fluorescent Indicators. Biochemistry. 2021;60(46).
154. Chamberlin NL, Du B, de Lacalle S, Saper CB. Recombinant adeno-associated virus vector: Use for transgene expression and anterograde tract tracing in the CNS. Brain Res. 1998;793(1–2):169–75.
155. Xiao X, Li J, McCown TJ, Samulski RJ. Gene transfer by adeno-associated virus vectors into the central nervous system. Exp Neurol. 1997;144(1):113–24.
156. Mathis A, Mamidanna P, Cury KM, Abe T, Murthy VN, Mathis MW, et al. DeepLabCut: markerless pose estimation of user-defined body parts with deep learning. Nat Neurosci. 2018 Sep 20;21(9):1281–9.
157. Moriya S, Yamashita A, Masukawa D, Kambe Y, Sakaguchi J, Setoyama H, et al. Involvement of supralemniscal nucleus (B9) 5-HT neuronal system in nociceptive processing: A fiber photometry study. Mol Brain. 2020;13(14).
158. Sych Y, Chernysheva M, Sumanovski LT, Helmchen F. High-density multi-fiber photometry for studying large-scale brain circuit dynamics. Nat Methods. 2019;16(6):553–60.
159. Nair J, Klaassen AL, Arato J, Vyssotski AL, Harvey M, Rainer G. Basal forebrain contributes to default mode network regulation. Proc Natl Acad Sci U S A. 2018;115(6):1352–7.
160. Lu C, Yang T, Zhao H, Zhang M, Meng F, Fu H, et al. Insular Cortex is Critical for the Perception, Modulation, and Chronification of Pain. Neuroscience Bulletin. 2016;32:191–201.
161. Gong S, Doughty M, Harbaugh CR, Cummins A, Hatten ME, Heintz N, et al. Targeting Cre recombinase to specific neuron populations with bacterial artificial chromosome constructs. Journal of Neuroscience. 2007;27:9817–23.
162. The Gene Expression Nervous System Atlas (GENSAT) Project, NINDS Contracts N01NS02331 & HHSN271200723701C to the Rockefeller University (New York, NY).
163. Goold CP, Nicoll RA. Single-Cell Optogenetic Excitation Drives Homeostatic Synaptic Depression. Neuron. 2010;68(3):512–28.
164. Morozov A, Sukato D, Ito W. Selective suppression of plasticity in amygdala inputs from temporal association cortex by the external capsule. Journal of Neuroscience. 2011;31(1):339–45.
165. Liu X, Ramirez S, Pang PT, Puryear CB, Govindarajan A, Deisseroth K, et al. Optogenetic stimulation of a hippocampal engram activates fear memory recall. Nature. 2012;484(7394):381–5.
166. Pascoli V, Turiault M, Lüscher C. Reversal of cocaine-evoked synaptic potentiation resets drug-induced adaptive behaviour. Nature. 2012;481(7379):71–6.
167. Tye KM, Mirzabekov JJ, Warden MR, Ferenczi EA, Tsai HC, Finkelstein J, et al. Dopamine neurons modulate neural encoding and expression of depression-related behaviour. Nature. 2013;493(7433):537–41.
168. Xie YF, Jackson MF, Macdonald JF. Optogenetics and synaptic plasticity. Acta Pharmacologica Sinica. 2013;34:1381–5.

169. Rogers-Carter MM, Djerdjaj A, Gribbons KB, Varela JA, Christianson JP. Insular cortex projections to nucleus accumbens core mediate social approach to stressed juvenile rats. Journal of Neuroscience. 2019;39(44):8717–29.
170. Haluk DM, Floresco SB. Ventral striatal dopamine modulation of different forms of behavioral flexibility. Neuropsychopharmacology. 2009;34(8):2041–52.
171. Aquili L, Liu AW, Shindou M, Shindou T, Wickens JR. Behavioral flexibility is increased by optogenetic inhibition of neurons in the nucleus accumbens shell during specific time segments. Learning and Memory. 2014;21(4):223–31.
172. Ragozzino ME. The contribution of the medial prefrontal cortex, orbitofrontal cortex, and dorsomedial striatum to behavioral flexibility. Annals of the New York Academy of Sciences. 2007:355–75.
173. Floresco SB. Prefrontal dopamine and behavioral flexibility: Shifting from an "inverted-U" toward a family of functions. Frontiers in Neuroscience. 2013.
174. del Arco A, Park J, Wood J, Kim Y, Moghaddam B. Adaptive encoding of outcome prediction by prefrontal cortex ensembles supports behavioral flexibility. Journal of Neuroscience. 2017;37(35):8363–73.
175. Ragozzino ME, Ragozzino KE, Mizumori SJY, Kesner RP. Role of the dorsomedial striatum in behavioral flexibility for response and visual cue discrimination learning. Behavioral Neuroscience. 2002;116(1):105–15.
176. Ragozzino ME, Jih J, Tzavos A. Involvement of the dorsomedial striatum in behavioral flexibility: Role of muscarinic cholinergic receptors. Brain Res. 2002;953(1–2):205–14.
177. Ragozzino ME, Mohler EG, Prior M, Palencia CA, Rozman S. Acetylcholine activity in selective striatal regions supports behavioral flexibility. Neurobiol Learn Mem. 2009;91(1):13–22.
178. Soares JCK, Oliveira MGM, Ferreira TL. Inactivation of muscarinic receptors impairs place and response learning: Implications for multiple memory systems. Neuropharmacology. 2013;73:320–6.
179. Goshen I. The optogenetic revolution in memory research. Trends in neurosciences. 2014;37:511–22.
180. Goshen I, Brodsky M, Prakash R, Wallace J, Gradinaru V, Ramakrishnan C, et al. Dynamics of retrieval strategies for remote memories. Cell. 2011;147(3):678–89.
181. Fink AJ, Axel R, Schoonover CE. A virtual burrow assay for head-fixed mice measures habituation, discrimination, exploration and avoidance without training. Elife. 2019;8(e45658).
182. Arnau RP, Paradiso E, Castaldi F, Sadeghi M, Yaqub M, Hoertnagl M, Goebel G and Ferraguti F. VIP-expressing interneurons in the anterior insular cortex contribute to sensory processing to regulate adaptive behavior. Cell Rep. 2022;39(9):110893.
183. Dombeck DA, Graziano MS, Tank DW. Functional clustering of neurons in motor cortex determined by cellular resolution imaging in awake behaving mice. Journal of Neuroscience. 2009;29(44):13751–60.
184. Hong W, Kim DW, Anderson DJ. Antagonistic control of social versus repetitive self-grooming behaviors by separable amygdala neuronal subsets. Cell. 2014;158(6):1348–61.
185. Dolensek N, Gehrlach DA, Klein AS, Gogolla N. Facial expressions of emotion states and their neuronal correlates in mice. Science. 2020;368(6486):89–94.
186. Ohara S, Tsutsui KI, Tobler PN, Iijima T, Ishii H. Inactivating Anterior Insular Cortex Reduces Risk Taking. Journal of Neuroscience. 2012;
187. Daniel ML, Cocker PJ, Lacoste J, Mar AC, Houeto JL, Belin-Rauscent A, et al. The anterior insula bidirectionally modulates cost-benefit decision-making on a rodent gambling task. European Journal of Neuroscience. 2017;46(10):2620–8.
188. Masui A, Kato N, Itoshima T, Tsunashima K, Nakajima T, Yanaihara N. Scratching behavior induced by bombesin-related peptides. Comparison of bombesin, gastrin-releasing peptide and phyllolitorins. Eur J Pharmacol. 1993;238(2–3):297–301.
189. Girard F, Aubé C, St-Pierre S, Jolicoeur FB. Structure-activity studies on neurobehavioral effects of bombesin (BB) and gastrin releasing peptide (GRP). Neuropeptides. 1983;3(6):443–52.
190. Gibbs J, Fauser DJ, Rowe EA, Rolls BJ, Rolls ET, Maddison SP. Bombesin suppresses feeding in rats. Nature. 1979;282:208–10.
191. Washington MC, Wright SA, Sayegh AI. Gastrin releasing peptide-29 evokes feeding responses in the rat. Peptides (NY). 2011;32(2):241–5.
192. Kyrkouli SE, Stanley BG, Leibowitz SF. Bombesin-induced anorexia: Sites of action in the rat brain. Peptides (NY). 1987;8(2):237–41.
193. O'Neill PK, Gore F, Salzman CD. Basolateral amygdala circuitry in positive and negative valence. Current Opinion in Neurobiology. 2018;49:175–83.
194. Namburi P, Beyeler A, Yorozu S, Calhoon GG, Halbert SA, Wichmann R, et al. A circuit mechanism for differentiating positive and negative associations. Nature. 2015;520(7549):675–678.

195. Burgos-Robles A, Kimchi EY, Izadmehr EM, Porzenheim MJ, Ramos-Guasp WA, Nieh EH, et al. Amygdala inputs to prefrontal cortex guide behavior amid conflicting cues of reward and punishment. Nat Neurosci. 2017;20(6):824–835.
196. Senn V, Wolff SBE, Herry C, Grenier F, Ehrlich I, Gründemann J, et al. Long-range connectivity defines behavioral specificity of amygdala neurons. Neuron. 2014;81(2):428–37.
197. Dumitriu D, Laplant Q, Grossman YS, Dias C, Janssen WG, Russo SJ, et al. Subregional, dendritic compartment, and spine subtype specificity in cocaine regulation of dendritic spines in the nucleus accumbens. Journal of Neuroscience. 2012;32(20):6957–66.
198. Nestler EJ. Cellular basis of memory for addiction. Dialogues Clin Neurosci. 2013;15(4):431–43.
199. Saddoris MP, Cacciapaglia F, Wightman RM, Carelli RM. Differential dopamine release dynamics in the nucleus accumbens core and shell reveal complementary signals for error prediction and incentive motivation. Journal of Neuroscience. 2015;35(33):11572–82.
200. Calipari ES, Bagot RC, Purushothaman I, Davidson TJ, Yorgason JT, Peña CJ, et al. In vivo imaging identifies temporal signature of D1 and D2 medium spiny neurons in cocaine reward. Proc Natl Acad Sci U S A. 2016;113(10):2726–31.
201. Ambroggi F, Ishikawa A, Fields HL, Nicola SM. Basolateral Amygdala Neurons Facilitate Reward-Seeking Behavior by Exciting Nucleus Accumbens Neurons. Neuron. 2008;59(4):648–61.
202. di Ciano P, Everitt BJ. Direct interactions between the basolateral amygdala and nucleus accumbens core underlie cocaine-seeking behavior by rats. Journal of Neuroscience. 2004;24(32):7167–73.
203. Gilpin NW, Herman MA, Roberto M. The Central Amygdala as an Integrative Hub for Anxiety and Alcohol Use Disorders. Vol. 77, Biological Psychiatry. 2015.
204. Schröder H, Moser N, Huggenberger S. The Mouse Caudate Putamen, Motor System, and Nucleus Accumbens. Neuroanatomy of the Mouse. Springer, Cham; 2020:305–18.
205. Urban A, Dussaux C, Martel G, Brunner C, Mace E, Montaldo G. Real-time imaging of brain activity in freely moving rats using functional ultrasound. Nat Methods. 2015;12(9):873–8.
206. Tiran E, Ferrier J, Deffieux T, Gennisson JL, Pezet S, Lenkei Z, et al. Transcranial Functional Ultrasound Imaging in Freely Moving Awake Mice and Anesthetized Young Rats without Contrast Agent. Ultrasound Med Biol. 2017;43(8):1679–89.
207. Knowland D, Lilascharoen V, Pacia CP, Shin S, Wang EHJ, Lim BK. Distinct Ventral Pallidal Neural Populations Mediate Separate Symptoms of Depression. Cell. 2017;170(2):284-297.e18.
208. Zingg B, Chou X lin, Zhang Z gang, Mesik L, Liang F, Tao HW, et al. AAV-Mediated Anterograde Transsynaptic Tagging: Mapping Corticocollicular Input-Defined Neural Pathways for Defense Behaviors. Neuron. 2017;93(1):33–47.